University of the Witwatersrand

Masters Dissertation

Evaluation of lightning location system over Johannesburg by high-speed cameras

Author:
Haydn Gareth Fensham

A Dissertation submitted in fulfillment of the requirements for the degree of Master of Science

in the

Lightning/EMC Research Group
School of Electrical and Information Engineering

August 2019

Declaration

I, **Haydn Gareth Fensham**, declare that this Dissertation titled, "**Evaluation of lightning location system over Johannesburg by high-speed cameras**" and the work presented in it are my own. I confirm that:

- This work was done wholly or mainly while in candidature for a research degree at this University.
- Where any part of this thesis has previously been submitted for a degree or any other qualification at this University or any other institution, has been clearly stated.
- Where I have consulted the published work of others, this is always clearly attributed.
- Where I have quoted from the work of others, the source is always given. With the exception of such quotations, this dissertation is entirely my own work.
- I have acknowledged all main sources of help.

Signed: ____

Date: ____

UNIVERSITY OF THE WITWATERSRAND

Abstract

Engineering and the Built Environment
School of Electrical and Information Engineering

Master of Science

Evaluation of lightning location system over Johannesburg by high-speed cameras

by Haydn Gareth FENSHAM

Supervisor: DR. HUGH HUNT, DR. CARINA SCHUMANN AND PROF. KEN NIXON

This research describes an approach to evaluating the performance of the South African Lightning Detection Network (SALDN) over Johannesburg, South Africa, using high-speed video footage of lightning events. The performance evaluation includes the flash detection efficiency, stroke detection efficiency and median location accuracy (locations of known attachments and flash cluster approach) of the SALDN. The proposed methodology has three subsections: time-correlating cloud-to-ground stroke data from the SALDN with ground truth lightning events (high-speed camera footage), determining the detection efficiency and determining the location accuracy. Results indicate that the SALDN has a flash detection efficiency of 84.9 %, stroke detection of 69.1 % and has a median location accuracy of 59.2 m and 124.4 m using locations of known attachments and flash cluster approaches respectively for cloud-to-ground lightning over Johannesburg.

I dedicate this to my parents, Verdell and Peter Fensham
and my sister, Jessica Albrecht

Thank you for always supporting and encouraging me, for the unconditional love and for the opportunity of allowing me to follow my passion.

Acknowledgements

I would like to thank my supervisors Dr. Hugh Hunt, Dr. Carina Schumann and Prof. Ken Nixon for their time and patience throughout this research. It has been a privilege working with such passionate and encouraging supervisors.

I would like to thank Tom Warner of ZT Research for the use of his equipment throughout this research.

I would like to thank my colleague Jesse Tasman for his help and support throughout the research.

I would like to thank the South African Weather Service (SAWS) for their support and for providing the SALDN data used in this research.

I would also like to thank Eskom for the support of the Lightning/EMC Research Group through the TESP programme.

Thanks are extended to the Department of Trade and Industry (DTI) for THRIP funding as well as to the National Research Foundation (NRF) for direct funding of the Research Group.

Contents

List of Figures

List of Tables

Abbreviations

LLS	**L**ightning **L**ocation **S**ystem
DE	**D**etection **E**fficiency
LA	**L**ocation **A**ccuracy
SALDN	**S**outh **A**frican **L**ightning **D**etection **N**etwork
SAWS	**S**outh **A**frican **W**eather **S**ervice
CG	**C**loud-to-**G**round
ICC	**I**nitial **C**ontinuing **C**urrent
IC	**I**nter/**I**ntra-**C**loud
RS	**R**eturn **S**troke
SRS	**S**ubsequent **R**eturn **S**troke
CC	**C**ontinuing **C**urrent
TOA	**T**ime-of-**A**rrival
MDF	**M**agnetic **D**irection **F**inding
GPS	**G**lobal **P**ositioning **S**ystem

Conferences and Publications

[Appendix A] **H. G. Fensham**, C. Schumann, H. G. P. Hunt, J. D. Tasman, K. J. Nixon, T. A. Warner and M. Gijben, "Performance evaluation of the SALDN using high-speed camera footage of ground truth lightning events over Johannesburg, South Africa", 34^{th} *International Conference on Lightning Protection (ICLP), 2018.*

[Appendix B] J. D. Tasman, **H. G. Fensham**, C. Schumann, H. G. P. Hunt, K. J. Nixon and T. A. Warner, "High-speed video analysis of lightning flashes over Johannesburg, South Africa", 26^{th} *Southern African Universities Power Engineering Conference (SAUPEC)*, 2018.

[Appendix C] C. Schumann, H. G. P. Hunt, J. D. Tasman, **H. G. Fensham**, K. J. Nixon, T. A. Warner and M. M. F. Saba, "High-speed video observation of lightning flashes over Johannesburg, South Africa 2017 - 2018", 34^{th} *International Conference on Lightning Protection (ICLP)*, 2018.

[Appendix D] J. D. Tasman, C. Schumann, H. G. P. Hunt, **H. G. Fensham**, K. J. Nixon, M. M. F. Saba and T. A. Warner, "Characterisation of lightning flashes from changing electric field measurements in Johannesburg, South Africa", 34^{th} *International Conference on Lightning Protection (ICLP)*, 2018.

CHAPTER 1

Introduction

Lightning events emit electromagnetic waves. A Lightning Location System (LLS) is a network composed of multiple sensors that can triangulate the propagated electromagnetic wave. An LLS can detect lightning events with a time stamp and provide an estimate of the geographical location [1]. Different countries around the world operate LLSs to collect lightning event data. LLS data is used for: warning systems, the forecasting of thunderstorms, insurance and forensic applications and determining if power outages and damages to the power utility are from lightning events [2].

LLS data is also used to develop ground-flash density maps. Ground-flash density maps provide information which can be used in risk assessments and lightning protection system designs. However, LLSs may not detect lightning events for a number of reasons, for example the strength of the emitted electromagnetic wave. LLSs may also not locate the lightning event accurately due to errors in the different location techniques. Therefore, Detection Efficiency (DE) and Location Accuracy (LA) are considered to be the most important performance measures of an LLS [3].

The Detection Efficiency (DE) of an LLS is an indication of how many lightning events an LLS is detecting. For instance, a DE of 80 % means that the LLS is detecting 80 % of lightning events. However, this means that 20 % of lightning events are not being detected. If this lightning data is used in a ground-flash density map, the map will underestimate the ground flash density in the area. This will affect risk assessments and lightning protection design. Therefore, it is important to understand the DE of a LLS in order to understand the accuracy of a flash-density map.

The Location Accuracy (LA) of an LLS is an indication of how accurately the LLS reports the location of a detected lightning event. The LA gives an indication of how accurately the LLS locates lightning events. Applications mentioned above such as the warning systems and the power utility outages and damages rely on this accuracy. If the median LA of a LLS is, for instance, 200 m the power utility will in most cases be able to rule out that an outage was caused from a lightning event that was reported to have occurred 2 km from a transmission line.

These performance measures are also used on the majority of LLSs throughout the world as it provides information which can be used to improve the network. For example, sensors might need to be repositioned or more sensors might need to be added to the network. Additionally, the performance evaluation after an upgrade to an LLS can be compared to the performance evaluation before the upgrade of an LLS. This will give an indication of how the upgrades to the LLS have changed the performance.

1.1 Problem statement

South Africa's Lightning Detection Network (SALDN) is operated by the South African Weather Service (SAWS). There was a performance evaluation on the SALDN in 2014. However, the stroke detection efficiency was not obtainable and the location accuracy was found for one location. This means the stroke detection efficiency of the SALDN is unknown and the location accuracy is unknown over a greater region. Therefore, the SALDN has not had a performance evaluation (detection efficiency and location accuracy) using high-speed cameras for all types of CG flashes over Johannesburg.

1.2 Research question

The problem statement above leads to the following research question which can be answered with the methodology in chapter 4.

"What is the performance of the SALDN in Johannesburg, South Africa?"

In this case the performance is defined as: flash DE, stroke DE and LA on downward and upward flashes. This research question can be answered by answering the following sub-questions:

1. What is the flash detection efficiency?
2. What is the stroke detection efficiency?
3. What is the location accuracy?

1.3 Structure of dissertation

This dissertation contains the answer to the research question presented above. This subsection provides an overview of chapters 2 to 7 which are found in the dissertation.

Chapter 2 presents lightning fundamentals that are important to comprehending the results presented in this document as well as the techniques used by an LLS to detect and provide a reported location of a lightning event. The performance evaluation of an LLS, previous studies which present the performance evaluations of different LLSs and LLS data that is used in ground-flash density maps are also discussed.

Chapter 3 presents a high-speed video investigation in Johannesburg discussing the equipment, the interpretation of high-speed lightning videos and the results of the investigation. The history of the South African Lightning Detection Network and the processing of the data collected from the SALDN are also presented.

Chapter 4 presents a methodology for time-correlating LLS data and ground truth lightning events, determining the flash detection efficiency and stroke detection efficiency and determining the location accuracy using locations of known attachment and using flash clusters.

Chapter 5 presents the results obtained by using the processed data in *chapter 3* and the methodology in *chapter 4*. The results include the time-correlated data, detection efficiency and location accuracy.

Chapter 6 discusses the results obtained in *chapter 5* this includes: the outliers found in the location accuracy data, a comparison between the location accuracy of the locations of known attachment method and the flash cluster method and a comparison between the results of the SALDN and the studies presented in chapter 2. Interesting cases found throughout the research are also discussed.

Chapter 7 provides a conclusion to the dissertation.

CHAPTER 2

Background

This chapter presents lightning fundamentals that are important to comprehending the results presented in this document as well as the techniques used by an LLS to detect and provide a reported location of a lightning event. The performance evaluation of an LLS, previous studies which present the performance evaluations of different LLSs and LLS data that is used in ground-flash density maps are also discussed.

2.1 Lightning fundamentals

There are two main types of lightning: Inter/Intra-Cloud (IC) and Cloud-to-Ground (CG). IC, the more common type of lightning, occurs within the clouds (Intra-Cloud) and between the clouds (Inter-Cloud) [4]. CG lightning terminates between the cloud and the ground, due to this CG is of more concern as it presents risks to humans and infrastructures. CG lightning can be sub divided into two categories: downward flashes and upward flashes. A downward and an upward flash can have either a negative or positive current polarity.

2.1.1 Downward flash

Given that 90 % of CG flashes are downward negative CG (nCG), the terminology associated with this type of flash will be discussed [5]. For a nCG flash to occur, a cloud with charge distribution is required as seen in the first image of figure 2.1. If there is a preliminary breakdown within this charge distribution, a conducting path of negative charge from the cloud may start to propagate towards the earth as seen in images 2 to 5. This is termed the negative stepped leader. The negative stepped leader may have multiple branches propagating towards the earth. This can look like an upside down tree with the branches facing the earth. It is termed "stepped" because the leader moves in discrete movements as opposed to a continuous movement. If the leader is propagating from the cloud towards the earth this is referred to as a downward flash. The duration of a stepped leader is in the order of tens of milliseconds [6].

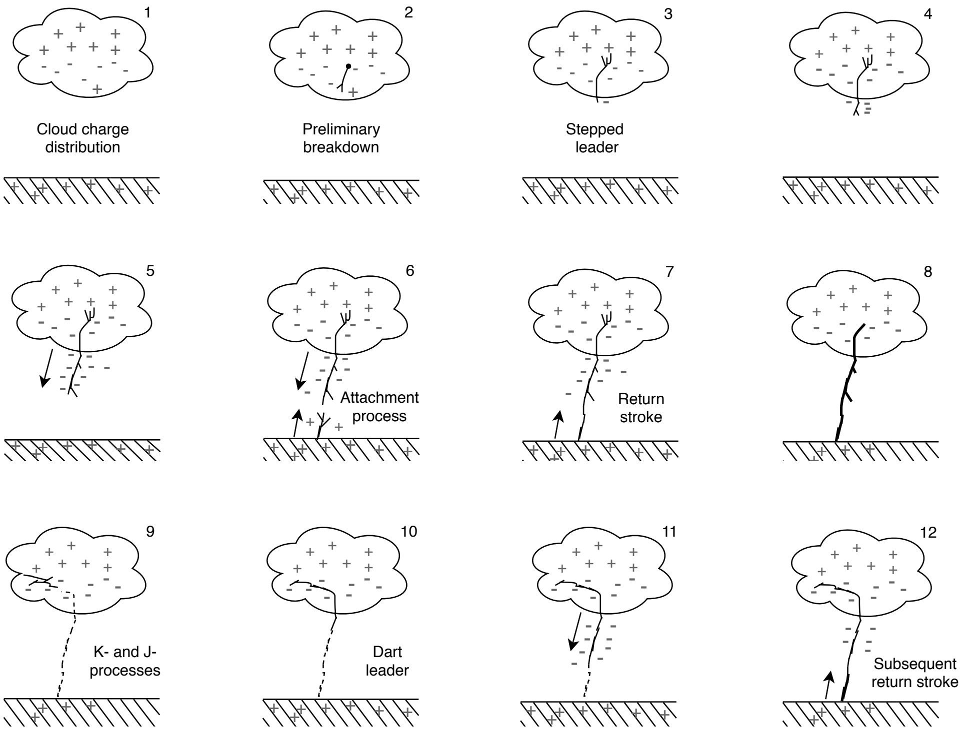

FIGURE 2.1: The sequence of processes in downward negative cloud-to-ground flash. Adapted from [6]

As the stepped leader propagates and approaches ground, the electric field on ground level enhances steadily as discussed in [7]. It is possible that leaders can be initiated from ground objects due to this enhancement as seen in image 6. These leaders will be attracted to the downward stepped leader. They are referred to as the upward connecting leaders which may attach to the downward stepped leader. The attachment process refers to contact between the downward stepped leader and the upward connecting leader as seen in image 6. This process is impulsive and is completed once contact is made between the downward stepped leader and the upward connecting leader. Once the leaders have made contact, a continuous ionised channel is formed which allows current to flow. The negative charges within the channel are transported to ground in an attempt to neutralise the charge within the downward stepped leader channel. This flow of current within the channel is referred to as the 1^{st} Return Stroke (RS) as seen in images 7 and 8 [6].

If the flash only contains the 1^{st} RS then it is referred to as a single-stroke flash [6]. However, about 80 % of nCG flashes have multiple strokes in a flash [8]. In the case where another stroke occurs in a flash, a downward leader propagates down the original channel of the 1^{st} RS. This downward leader is referred to as the dart leader. It is termed "dart" because it moves in a continuous movement towards the earth. The dart leader occurs from J- and K- processes which have taken place within the cloud after the 1^{st} RS as seen in image 9. This dart leader attaches in a similar manner to the attachment process of the 1^{st} RS, as seen in image 10 and 11. The channel of current is formed again and is called the Subsequent Return Stroke (SRS) as seen in image 12 [6]. The SRS attempts to neutralize the charge in the leader channel, recharged by the dart leader [6]. The process of a SRS forming may occur numerous times resulting in a number of strokes in one flash. SRSs may have a smaller peak current magnitude than the 1^{st} RS since an ionised channel already existed. All strokes (1^{st} RS and SRSs) in this process are considered part of the flash.

There is an important relationship between the current in a channel of a stroke and the luminosity of that channel. The luminosity of a channel has been found to be proportional to the amount of current flowing in the channel [9]. This means that as a stroke is formed (impulsive phase) and there is a large flow of current there is also a large increase in luminosity of the channel. The luminosity of channels start to decrease as the current in the channel starts to decay. Figure 2.2 below illustrates the changes in luminosity of the channel with the 1^{st} RS and a SRS.

It is important to note that after the impulsive phase of a stroke (1^{st} RS or SRS) which has a duration of a few microseconds, there can be a Continuing Current (CC) phase which can have a duration of hundreds of milliseconds. CC is the relatively low current that flows through the channel immediately after the impulsive phase. If there are transient effects (luminosity fluctuations in the channel) during the CC phase, this can be what is referred to as M-components [6]. Figure 2.2 shows an example of M-components during the continuing current phase of a SRS.

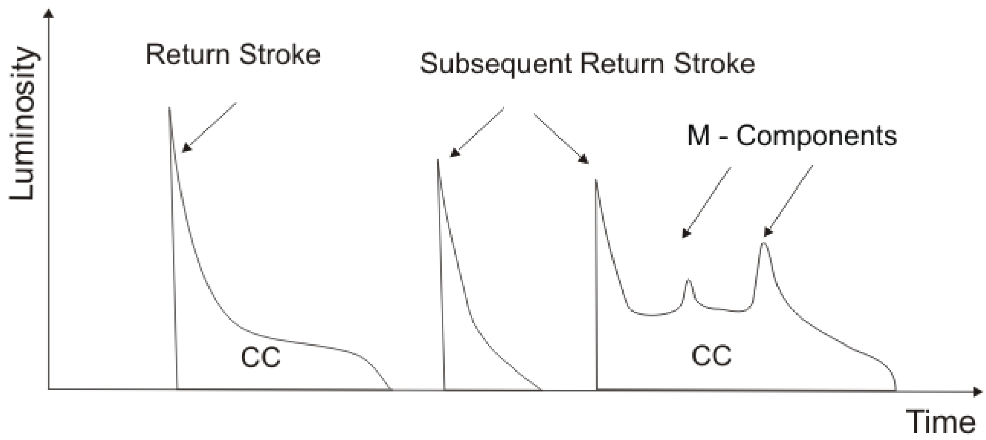

FIGURE 2.2: The luminosity changes, during different processes, in a downward flash against time. Adapted from [10]

2.1.2 Upward flash

Upward flashes are similar to downward flashes, however, the upward leader originates from a structure on the ground and propagates into the cloud. The upward leader can be initiated in two ways: nearby-lightning-triggered or self-initiated [11]. Thus, there are two types of upward flashes as seen below [12].

- Nearby-lightning-triggered upward flash
- Self-initiated upward flash

In the case of a nearby-lightning-triggered upward flash, the upward leader will be initiated by a lightning event (CG or IC) in the vicinity of the structure. Even lightning events as far as tens of kilometres can initiate the upward leader. In the case of a self-initiated upward flash, there is no lightning event (CG or IC) in the vicinity of the structure. Instead, the upward leader is initiated from a structure due to an intense electric field [12]. Upward leaders may or may not branch as they propagate towards the cloud base [13].

A negative upward flash implies a positive upward leader [6]. Once an upward leader has been initiated and has been propagating towards the cloud base, an Initial Continuous Current (ICC) flows through the channel [13]. The first event in figure 2.3 illustrates how the ICC luminosity would appear. It is important to note the slow rise time of this ICC, which will be discussed in section 2.3. Transient effects that occur on the upward leader channels are known as ICC pulses. ICC pulses are superimposed on the upward leader and are seen by luminosity fluctuations in the upward leader as seen in figure 2.3 [6].

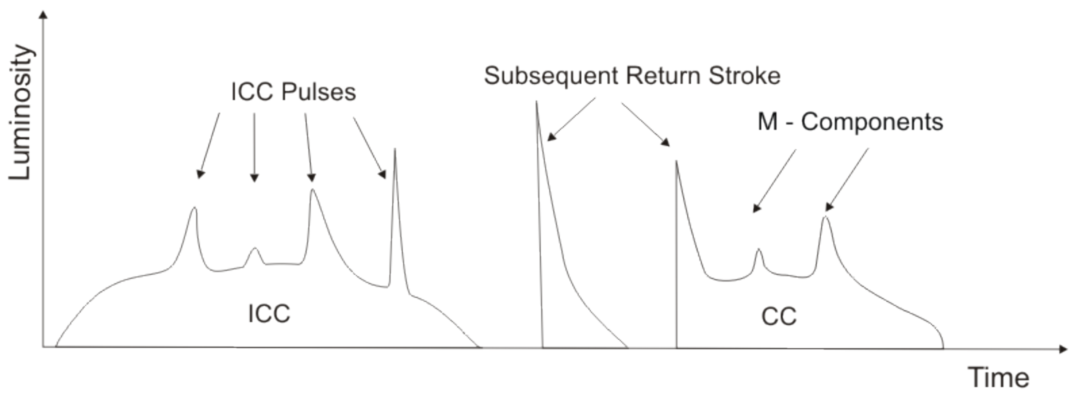

FIGURE 2.3: The luminosity changes, during different processes, in an upward flash against time. Used with permission [13]

After a period where the current ceases (no luminosity from the channel) dart leaders may propagate through the ionised channels and make attachment with the structure forming SRSs [13]. This is similar to the SRSs that are formed in downward flashes. M-components can also occur during the CC phase of the SRS in upward flashes. The SRSs and M-components can be seen in figure 2.3. A downward flash can consist of a 1^{st} RS and SRSs, however, an upward flash in terms of strokes will only have SRSs.

Figures 2.2 and 2.3 illustrate that the luminosity of a channel can be used to distinguish between certain processes in a flash. This means a camera will be able to see the different processes discussed above as the luminosity of the channel is visible and will allow the type of flash and all its processes to be determined and analysed. A video can be used as evidence of ground truth lightning events since there is physical evidence of the flash. The flashes can be classified as negative downward, negative upward, positive downward or positive upward [6]. Each lightning event emits an electromagnetic wave.

2.2 Lightning location systems

An LLS measures the electromagnetic waves which are propagated from a lightning event. This electromagnetic wave allows the LLS to detect CG and IC flashes [4]. There are several techniques which use different components of the electromagnetic wave to firstly, identify if there was a lightning event and secondly determine where the lightning event occurred. The two main techniques used to locate lightning events are Magnetic Direction Finding (MDF) and Time-of-Arrival (TOA) [14]. These two techniques can also be used in combination, this is know as IMPACT.

2.2.1 Magnetic direction finding

MDF uses two orthogonal antennas to measure the magnetic field from the lightning event. The Azimuth angle is calculated from the voltages induced in each of the antennas. The Azimuth angle is the horizontal angle which is measured from fixed angle in a clockwise direction. This angle gives the direction in which the lightning event occurred. Figure 2.4 below shows how MDF can be used to find the direction of the lightning event as well as the location. In this figure, three sensors have detected a lightning event. The solid lines illustrate the Azimuth angles from the sensors, showing that the lightning event should be located somewhere along the solid line for each sensor. Ideally, the three solid lines should intersect at the same point indicating the location of the lightning event. However, metal bodies and other irregularities on the surface of the earth can affect the accuracy of the MDF. Due to this, these solid lines may not intersect perfectly and therefore an area of uncertainty will form [15]. The lightning event location is then calculated by a least square optimization algorithm. However, the calculated location might not be the same as the true location of the lightning event.

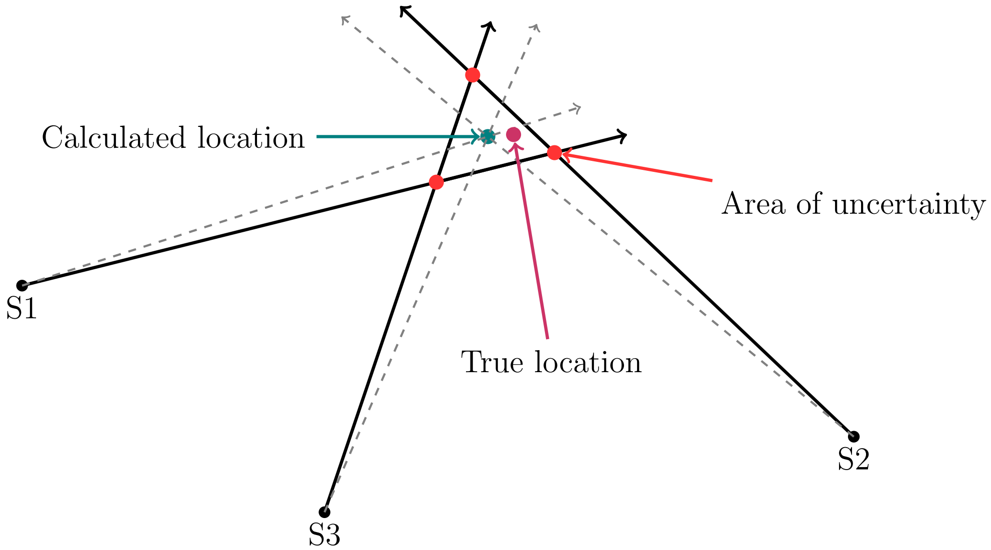

FIGURE 2.4: MDF technique for finding the location of a lightning event. Adapted from [15]

2.2.2 Time-of-arrival

TOA relies on the electric field generated by a lightning event and more specifically the radiation field component of this electric field. TOA measures the time difference between when each sensor detects the radiation field. Knowing the distances between all of the sensors and measuring the time difference in which each sensor detects the electric field, leads to a hyperbola which can be drawn for each pair of sensors. Figure 2.5 shows three sensors which detected a lightning event and their respective hyperbolae (solid lines). Theoretically, these hyperbolae should all intersect at the same point indicating the lightning event location. However, if the ground conductivity is low and the earth has an irregular surface this can affect the accuracy of the TOA. Thus, as with the MDF technique, an area of uncertainty is formed between the intersections of the hyperbolae [15]. The lightning event location is then calculated by a least square optimization algorithm.

However, the calculated location might not be the same as the true location of the lightning event.

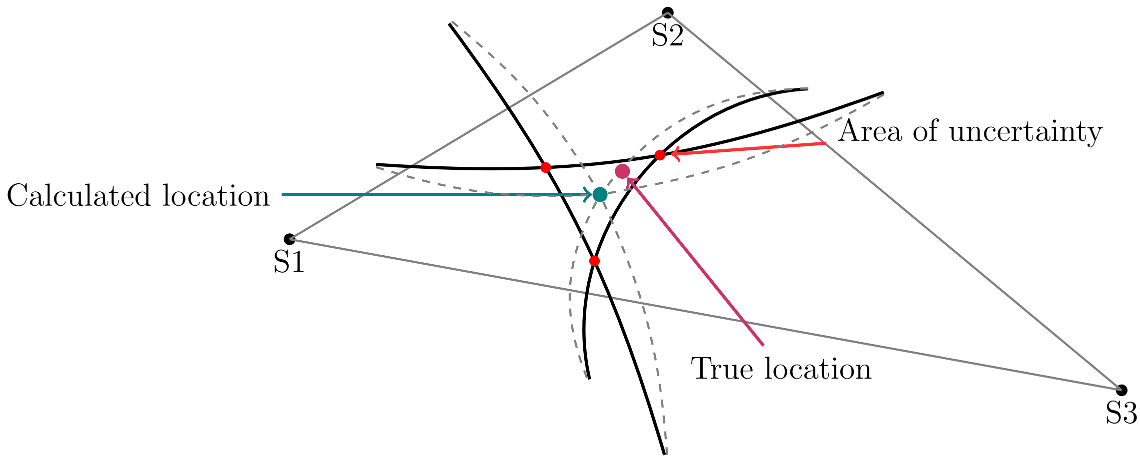

FIGURE 2.5: TOA technique for finding the location of a lightning event. Adapted from [15]

2.3 Performance of an LLS

The main performance measure of an LLS is the detection efficiency and location accuracy [3]. As discussed before, a flash consists of multiple strokes. The DE can be defined in terms of two parameters, the flash DE and the stroke DE. The flash DE is the percentage of flashes detected by the network versus the number of ground truth flashes. The stroke DE is the percentage of strokes (1^{st} RS and SRSs) detected by the network versus the number of ground truth strokes. The flash and stroke DE gives an indication of how well the LLS is detecting lightning. The flash DE will be greater than that of the stroke DE because the LLS only needs to detect one of the strokes in a given flash in order to detect this flash. [16].

LLSs provide a reported location of a detected lightning event. Location error is the distance between the actual location of a lightning event and the reported LLS location of the lightning event. An illustration of this can be seen in figure 2.6. The LA is a dataset of multiple location errors which can represented by using statistics such as the maximum, minimum, median, standard deviation, mode and mean of the location errors [17].

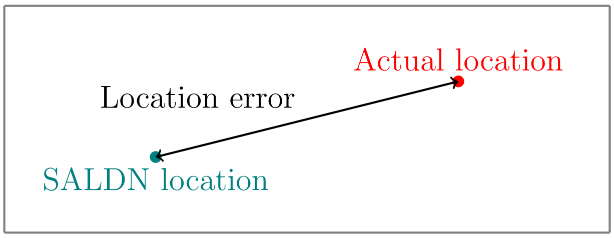

FIGURE 2.6: Location error (m) between SALDN location and actual location

Other performance measures of an LLS that may be considered are peak current estimation accuracy and lightning type classification accuracy [2]. Peak current estimation accuracy is how accurately an LLS reports the actual current of a cloud-to-ground flash. This requires a ground truth current measurement of the actual lightning event in order to compare it to the reported current of the LLS. LLSs can misclassify CG and IC flashes. This means that the lightning event can be detected but it will be classified as the wrong type of flash. Generally, IC flashes have lower peak currents. Therefore, if a positive CG flash is below a certain peak current, the LLS may classify this lightning event as a IC flash [18]. Lightning type classification accuracy is a ratio of misclassified to classified lightning events.

It is important to note that an LLS detects impulsive events so, in the case of upward flashes, the upward leader will not be detected by the LLS due to the slow rise time as seen in figure 2.3. However the CG trigger event, if there is one, has a good chance of being detected [13]. This is however, not strictly a detection of the upward flash. ICC pulses and SRS can be detected due to their impulsive nature [13]. Therefore, it is not expected that the LLS will detect upward flashes as good as downward flashes. In some cases the DE is only provided on downward flashes due to this.

2.4 Previous studies on LLS performance

The following subsection presents studies which have previously evaluated the performance of an LLS.

The European LLS, EUCLID (European Cooperation for Lightning Detection) was evaluated using various ground truth data. The LA, DE and current estimations of EUCLID were evaluated. The LA was calculated by using the Gaisberg Tower measurement system and the data obtained from EUCLID. With the lightning terminating on the tower, the actual location of the lightning event was known and this could be compared to the location estimated from EUCLID. The DE was presented using two different methods, the first being the instrumented tower and the second being the video and E-field data. The flash DE and stroke DE was found to be 96 % and 70 % using the Gaisberg Tower. In Austria, EUCLID had a flash DE and stroke DE of 98 % and 84 % using high-speed cameras for flashes to the tower which had at least one SRS. With improvements to the LLS, the last 100 strokes on the Gaisberg Tower had a median LA of 89 m. There has been a continuous improvement to the LA of EUCLID with software and hardware improvements [19].

In Hong Kong, the LLS in operation is the Guangdong-Hongkong-Macau Lightning Location System (GHMLLS). The flash DE, stroke DE, LA and peak current estimation accuracy of the GHMLLS was evaluated. Two methods were used to gather ground truth data. The first was lightning triggered experiments which took place in Conghua and the second was the observation of natural flashes on tall structures using high speed video footage along with other sensors, which took place in Guangzhou. Data over many years was obtained and evaluated to determine the performance measures of the GHMLLS. The results obtained were: flash DE of 95 %, stroke DE of 90 % and median LA of 410 m. These results showed a significant improvement in the performance of the LLS after an upgrade in 2012 [3].

In Brazil, the LLS is referred to as the Brazilian Integrated Lightning Detection Network (RINDAT). This network has seen multiple upgrades to increase the DE and LA. A performance evaluation of the network used high-speed camera footage of negative downward flashes as the ground truth data. The RINDAT was found to have a flash DE of 87.4 % and a stroke DE of 54.7 %. These values were in agreement with the expected DE by the manufacturer. The LA was determined by taking the maximum distance between strokes within a flash. Thus, this LA is a overestimation of the network. The median LA was found to be 3.4 km. This was the first performance evaluation of the RINDAT where all sensors were operating normally [20].

The U.S. National Lightning Detection Network (NLDN) has had multiple performance evaluations where the DE, LA and peak current estimation accuracy were determined. These performance evaluations used rocket triggered lightning in the Florida region. The location errors were defined as the distance between the rocket launcher and the reported location of the lightning event from the NLDN. Using data from 2004 to 2013 the following results were obtained: The flash DE, stroke DE and median LA was 94 %, 75 % and 309 m respectively. These results show the constant improvement of the NLDN since performance evaluations in 2005, 2011 and 2014 [21].

In 2014, there was a performance evaluation on the SALDN using low-speed cameras, the flash DE was found to be 76 % in the last season (2012-2013) with a median LA of 280 m for data collected between 2009-2013 [17].

It can be seen in the studies above that countries evaluate the performance of their LLS by finding the DE and LA of the network. The studies use various methods of obtaining ground truth lightning events to evaluate the LLS. This research makes use of ground truth lightning events from high-speed cameras.

2.5 LLS data used in ground-flash density maps

LLS data and ground-flash density maps are used for a number of investigations: risk assessments regarding lightning flashes, power utility damages and outages, lightning protection designs as well as forensic and insurance investigations are some examples [2]. A ground-flash density map shows the amount of flashes, grouped by time and location, per square kilometre per year over a geographical map. In South Africa, ground-flash density maps are formulated by using the lightning data from the SALDN [5]. The accuracy of the ground-flash density map is directly proportional to the performance of the SALDN. Figure 2.7 is a ground-flash density map of South Africa using data from 2006 to 2010 [22].

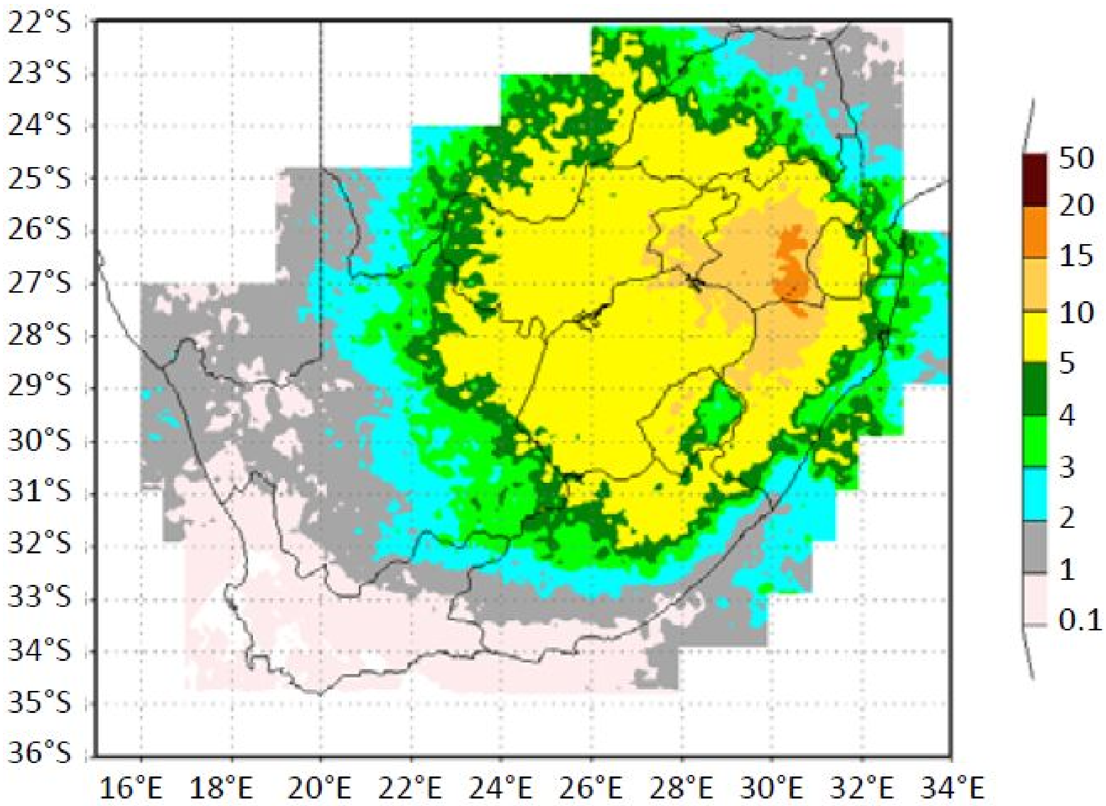

FIGURE 2.7: Ground-flash density map of South Africa. Used with permission [22]

It is also important to note that strokes in a CG flash can produce multiple ground terminations, this is referred to as Multiple Ground Contacts (MGC) [23]. MGCs lead to an underestimation of the probability that a structure will be struck by lightning based on the ground-flash density maps information [24]. Thus, it has been advised that Ground Strike Point (GSP) density maps need to be formulated and used for risk assessment [25]. A GSP refers to the geographical locations of which strokes terminated. Therefore, a GSP map contains the geographical location of the termination point of strokes as opposed to flashes in the case of ground-flash density maps. GSP density maps rely on stroke data from the LLS. Therefore, it is important to know the stroke DE and LA in order to know how viable GSP density maps are using data from a certain LLS [26].

2.6 Summary

Cloud-to-ground lightning consists of downward and upward flashes. Flashes can have multiple strokes. In the case of a downward flash the first stroke is referred to as the 1^{st} return stroke and the following strokes are referred to as the subsequent return strokes. A stroke may have continuing current, any transient effects during this phase are referred to as M-components. An upward flash may have transient effects during the initial continuous current phase of the upward leader, these are referred to as initial continuing current pulses. Ground truth lightning event data is physical evidence of a lightning event. LLSs use time-of-arrival and magnetic direction finding techniques to detect and locate flashes. However, there are factors that affect the accuracy of detecting and providing a reported location of a lightning event. This can be quantified by evaluating the detection efficiency and location accuracy of an LLS. The results of performance evaluations of different LLSs are presented. LLS data is used in ground-flash density maps which are important for risk assessments and lightning protection design. The ground-flash density map is only as accurate as the LLS itself.

The following chapter presents the equipment and data processing in the research.

CHAPTER 3

Equipment and Data Processing

This chapter presents a high-speed video investigation in Johannesburg discussing the equipment, the interpretation of high-speed lightning videos and the results of the investigation. The history of the South African Lightning Detection Network and the processing of the data collected from the SALDN are also presented.

The ground truth performance evaluation of an Lightning Location System (LLS) requires two forms of data, ground truth lightning data and the LLS data. Ground truth lightning data is important as it provides evidence that a flash or stroke occurred. LLS data can be compared to ground truth lightning data to establish if the ground truth lightning event was detected or not. In this research, the ground truth lightning data is collected using high-speed video cameras over Johannesburg, South Africa. The LLS data is provided by the South African Weather Service and is in the form of Cloud-to-Ground (CG) stroke South African Lightning Detection Network (SALDN) data.

3.1 High-speed video investigation in Johannesburg

High-speed cameras are one way to gather ground truth lightning events [19]. They can capture videos at thousands of frames per second. This allows processes such as the leader and the strokes within a flash to be observed and analysed.

The ground truth data for this research was collected using two high-speed cameras, the Phantom v310 (15 000 fps) and the Phantom v7.1 (5 000 fps), which overlook Johannesburg, South Africa. The high-speed cameras are positioned approximately 6 km away from Johannesburg Central Business District (CBD). The blue camera icon situated at (26.16283 °S, 27.95986 °E) in figure 3.1 is where the cameras are positioned. Within the Johannesburg CBD there are two tall towers, the Hillbrow and Sentech Tower. The Hillbrow (26.18696 °S, 28.04948 °E) and Sentech (26.1925 °S, 28.00666 °E) Tower are situated within the field of view (black lines) as seen in figure 3.1. The towers are represented as the black tower icons.

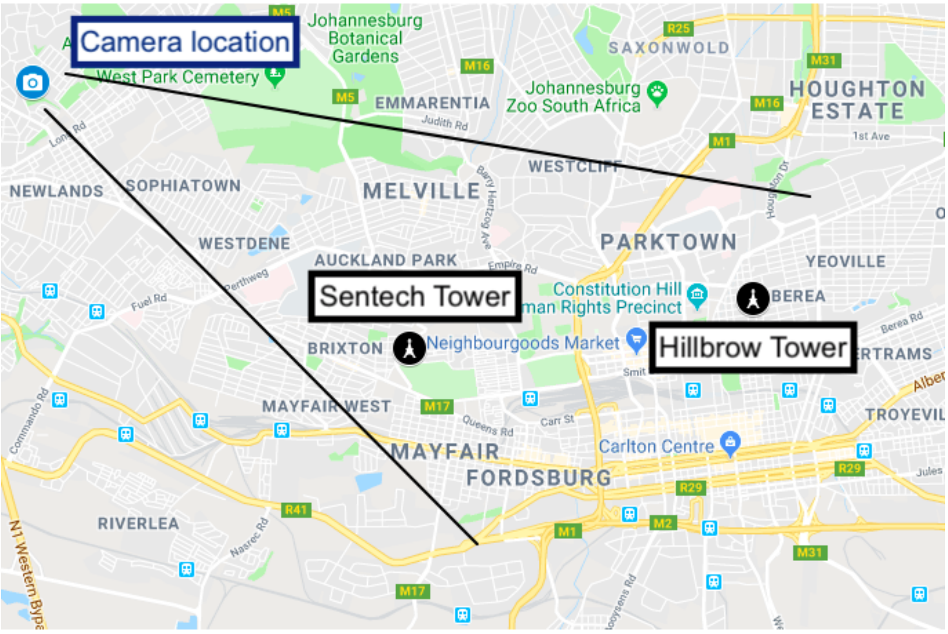

FIGURE 3.1: Map showing the geographical location of the cameras, towers and the field of view

Figure 3.2 illustrates the cameras field of view, the Hillbrow and Sentech Tower can be seen clearly. The Hillbrow and Sentech Tower have a height of 270 m and 232 m respectively.

FIGURE 3.2: Field of view from the cameras location

The cameras are manually triggered once a flash has been observed. Therefore, each day a weather forecast is used to determine if there is a possibility of a thunderstorm. The cameras are switched on before a thunderstorm and adjustments are made for the ambient light level. The cameras have a pre-trigger and post-trigger time of 1.6 s and 0.2 s respectively. Figure 3.3 below shows the Phantom v310 (camera on the left) and the Phantom v7.1 (camera on the right) positioned with the field of view shown previously. The camera mount rail allows the field of view of the cameras to be adjusted if need be.

FIGURE 3.3: Image showing the setup of the high-speed cameras

The high-speed camera investigation over Johannesburg collected data between the 5th February 2017 and 6th February 2018 during the summer season. Thunderstorms are expected during the summer season in Johannesburg, South Africa. It must be noted the high-speed video investigation is not based on all lightning events over Johannesburg but rather interesting cases which have been captured on the high-speed cameras.

3.1.1 Interpretation of high-speed lightning videos

In chapter 2 it is discussed that the current in a channel (therefore the luminosity from that channel) can be used to distinguish different processes in a flash. The high-speed camera images in this subsection will help visualise these processes.

Figure 3.4 shows an example of a downward flash. The downward stepped leader is the first visible process as seen in the first image. It is important to note the branches on the stepped leader. The branches are pointing towards the earth like an upside down tree, indicating a downward flash. The second image shows attachment, which is associated with a large increase in luminosity over a short period of time (impulsive event). This can now be referred to as the 1^{st} Return Stroke (RS) as seen in the third image. Once the luminosity of the 1^{st} RSs channel ceases, there can be a dart leader looking for attachment down the ionised channel as seen in the fourth image. Once attachment is made, a Subsequent Return Stroke (SRS) is formed as seen in the fifth image. These videos also allow the duration of the 1^{st} RS and SRS to be obtained.

FIGURE 3.4: The different processes in downward flashes caught with a high-speed camera

Figure 3.5 shows an example of an upward flash. The first visible stage is the upward leader. In the first image the upward leader has multiple branches as seen with the downward flash, however, these branches are facing the clouds. The second image shows a fluctuation in the luminosity of one of the branches. This is an Initial Continuous Current (ICC) pulse as discussed previously and is superimposed on the upward leader. Any luminosity fluctuation on an entire upward leader branch was considered an ICC pulse. Once the flow of current in the upward leader ceases, a dart leader can propagate down the channel. The third image illustrates the dart leader propagating towards earth. Once attachment is made, as seen in the fourth image, a large increase in luminosity is seen and the SRS is formed as seen in the fifth image.

Recoil leaders allow the polarity of a downward or upward flash to be determined from a high-speed video. If recoil leaders appear in the video, then the polarity of the channel is positive. If there are no recoil leaders, then the current of the channel is negative.

FIGURE 3.5: The different processes in upward flashes caught with a high-speed camera

3.1.2 Results of the high-speed video investigation

The camera footage was collected between the 5th February 2017 and the 6th February 2018. This was the first year high-speed videos cameras were used to capture ground truth lightning events. The footage needed to be watched and analysed in order to develop the ground truth dataset. The ground truth data is used in the methodology found in chapter 4. The ground truth data were categorised in a data sheet comprising of information such as: Time of attachment of the stroke, strike point, type of lightning, if there was Inter/Intra-Cloud (IC) or an attempted leader and the duration of each stroke. The ground truth data should describe the processes that occurred in the high-speed videos.

Table 3.1 shows an example of the ground truth data obtained from analysing a high-speed video. Row 1 and 4 of the data sheet are 1^{st} return strokes because of the different strike points in the flash. This is a case of multiple ground contacts within a flash. This was discussed in chapter 2, section 2.5. The remaining strokes are subsequent return strokes. In the case where there was a CG triggered upward flash, the triggering event was considered as a downward flash. This means the triggering event was not classified as part of the upward flash.

TABLE 3.1: High-speed video of a downward flash analysed into a data sheet

Reference	**Time**	**Process**	**Strike Point**	**Polarity**	**Visible**	**Duration (ms)**
1	14:58:34:070	Stroke	1	Negative	yes	7
1	14:58:34:103	Stroke	1	Negative	yes	6
1	14:58:34:121	Stroke	1	Negative	yes	5
1	14:58:34:208	Stroke	2	Negative	no	
1	14:58:34:256	Stroke	2	Negative	no	
1	14:58:34:292	Stroke	2	Negative	no	

Table 3.2 summarises the ground truth data captured over Johannesburg. 206 flashes and 667 strokes were recorded during the 24 thunderstorms. Of the 206 flashes, 163 are downward flashes and 43 are upward flashes. The majority of these upward flashes occurred on the Hillbrow and Sentech Tower. The data shows that there were 55 upward leaders which is greater than the amount of upward flashes. This means that certain upward flashes had multiple upward leaders coming from different objects on the ground. An interesting observation is the large amount of ICC pulses which were recorded. On average there are 9 ICC pulses per upward flash.

TABLE 3.2: High-speed camera data (ground truth data)

Lightning events	**High-speed camera events**
Thunderstorms	24
Flashes	206
Strokes	667
Downward flashes	163
Strokes	604
M-components	101
Upward flashes	43
Upward leaders	55
ICC pulses	387
Subsequent Return Strokes	63
M-components	10

3.2 The South African Lightning Detection Network

The SALDN is owned by the South African Weather Service. The SALDN was established in 2005 and consisted of 19 sensors. In 2010, 3 sensors were added to the network. In 2011, 2 sensors where added and 2 sensors were relocated. Currently the SALDN consists of 24 Vaisala LS7000 sensors which are positioned as seen in figure 3.6 [17]. The sensors have a mean distance of approximately 250 km between the each other, this was found by using the figure as a reference for the location of sensors. The self-evaluated performance of the SALDN is 90 % for the flash DE and 0.5 km for the median location accuracy [22]. The self-evaluated performance is based on median error ellipse calculations of downward flashes.

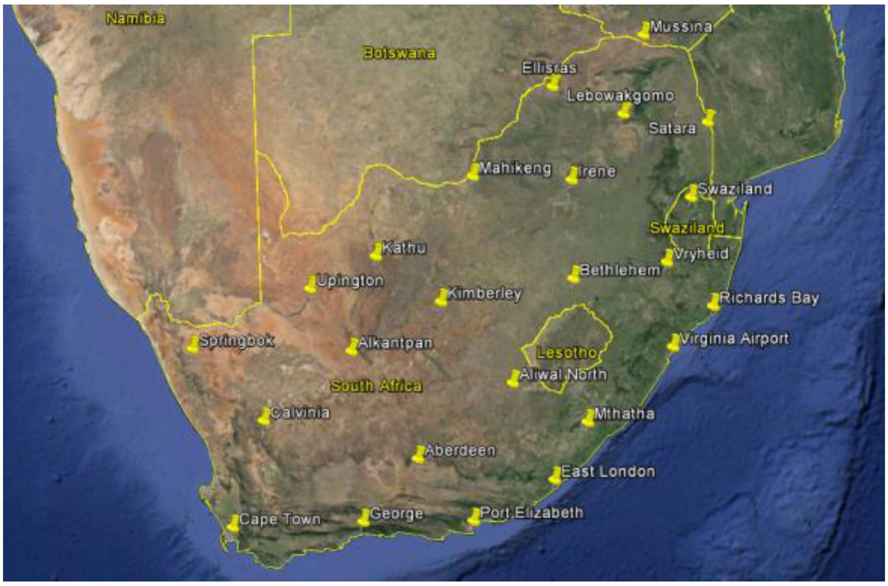

FIGURE 3.6: Location of the 24 Vaisala sensors in South Africa as of 2014 [17]

In 2014, the performance of the SALDN was evaluated using low-speed camera footage of CG flashes terminating on the Sentech Tower [17]. The flash DE and the LA of the SALDN was determined. However, with the use of a low-speed camera, the stroke DE could not be determined as individual strokes could not be observed. Secondly, the only flashes which were captured were those that terminated on the Sentech Tower. Therefore the flash DE and LA were calculated for only one location. Lastly, only lightning events terminating on the Sentech Tower were gathered meaning the results are based on predominately upward flashes. This means that the flash DE, stroke DE and LA performance of the SALDN for all types of CG flashes (downward and upward flashes) over Johannesburg is unknown as mentioned in the problem statement.

3.2.1 SALDN data over Johannesburg

SALDN CG stroke data were obtained for the 24 thunderstorms in the ground truth data. The SALDN data received was for the whole of South Africa. Therefore, the SALDN data were filtered between coordinates as seen in table 3.3. This area can be seen in figure 3.7 where the red icons illustrate the region that the SALDN data were filtered for. This area was chosen as it enclosed the field of view of the cameras and also allowed for errors which might occur in the SALDN reported locations. In this figure, the cameras (blue camera icon) and the Hillbrow and Sentech Tower (black tower icons) can also be seen. The filtering gives stroke data over a more localised area of Gauteng rather than the whole of South Africa.

TABLE 3.3: Coordinates which the SALDN stroke data were filtered by

Latitude	Longitude
-26.0	27.8
-26.5	28.3

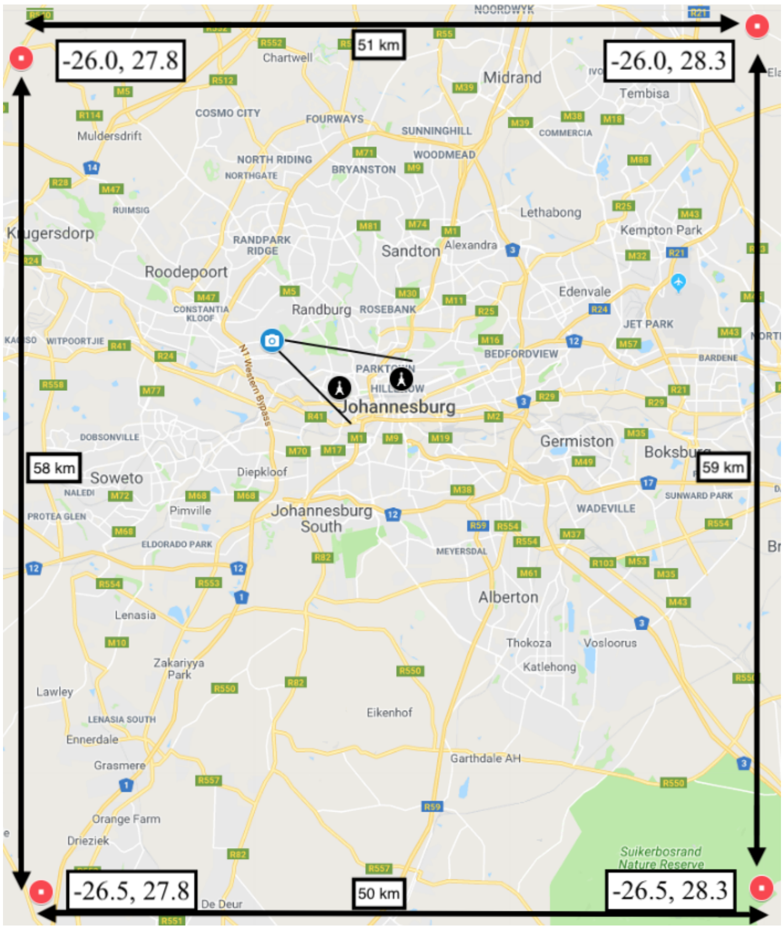

FIGURE 3.7: Map of region which SALDN data is filtered by (2939 km^2), camera location and Hillbrow and Sentech Tower

26 598 strokes were detected by the SALDN in the filtered area for the 24 thunderstorms which the cameras collected data from. Table 3.4 gives an example of the filtered SALDN data. In this case the data were already time-correlated to the video data in table 3.1. The table shows the data which is provided by the SALDN. Each stroke contains the time (Time) at which the event occurred, the latitude

(lat) and longitude (lon) of the lightning event, the peak current (peak_kA), chi square (chi_square) value and number of detected sensors (num_dfrs).

Table 3.4: SALDN data which detected a downward flash

Time	**lat**	**lon**	**peak_kA**	**chi_square**	**num_dfrs**	**Video**
14:58:34:071	-26.1770	27.9882	-21	0.6	12	1
14:58:34:104	-26.1778	27.9873	-24	1.4	3	
14:58:34:121	-26.1770	27.9883	-9	0.3	6	
14:58:34:208	-26.1762	27.9773	-23	0.5	13	
14:58:34:256	-26.1760	27.9772	-16	0.2	8	
14:58:34:292	-26.1762	27.9770	-13	0.4	7	

3.3 Summary

Two high speed cameras were used in a high-speed video investigation in Johannesburg. In the investigation 206 flashes were captured over Johannesburg, South Africa in a year. Of these 206 flashes, 163 were downward flashes and 43 were upward flashes. The South African Lightning Detection Network consists of 24 Vaisala LS7000 sensors and has a self-evaluated performance of 90 % for flash detection efficiency and a median location accuracy of 0.5 km. The South African Lightning Detection Network cloud-to-ground stroke data were obtained for the thunderstorms which the high-speed video investigation captured. This data were filtered between -26.0 and -26.5 latitude and 27.8 and 28.3 longitude in order to reduce the size of the data. The filtered South African Lightning Detection Network stroke data contained 26 598 detected strokes.

The following chapter presents the methodology that is applied in this research.

CHAPTER 4

Performance Evaluation Methodology

> This chapter presents a methodology for time-correlating LLS data and ground truth lightning events, determining the flash detection efficiency and stroke detection efficiency and determining the location accuracy using locations of known attachment and using flash clusters.

This methodology is a general method to finding the Detection Efficiency (DE) and Location Accuracy (LA) of an Lightning Location System (LLS) using ground truth lightning events. The detection efficiency includes the flash and stroke detection efficiency. The location accuracy includes determining the location accuracy using lightning events which attached to known locations as well as by using a flash cluster method.

This methodology requires GPS time stamped Cloud-to-Ground (CG) LLS stroke data and GPS time stamped ground truth lightning event data. Ground truth lightning data can be collected from not only high-speed videos but by instrumented towers or rocket triggered lightning [19]. However, for the flash cluster method used to find the location accuracy, the ground truth data will need to provide evidence that the strokes are within the same channel and therefore have the same Ground Strike Point (GSP). It can be seen from high-speed videos if strokes have the same channel and therefore the same ground strike point.

As discussed in chapter 3 the ground truth lightning data in this research is high-speed videos and the LLS data is stroke data from the SALDN.

4.1 Time-correlation between LLS data and ground truth lightning events

The following methodology is used to time-correlate CG LLS stroke data and ground truth lightning events. The ground truth lightning events is high-speed videos and the LLS data is stroke data from the SALDN as seen in chapter 3. This time-correlation between LLS data and ground truth lightning events forms a *time-correlated dataset* in which the lightning events within the video have either been noted as detected or not detected by the SALDN. As mentioned in chapter 3, section 3.1, the high-speed video investigation is not based on all lightning events over Johannesburg but rather interesting cases which have been captured on the high-speed cameras.

1. Create a dataset of the recorded ground truth lightning events. This will be referred to as the *ground truth dataset*. Include the following in the dataset:
   - The GPS time stamp of the lightning event
   - The type of lightning (leaders, strokes, M-components, ICC pulses, positive or negative current polarity)
   - The number of strike points
   - The duration of the strokes
   - Make note if lightning event attached to a structure of interest
2. Filter the CG LLS stroke data by date, time and area of the thunderstorms in which ground truth lightning events were captured. This data will be referred to as the *filtered LLS dataset*.
3. Time-correlate the *ground truth dataset* and the *filtered LLS dataset*. If the filtered LLS data detected the same lightning event as the ground truth data, indicate this and insert the coordinates of the flash given by the LLS data next to that entry in the *ground truth dataset*. This completed dataset will now be referred to as the *time-correlated dataset*.

4.2 Determining the detection efficiency

The *time-correlated dataset* is used to determine the flash DE and the stroke DE of an LLS. The following two subsections will describe the methodology that is used to obtain the flash DE and stroke DE.

4.2.1 Flash detection efficiency

The following methodology is used to determine the flash DE from the *time-correlated dataset.*

1. Determine the number of ground truth flashes in the *time-correlated dataset.*
2. Determine if any lightning events in a flash were detected by the LLS. If so, indicate that the flash has been detected in the *time-correlated dataset.*
3. Calculate how many flashes were detected by the LLS in the dataset. This is the number of detected LLS flashes in the *time-correlated dataset.*
4. Using equation 4.1 calculate the flash detection efficiency.

$$\mathrm{D}E_{Flash} = \frac{no.\ detected\ LLS\ flashes\ in\ time\ correlated\ dataset}{no.\ ground\ truth\ flashes\ in\ time\ correlated\ dataset}\% \tag{4.1}$$

4.2.2 Stroke detection efficiency

The following methodology is used to determine the stroke DE from the *time-correlated dataset.* Stroke refers to 1^{st} Return Stroke (RS) and Subsequent Return Stroke (SRS) for downward flashes as well as SRS for upward flashes.

1. Determine the number of ground truth strokes in the *time-correlated dataset* for downward and upward flashes.

2. Calculate the total number of strokes which were detected by the LLS data in the *time-correlated dataset*. This is the number of detected LLS strokes in the *time-correlated dataset*.

3. Using equation 4.2 calculate the stroke detection efficiency.

$$\mathrm{D}E_{Stroke} = \frac{no.\ detected\ LLS\ strokes\ in\ time\ correlated\ dataset}{no.\ ground\ truth\ strokes\ in\ time\ correlated\ dataset}\% \qquad (4.2)$$

4.3 Determining the location accuracy

Two approaches are used in this methodology to evaluate the location accuracy. The first method utilizes known locations where strokes have terminated and the second is using the differences in reported locations of SRSs with regards to the 1^{st} RS that occurred in the same channel within a flash (flash cluster).

4.3.1 Locations of known attachment

The LA can be found by using lightning events which have terminated on known locations. Since the location of the structure is known, the location error between the structure and the reported LLS location can be determined. This method requires entries in the *time-correlated dataset* that have terminated on known locations and have been detected by the LLS.

1. From the *time-correlated dataset*, create a subset of data which only includes detected lightning events which terminated on the known locations. This will be referred to as the *known location dataset*.

2. Calculate the location errors in meters between the coordinates of the known location and the coordinates given by the LLS data for the lightning events.

3. Determine the maximum, minimum, median, standard deviation, mode and arithmetic mean of the calculated location errors.

4.3.2 Flash cluster

The flash cluster method is described by Schulz et al [27]. The method determines the LA by using Negative Cloud-to-Ground (nCG) flashes. The high-speed cameras allow one to determine if the 1^{st} RS and SRSs are in the same channel and therefore can be assumed to have the same GSP, meaning they terminate at the same location. Ideally, the LLS should report all the locations of the 1^{st} RS and SRS as the same since they terminate at the same GSP. However, there are differences between these reported locations and the location error can be found between the different locations [27].

The stroke with the highest peak current estimate within a flash can be considered to the most accurately located stroke since it is more likely to be detected by multiple sensors. The more sensors that detect a stroke the better the LA of that stroke [14]. The 1^{st} RS generally has the highest peak current in a flash and therefore can be considered the most accurate location of the flash. The difference in reported locations between the 1^{st} RS and the SRSs in the flash form the dataset of location errors. The statistics of the LA can then be calculated.

Figure 4.1a, gives an example of how the location error is defined. Figure 4.1b, is the same flash represented in figure 3.4. The flash consisted of 5 strokes. The red number 1 illustrates the 1^{st} RS and the blue number 2 represents the first SRS as seen in figure 3.4. This is seen as the flash cluster. The high-speed camera was used to determine if all the SRS strokes were in the same channel.

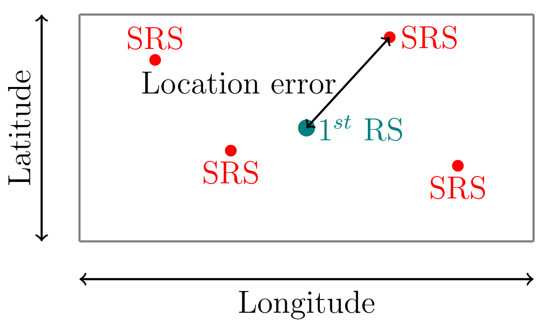

(a) The location error within a flash cluster

(b) Captured and detected flash cluster

FIGURE 4.1: The location error within a flash cluster and an example of a flash cluster captured in this research

Figure 4.2, shows the flow diagram used to determine the LA using the flash cluster approach. The method requires the *time-correlated dataset* and requires flashes within that dataset to have the 1^{st} RS detected as well as a minimum of one SRS detected. If this is satisfied, the geographical location of the flash should be that of the 1^{st} RS. Then the location errors between the flash location and the SRSs need to be calculated for all the flashes. Once all the flashes that meet the criteria have been processed, the LA can be calculated from the location errors.

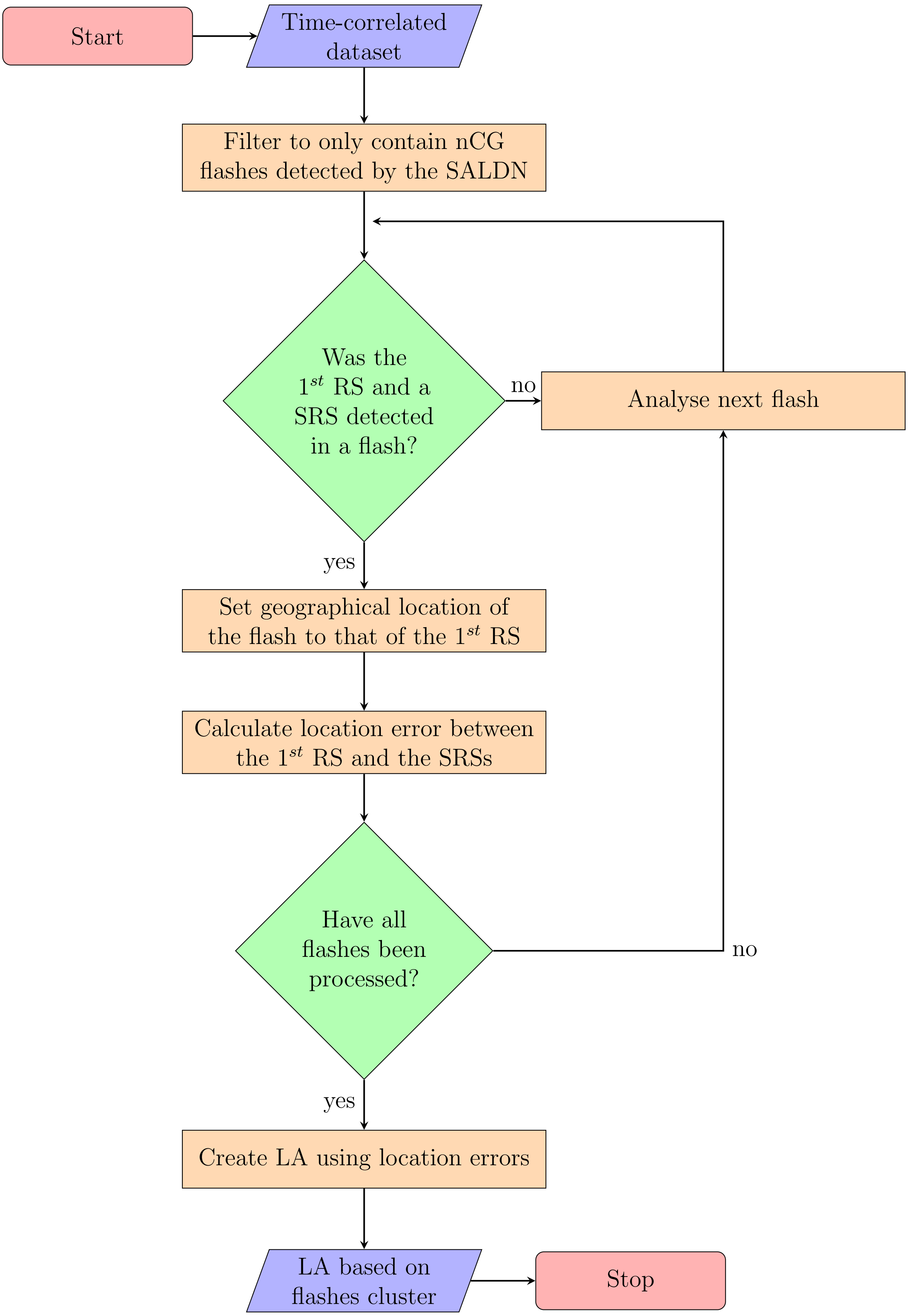

FIGURE 4.2: Flow diagram explaining how the LA is found by using the location errors in a flash cluster

4.4 Summary

The methodology can be used to determine the flash detection efficiency, stroke detection efficiency and location accuracy with the use of GPS time-stamped cloud-to-ground LLS data and ground truth lightning events. The flash detection efficiency is the percentage of the amount of flashes detected by the LLS over the amount of ground truth flashes. Stroke detection efficiency is similar however it is the percentage to the number of strokes. Location accuracy can be determined if ground truth data has captured lightning events terminating on known locations which were also detected by the LLS. This allows the location error between the actual location of the structure and the reported location of the LLS to be calculated. Location accuracy can also be found using the location errors between subsequent return strokes and the 1^{st} return stroke within a flash provided they were detected and had the same ground strike point.

The following chapter presents the results of the research which answers the research question.

CHAPTER 5

Results

> This chapter presents the results obtained by using the processed data in *chapter 3* and the methodology in *chapter 4*. The results include the time-correlated data, detection efficiency and location accuracy.

The results in this chapter were found by applying the methodology in chapter 4 to the data discussed in chapter 3. These results are the performance evaluation of the South African Lightning Detection Network (SALDN) which include the flash Detection Efficiency (DE), stroke detection efficiency and Location Accuracy (LA). The results can be compared to the self-evaluation index of the SALDN as well as other performance evaluations of Lightning Location Systems (LLS). This will provide a reference as to how well the system performs. This data can also be used in future research to compare with a performance evaluation of an upgraded SALDN. Additionally, with Ground Strike Point (GSP) maps being considered for use in the future, it is beneficial knowing the stroke detection efficiency of an LLS.

5.1 Time-correlated data

The *time-correlated data* can be seen in table 5.1. This data allows the DE to be calculated. The high-speed camera events column refers to the ground truth data that was recorded and analysed. The SALDN events column refers to the SALDN stroke data that was time-correlated with the ground truth data. As seen in the table, 175 flashes were detected by the SALDN out of 206 filmed flashes, 457 strokes were detected by the SALDN out of 667 filmed strokes.

Table 5.1: Time-correlated data of the high-speed video camera data and the SALDN data

Lightning events	**High-speed camera events**	**SALDN events**
Flashes	206	175
Strokes	667	457
Downward flashes	163	151
Strokes	604	417
M-components	101	12
Upward flashes	43	24
Upward leaders	55	0
ICC pulses	387	57
Subsequent return strokes	63	40
M-components	10	3

5.2 Detection efficiency

The following section presents the results for the flash DE and stroke DE. The flash DE and stroke DE for downward and upward flashes will also be discussed separately. As mentioned earlier, the network has a greater chance of detecting a flash compared to a stroke because a single detected stroke, within a flash, will constitute a detected flash [16].

5.2.1 Flash detection efficiency

The SALDN detected 175 flashes of the 206 flashes that were filmed using the high-speed camera as seen in table 5.1. These numbers include downward and upward flashes. Table 5.2 shows the flash DE of the SALDN to be 84.9 %. This is also shown as a bar graph in figure 5.1. The first bar represents downward flashes and the second bar represents upward flashes. The green is the amount of flashes detected by the SALDN and the blue is the amount of flashes captured by the high-speed cameras. The flash DE of downward and upward flashes will be discussed separately below.

Table 5.2: Overall flash detection efficiency of the SALDN

Flash information	**Quantity**
High-speed video flash count	206
SALDN flash count	175
Overall flash DE	84.9 %

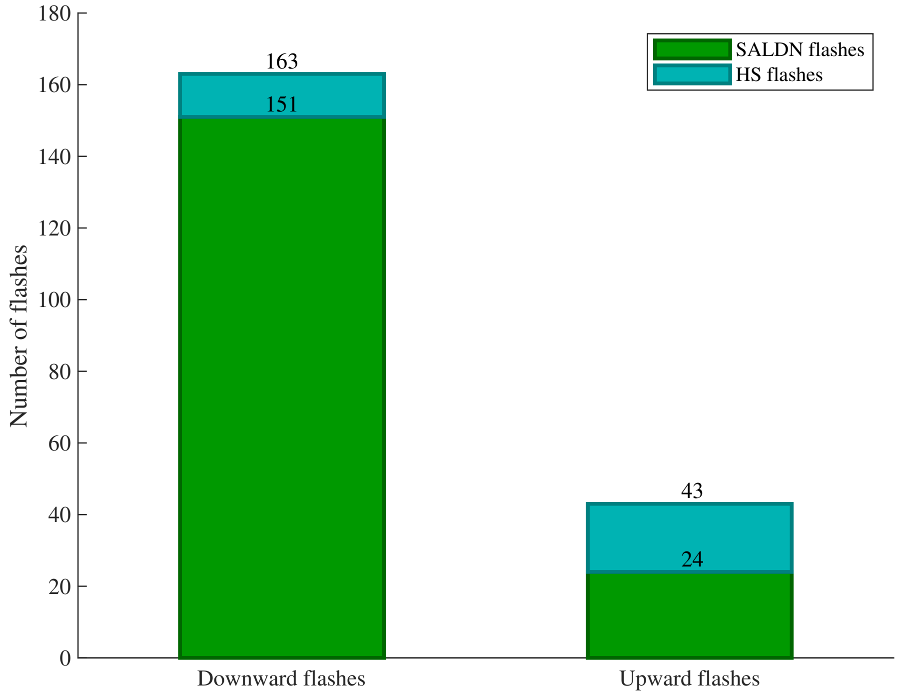

Figure 5.1: Bar graph illustrating the number of downward and upward flashes captured on the high-speed cameras and detected by the SALDN

5.2.1.1 Downward flashes

The downward flash DE can be seen in table 5.3. The SALDN detected 151 downward flashes from the 163 that were filmed with the high-speed camera. This means the SALDN detects 92.6 % of downward flashes.

Table 5.3: Downward flash detection efficiency of the SALDN

Flash information	**Quantity**
High-speed video downward flash count	163
SALDN downward flash count	151
Downward flash DE	92.6 %

5.2.1.2 Upward flashes

Table 5.4 below shows the upward flash DE is 55.8 %. Upward flashes can be categorised into upward flashes with Subsequent Return Strokes (SRSs) and upward flashes without SRSs. It is seen that upward flashes with SRSs were detected 93.7 % of the time whereas upward flashes without SRS were detected 33.3 % of the time.

Table 5.4: Upward flash detection efficiency of the SALDN

Flash information	**HS**	**LLS**	**Percentage**
Upward flash DE	43	24	55.8 %
Upward flash DE (SRS)	16	15	93.7 %
Upward flash DE (no SRS)	27	9	33.3 %

5.2.2 Stroke detection efficiency

A total of 667 strokes were filmed by the high-speed cameras, of this, 457 strokes were detected by the SALDN. The SALDN has a stroke DE of 68.5 % as seen in table 5.5. This can also be seen in figure 5.2. The first bar represents downward strokes (1^{st} return strokes and subsequent return strokes) and the second bar represents strokes in upward initiated flashes (subsequent return strokes). The red aspect of the bars represent the number of strokes detected by the SALDN and the grey represents the number of strokes captured on the high-speed cameras.

Table 5.5: Overall stroke detection efficiency of the SALDN

Stroke information	**Quantity**
Video stroke count	667
SALDN stroke count	457
Overall Stroke DE	68.5 %

Table 5.6 below shows the stroke DE for downward and upward strokes. Within the downward flashes, strokes (1^{st} return strokes and subsequent return strokes) are of interest. It can be seen that the DE for a downward stroke is 69.0 %. Upward strokes refer to the SRSs which can occur in an upward flash. It can be seen in table 5.6 that the upward stroke DE is 63.4 %.

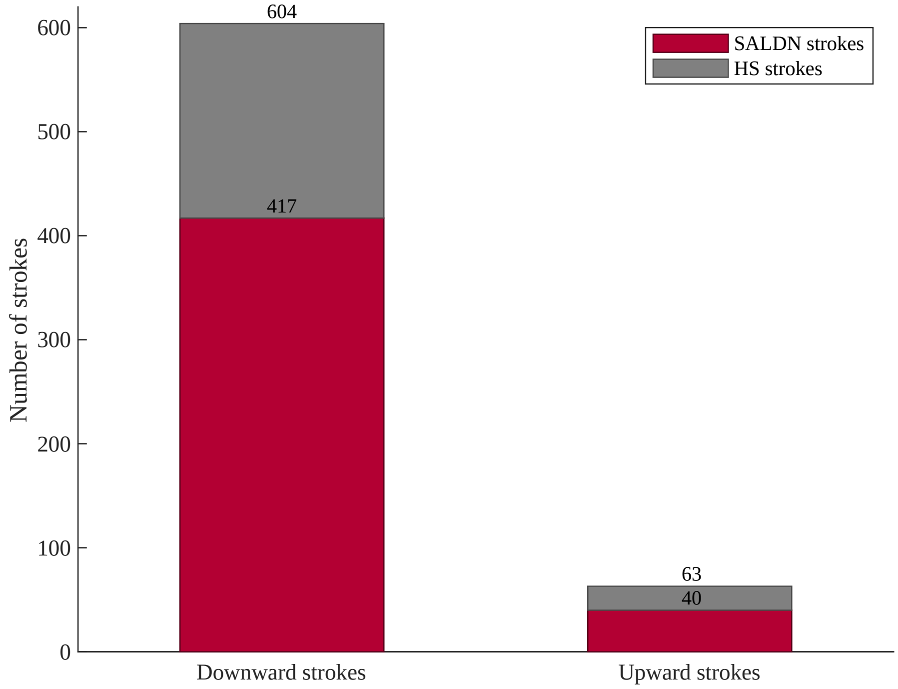

FIGURE 5.2: Bar graph illustrating the number of downward and upward strokes captured on the high-speed cameras and detected by the SALDN

TABLE 5.6: Downward and upward stroke detection efficiency of the SALDN

Flash information	**HS**	**LLS**	**Percentage**
Downward stroke DE	604	417	69.0 %
Upward stroke DE	63	40	63.4 %

5.3 Location accuracy

Two methods have been used to determine the LA of the SALDN. The first is the use of locations of known attachment and the second is the flash cluster method.

5.3.1 Locations of known attachment

This method required known locations where lightning had terminated as discussed in chapter 4. In this research the locations of known attachment were the Sentech and Hillbrow Tower shown in chapter 3. These two locations provided the true coordinates of the attachment of the lightning event which could be compared to the locations reported by the SALDN. Figure 5.3 shows the locations of the cameras and the Sentech and Hillbrow Tower with the y-axis indicating the latitude and the x-axis indicating the longitude. The reported locations of the lightning events which terminated on the towers have also been plotted. This figure can be compared to figure 3.1 in chapter 3.

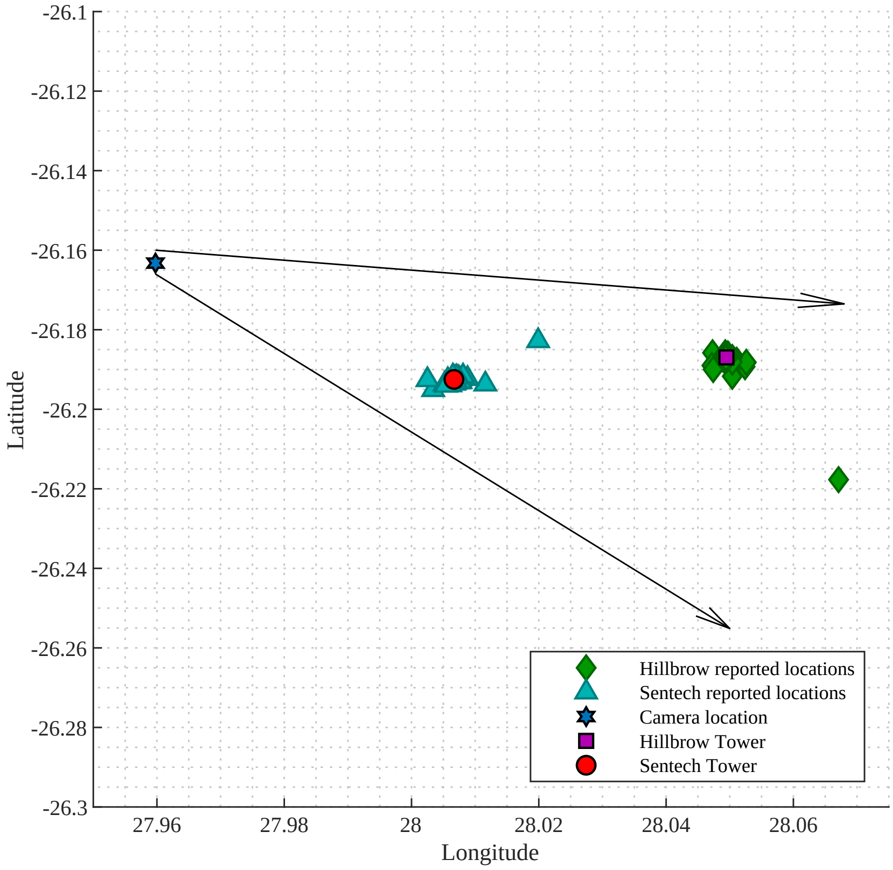

FIGURE 5.3: Camera location and field of view with respect to the reported locations for the Hillbrow and Sentech Tower

Table 5.7 below gives the overall location accuracy for both towers and the location accuracy for each tower separately. As seen in the table, a total of 98 detected strokes and ICC pulses terminated on the towers. With these 98 events the SALDN has a median LA of 59.2 m.

TABLE 5.7: Location accuracy of the tower events

Tower	**N**	**Max**	**Min**	**Median**	σ	**Mode**	**Mean**
Both towers	98	3847.3 m	4.9 m	**59.2 m**	423.0 m	4.9 m	152.2 m
Sentech Tower	45	1707.1 m	11.8 m	74.7 m	259.3 m	53.9 m	139.8 m
Hillbrow Tower	53	3847.3 m	4.9 m	51.0 m	522.9 m	4.9 m	162.8 m

5.3.1.1 Sentech Tower

45 detected strokes and ICC pulses terminated on the Sentech Tower. Figure 5.4 shows the reported locations of the events around the tower with the y-axis and x-axis as a distance in metres. The reported SALDN locations are grouped within 450 m of the tower. This figure excludes the one large location error seen in figure 5.3. Table 5.8 shows that the SALDN has a median location accuracy of 74.7 m at the Sentech Tower.

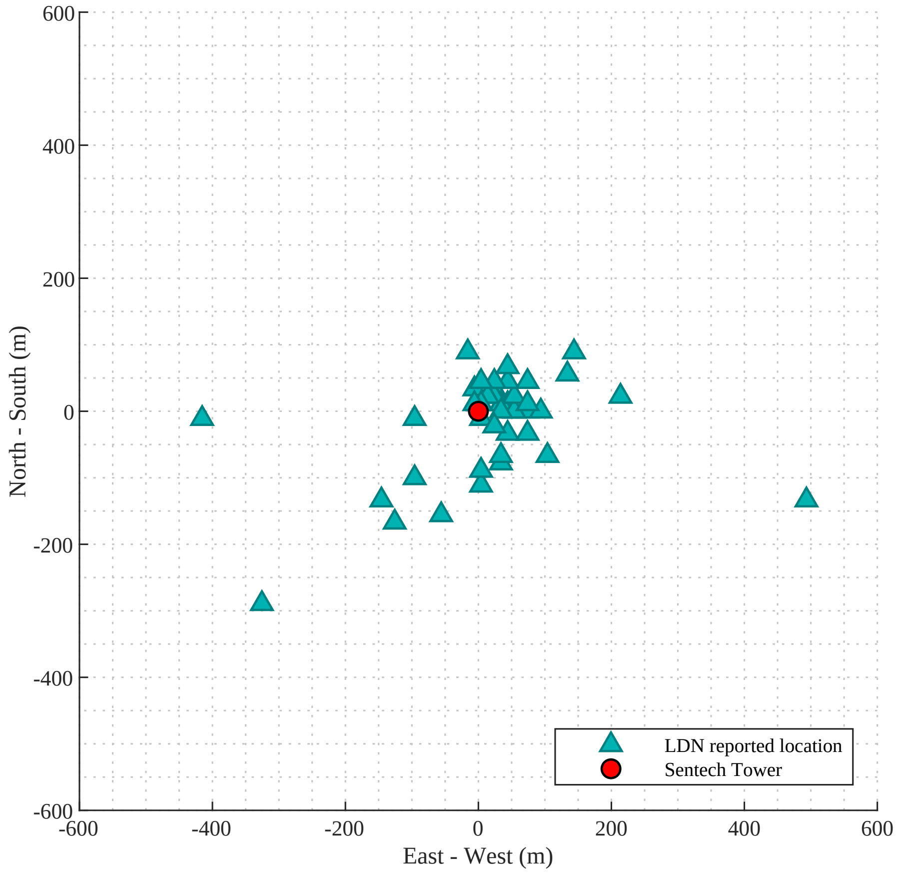

FIGURE 5.4: Reported locations of lightning events, excluding one large location error, which occurred on the Sentech Tower

TABLE 5.8: Location accuracy of Sentech Tower events

Statistical parameters	**Value**
Count (N)	45
Median location error	74.7 m
Mean location error	139.8 m
10 %	32.7 m
90 %	212.6 m

5.3.1.2 Hillbrow Tower

53 detected strokes and ICC pulses terminated on the Sentech Tower. Figure 5.5 illustrates the distance in metres between the reported locations and the Hillbrow Tower. The x and y-axis are a distance in metres and the reported SALDN locations are grouped within 550 m of the tower. As with the Sentech Tower this figure excludes one large location error which is seen in figure 5.3. Table 5.9 shows that the SALDN has a median location accuracy of 51.0 m at the Hillbrow Tower.

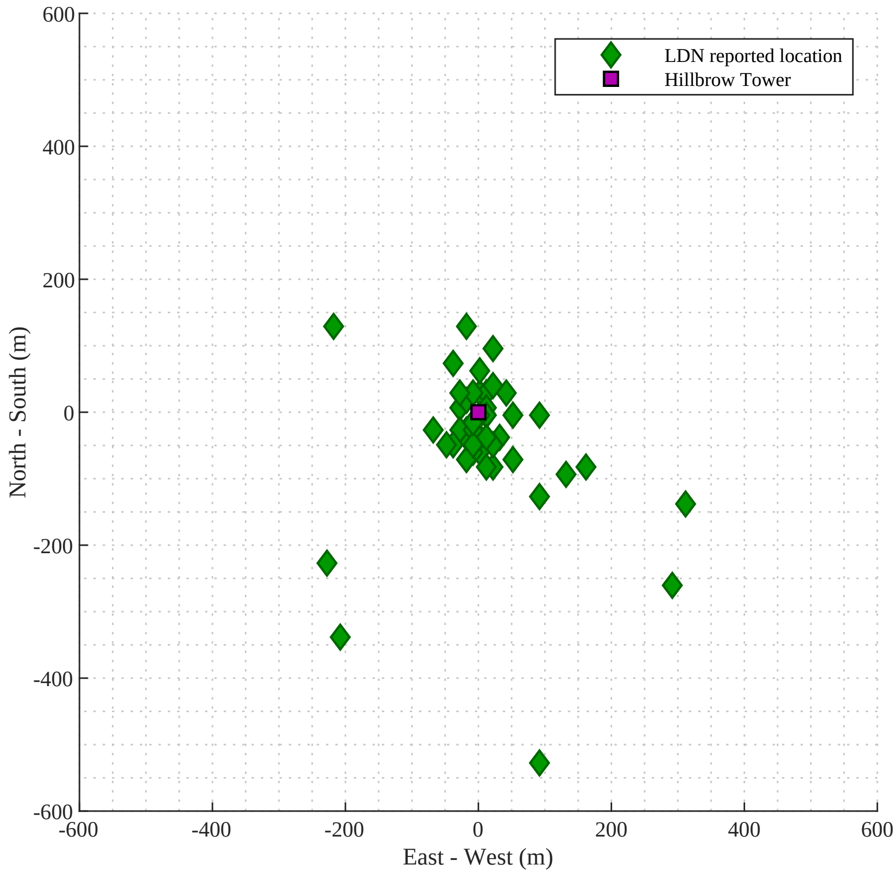

FIGURE 5.5: Reported locations of lightning events, excluding one large location error, which occurred on the Hillbrow Tower

TABLE 5.9: Location accuracy of Hillbrow Tower events

Statistical parameters	**Value**
Count (N)	53
Median location error	51.0 m
Mean location error	162.8 m
10 %	14.5 m
90 %	307.9 m

5.3.2 Flash cluster

Using the flash cluster method discussed in chapter 4, figure 5.6 shows the location accuracy distribution. The y-axis represents the number of SRSs and the x-axis represents the distance the SRSs are from the 1^{st} return stroke. From the graph it can be seen that approximately 105 SRS are within 100 m of the 1^{st} return stroke. This graph accounts for 241 SRSs out of a total of 245 SRSs. Therefore, 4 SRSs were greater than a distance of 2 km from the 1^{st} return stroke.

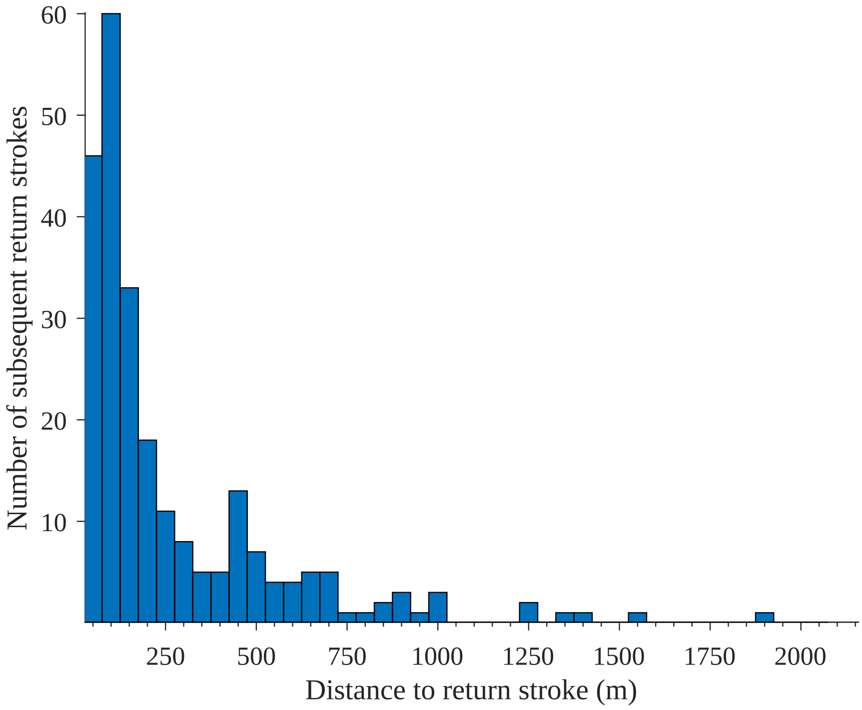

FIGURE 5.6: Location accuracy distribution from flash cluster

Table 5.10 shows the results of the flash cluster method. The table shows a median location accuracy of 124.4 m.

TABLE 5.10: Location accuracy from flash cluster method

N	**Max**	**Min**	**Median**	σ	**Mode**	**Mean**
318	25711.3 m	0.0 m	**124.4 m**	1675.5 m	22.3 m	38.5 m

5.4 Summary

The overall flash detection efficiency which includes downward and upward flashes is 85 %. The downward and upward flash detection efficiency is 93 % and 56 % respectively. 33 % of upward flashes without subsequent return strokes were detected by the SALDN and 94 % of upward flashes with subsequent return strokes were detected by the SALDN.

The overall stroke detection efficiency is 69 %. The stroke detection efficiency of downward (1^{st} return strokes and subsequent return strokes) and upward strokes (subsequent return strokes) is 69 % and 63 % respectively.

Two methods were used to determine the location accuracy. Using locations of known attachment, the location accuracy is 59 m from 98 detected strokes and ICC pulses that terminated on the Sentech and Hillbrow Tower. Using a flash cluster method, the median location accuracy is 124 m from 318 strokes that were recorded.

The following chapter is a discussion of the results from this chapter as well as interesting cases which were found throughout the research.

CHAPTER 6

Discussion

> This chapter discusses the results obtained in *chapter 5* this includes: the outliers found in the location accuracy data, a comparison between the location accuracy of the locations of known attachment method and the flash cluster method and a comparison between the results of the SALDN and the studies presented in chapter 2. Interesting cases found throughout the research are also discussed.

The results in chapter 5 allow for further discussion. The performance evaluation of the South African Lightning Detection Network (SALDN) can be analysed more in depth and can be compared to the performance evaluations of other LLS such as those in chapter 2. The performance evaluation can also be compared to the self-performance evaluation of the SALDN. Additionally, from the data collected in this research the Detection Efficiency (DE) and the reported peak current for the first 10 strokes in a downward negative flash can be determined. The large location errors found in the known location of attachment results, for the Location Accuracy (LA), can also be analysed to find out why these outliers occurred.

There are a number of interesting cases which appeared these include: nearby-lightning-triggered upward flashes, the detection of M-components and Initial Continuing Current (ICC) pulses by the SALDN and dual stroke entries which entails strokes that have the exact same time stamp and similar geographical location. It must be noted that these interesting cases do not have a direct effect on the performance evaluation.

6.1 Detection efficiency

The flash and stroke detection efficiency of the SALDN were found to be 84.9 % and 68.5 % respectively. The following subsections will discuss the results of the flash detection efficiency, stroke detection efficiency and the detection efficiency of different strokes in a flash.

6.1.1 Flash detection efficiency

As shown in table 5.2, the overall flash DE, including downward and upward flashes is 84.9 %. Evaluating the DE of the flashes separately, the downward and upward flash DE were found to be 92.6 % and 55.8 % respectively in tables 5.3 and 5.4. The greater DE of a downward flash is expected. 1^{st} Return Strokes (RS) and Subsequent Return Strokes (SRS) have fast rise times, which aid in the detection of a flash. Upward flashes are not expected to be detected by the SALDN due to the slow rise time of the upward leader, as can be seen in table 5.1 where no upward leaders were detected by the SALDN. An upward flash is detected due to a strong Initial Continuous Current (ICC) pulse that is superimposed on the upward leader or the detection of a SRS after the upward leader.

An evaluation of the SALDNs DE of downward flashes against that of upward flashes which contained SRSs can be performed. The SALDN detected 93.7 % of upward flashes which contained SRSs as seen in table 5.4. This value is very similar to that of downward flashes which are detected 92.6 % of the time. However, the SALDN only detected 33.3 % of upward flashes which did not contain SRSs. Therefore, SRSs increase the chances of an upward flash being detected by about 60 %.

6.1.2 Stroke detection efficiency

The overall stroke DE of the SALDN is 68.5 % as seen in table 5.5. This, as expected, is less than the flash DE since only one stroke needs to be detected to constitute the detection of a flash [16]. The SALDN DE of downward strokes and upward strokes is 69.0 % and 63.4 % respectively as seen in table 5.6. These values are similar. This is expected since a SRS during an upward flash is similar to that of a SRS during a downward flash. This means that if an upward flash contains a SRS, it should have a very similar chance of being detected. This is in agreement with the results obtained where the flash DE of upward flashes containing SRSs is very similar to that of downward flashes.

Figure 6.1 shows the average detection efficiency of the strokes in negative cloud-to-ground flashes. The x-axis is the strokes in a flash and the y-axis is the detection efficiency. The 1^{st} RS is seen to have the highest DE of 80.7 % which is expected since this stroke should have the highest peak current within a flash. The DE decreases as the number of the SRS increases. The number of strokes detected for each stroke category on the x-axis is shown at the bottom of each bar. For instance there was 165 detected 1^{st} RSs. The 1^{st} RSs had a detection efficiency of 80.7 %.

6.2 Location accuracy

The median LA of the SALDN using the location of known attachment and flash cluster method is 59.2 m and 124.4 m respectively as seen in tables 5.7 and 5.10. There are two outliers in the location of known attachment results, these will be discussed. Evidence why the 1^{st} return stroke can be considered as the most accurate location of a flash and a comparison of the two methods for determining the location accuracy is discussed.

6.2.1 Outliers in tall tower result

As seen in chapter 5, figure 5.3, the locations of known attachment were the Hillbrow and Sentech Tower. It must be noted that the majority of flashes which terminated on these towers were upward flashes. Therefore, the data for this

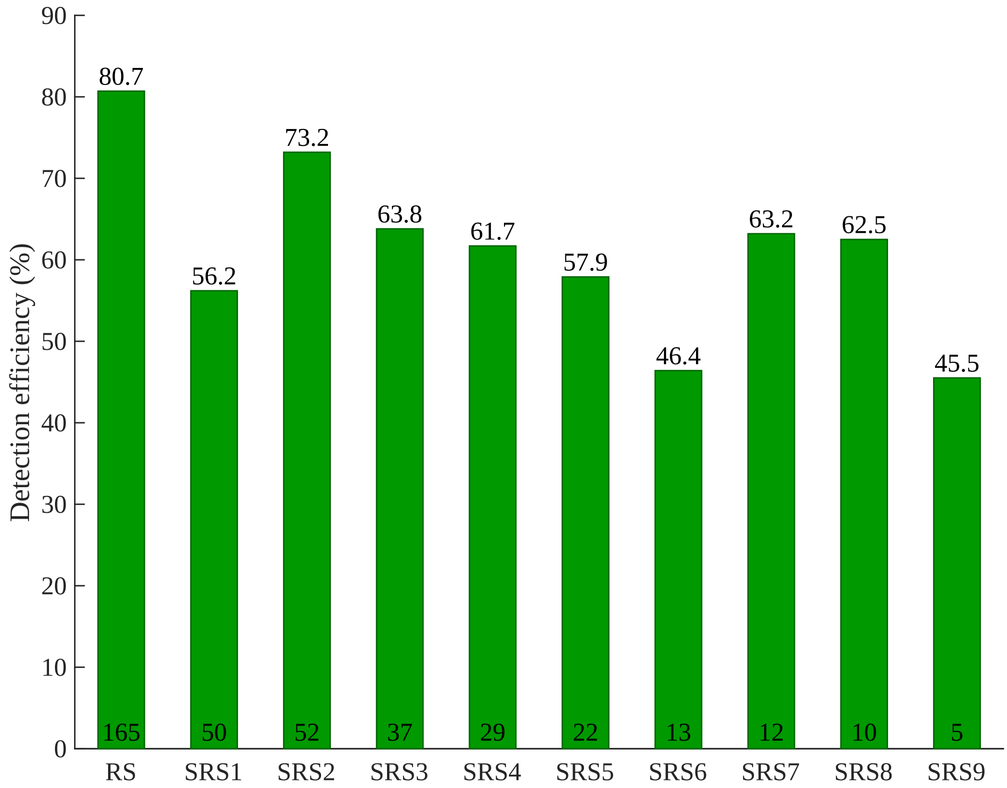

FIGURE 6.1: Bar graph illustrating the detection efficiency of the strokes within negative cloud-to-ground flashes. The number within the bar represents the amount, of that specific stroke, detected by the SALDN

method consists of detected ICC pulses and mostly SRS. There was a small amount of 1^{st} return strokes which occurred on the towers. It was seen that there were outliers for both towers. These outliers were time-correlated with the events that were filmed attaching to the towers. However, the SALDN reported location had large location errors. The subsections below will discuss these outliers and explain why they occurred.

6.2.1.1 Sentech Tower outlier

The Sentech Tower outlier seen in figure 5.3 can be examined using figure 6.2. At the time in which the SALDN detected a lightning event, there was an IC flash which appeared as seen in figure 6.2. Within the same millisecond of this IC flash there was an ICC pulse. Therefore according to the way the data were time-correlated, this ICC pulse was considered as detected. However, it was the nearby IC that was detected. At no point did the IC connect with the upward leader channel causing an ICC pulse. This IC was situated over the Hillbrow Tower. This is in agreement with the location of the outlier in figure 5.3 where the outlier is almost in line with the Hillbrow Tower looking from the perspective of the camera. The SALDN estimated the peak current of the IC flash to be -5 kA. This is relatively small and coincides with being an IC event [18]. Therefore, in this instance, it seems that the SALDN misclassified an IC event as a CG stroke.

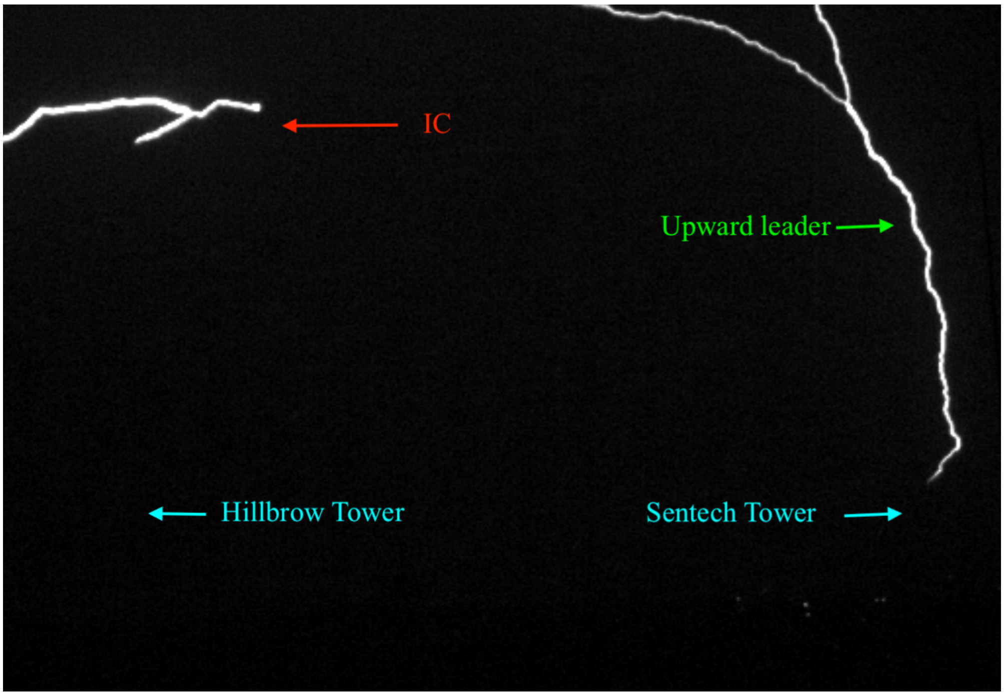

FIGURE 6.2: Image explaining the outlier in the Sentech Tower data

6.2.1.2 Hillbrow Tower outlier

The outlier which is seen in figure 5.3 can be explained by using the images seen in figure 6.3. The upward flash in question was of a negative polarity, in other words a positive upward leader. In the first image of figure 6.3 an attempted ICC pulse can be seen occurring on the Hillbrow Tower. In the second image, a positive SRS makes attachment with the negative attempted ICC pulse in mid-air. The SALDN detected this attachment giving the geographical location of the outlier seen in figure 5.3 with a peak current of +41 kA. Figure 5.3 shows that the reported location of the outlier is to the right of the tower from the cameras perspective. This agrees with where the attachment took place in the second image in figure 6.3.

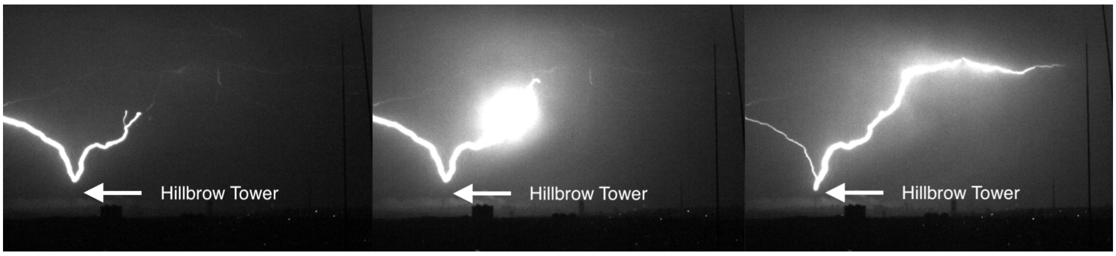

FIGURE 6.3: Sequence of images explaining the Hillbrow Tower outlier

Additionally, the chi-square value for this SALDN entry was reported to be 1.7. This is relatively high. Figure 3.4 in chapter 3 gives an indication of the chi-square values of strokes. The chi-square value is one of the parameters used to describe the quality of the geographical location reported by a LLS [2]. This high chi-square value indicates a greater level of uncertainty to the geographical location reported for this outlier. These figures and chi-square values explain the outlier event which occurred 3.8 km from the tower.

6.2.2 Flash cluster

The flash cluster method collects the location errors between the 1^{st} RS and the SRSs of the same flash. The location errors are calculated from the SALDN reported locations. It was discussed in the methodology section 4.3.2 that the 1^{st} RS in a flash generally has the highest peak current compared to the SRSs. This makes it in most cases, the most accurately located stroke in a flash. Figure 6.4 below shows the average reported peak current for 10 strokes in a nCG flash from the SALDN data in this research. The x-axis is the strokes in the flashes and the y-axis is the average reported peak current. The number of strokes detected for each stroke category on the x-axis is shown at the bottom of each bar. It can be seen that the 1^{st} RS has, on average, the highest peak current values. This confirms the use of the 1^{st} RS as the location of the flash in this method.

This figure also follows a similar trend to the one seen in figure 6.1 where the DE of the strokes in a flash are illustrated. Figure 6.4 agrees with figure 6.1 since

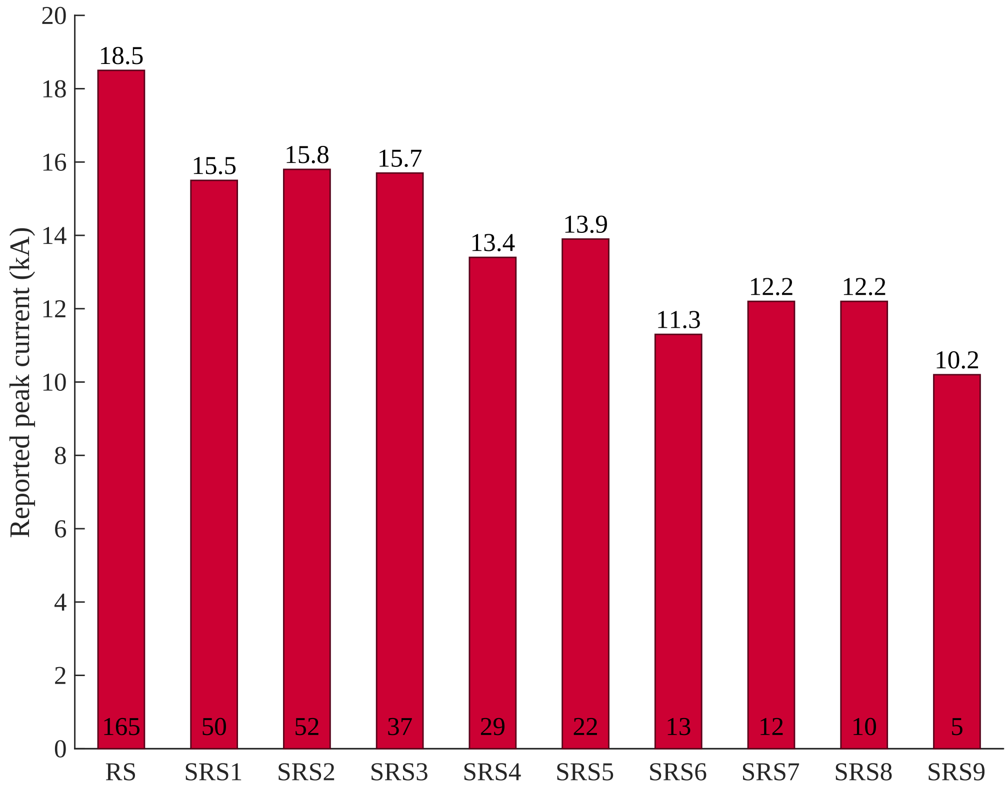

FIGURE 6.4: Bar graph illustrating the average peak current reported for the strokes within negative cloud-to-ground flashes. The number within the bar represents the amount, of that specific stroke, detected by the SALDN

the 1^{st} return stroke has the highest reported peak current and is also the stroke detected most often. The shape of the graphs are also similar confirming the relationship between the peak current of a stroke and the detection efficiency.

6.2.3 Comparison of location accuracy methods

The two location accuracy methods can be compared. Table 6.1 below compares the results of the locations of known attachment method versus the flash cluster method. It can be seen that the flash cluster method has a median location accuracy which is 65.2 m greater than that of the known location terminations. However, as described in reference [27] the flash cluster method provides the upper bounds of the location accuracy due to the fact that the ground strike points within a flash cluster may vary slightly.

TABLE 6.1: Comparison of location accuracy methods

Method	N	Max	Min	Median	σ	Mode	Mean
Both towers	98	3847.3 m	4.9 m	**59.2 m**	423.0 m	4.9 m	152.2 m
Flush cluster	318	25711.3 m	0.0 m	**124.4 m**	1675.5 m	22.3 m	38.5 m

Based on these results the flash cluster method is a suitable method for finding the LA of a LLS. This method can be used if there are no locations of known attachment. It is also easier to gather data for the flash cluster method because all that is needed is high-speed videos of flashes as opposed to high-speed videos of flash terminating on specific locations.

6.3 SALDN performance evaluation comparison

This section compares the performance evaluation of the SALDN to the performance evaluations of the studies presented in chapter 2. Table 6.2, shows the results for the studies compared to the SALDN. The SALDN (Overall) row refers to the overall DE (upward and downward flashes) of the SALDN. The overall LA value in this row is from the location of known attachments method. The SALDN (Downward flashes only) row refers to the DE of the SALDN for downward flashes. The LA value in this row is from the flash cluster method.

TABLE 6.2: Comparison of SALDN performance evaluation to other studies

LLS	Flash DE	Stroke DE	Median LA
EUCLID [19]	98 %	84 %	89 m
GHMLLS [3]	95 %	90 %	410 m
RINDAT [20]	87 %	55 %	3400 m
NLDN [21]	94 %	75 %	309 m
SALDN (Overall)	85 %	69 %	59 m
SALDN (Downward flashes only)	93 %	69 %	124 m

The DE of downward flashes for the SALDN is more in-line with the flash DE of the studies. The LA values obtained from the locations of known attachment and the flash cluster method show how well the SALDN locates lightning events. The results show that the ground-flash density map accuracy in South Africa is similar to those seen in other countries. This result also gives information on how accurate the ground strike point density maps would be with the SALDN data.

The results of the SALDN performance evaluation can be compared to the performance evaluation completed in 2014 [17]. In 2014, the overall flash DE was found to be 76 % in the last season, this value has now increased to an overall flash DE of 85 %. However, the study in 2014 would have been an underestimate of the overall flash DE of the SALDN. The majority of flashes analysed were upward flashes because the ground truth data were collected from lightning events terminating on the Sentech Tower. As discussed previously, it is not expected that an LLS will detect upward flashes without any SRS because of the slow rise time of the upward leader. The median location accuracy in 2014 was found to be 280 m based on data over the past 4 years. This has now reduced to 59 m. This shows the improvement of the SALDN over the last 5 years.

The SALDN flash DE and LA can also be compared to the self-performance evaluation presented in chapter 3. The self-evaluated flash detection efficiency of the SALDN is 90 %, this compared to the current flash detection efficiency of 84.9 % shows a 5 % difference. However, it is not expected that the SALDN will detect upward flashes as discussed previously, it is also mentioned in chapter 3 section 3.2 that the self-evaluated performance of the SALDN is based on downward flashes. Therefore if the flash detection efficiency of downward flashes is used, which is 92.6 %, this would indicate that the SALDN is exceeding the self-performance flash detection efficiency. The self-performance median location accuracy of the SALDN is 500 m. The median location accuracy of 59 m is well within 500 m. This result indicates that the SALDN performance is exceeding the expected location accuracy.

6.4 Interesting cases

A number of interesting cases were observed. There were upward triggering events seen on the camera and detected by the SALDN which showed nearby-lightning-triggered upward flashes, a certain percentage of M-components and ICC pulses were detected as strokes by the SALDN and there were a number dual strokes SALDN entries.

6.4.1 Upward triggering event

As discussed in chapter 2 section 2.1.2, there are two types of upward flashes: nearby-lightning-triggered upward flash and self-initiated upward flash [11]. This section will discuss the amount of CG nearby-lightning-triggered flashes that was seen on camera and/or detected by the SALDN.

Of the 43 upward flashes seen in the high-speed camera footage, 14 had a nearby CG triggering event. Of the 14 triggering events, 6 were seen on the high-speed camera and were detected by the SALDN. The remaining 8 triggering events were out of the field of view of the camera but were detected by the SALDN as a positive CG flashes. Although these detected triggering events were out of view, the upward leader being initiated from the Hillbrow and Sentech Tower was still seen on the high-speed camera.

Table 6.3 below shows the triggering events detected by the SALDN that were out of view of the high-speed camera. “Tower of flash” refers to the tower from which the upward leader was initiated. The distance between the trigger event and the Sentech and Hillbrow Tower is included in the table and the “Timing of trigger” refers to when the trigger occurred in relation to when the upward leader was seen on the high-speed camera. “Estimated current” is the current value of the triggering event, measured by the SALDN.

TABLE 6.3: Upward flash triggering events detected by the SALDN and out of view from the cameras

Count	Tower of flash	Distance to Sentech Tower	Distance to Hillbrow Tower	Timing of trigger	Estimated current
1	Sentech	**14.1 km**	-	60 ms before	21 kA
2	Both	**5.8 km**	**6.2 km**	1 ms during	50 kA
3	Hillbrow	-	**14.5 km**	253 ms during	31 kA
4	Sentech	**14.6 km**	-	12 ms before	64 kA
5	Sentech	**33.7 km**	-	629 ms before	11 kA
6	Both	**14.0 km**	**18.2 km**	7 ms before	106 kA
7	Sentech	**22.0 km**	-	60 ms before	54 kA
8	Hillbrow	-	**21.2 km**	42 ms before	28 kA

Figure 6.5 below is a scatter plot containing all 14 nearby-lightning-triggered upward flashes. Of the 14 upward flashes, 4 of them had upward leaders on both of the towers. The figure illustrates the distance the trigger event was to the towers versus the timing of the trigger events (when the upward leader was initiated).

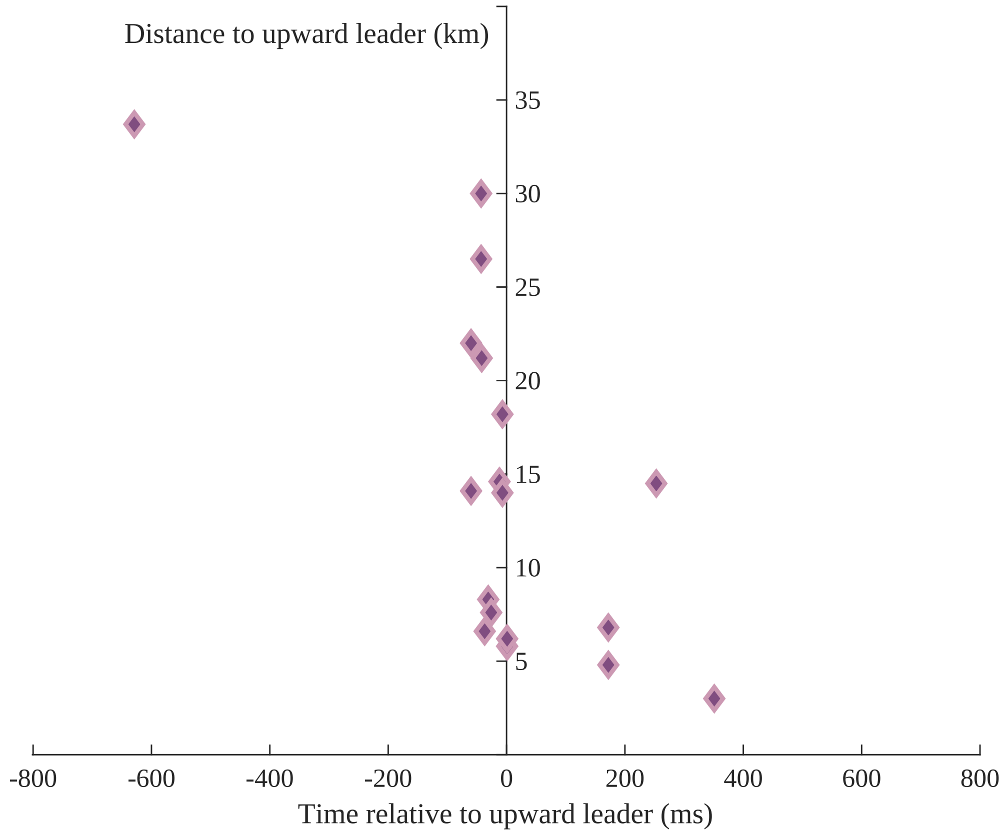

FIGURE 6.5: Scatter plot illustrating the triggering events with respect to the distance from the tower and the time to initiate the upward leader

If the triggering events in figure 6.5 are to the left of the y-axis, the triggering events occurred before the upward leader was initiated. If the triggering events are to the right of the y-axis, the triggering event occurred during the upward flash. The y-axis illustrates how far the triggering event was from a tower.

In figure 6.5, 14 of the 18 triggering events are to the left of the y-axis while the remaining 4 are to the right of the y-axis. Therefore, according to the data in the figure, 77.8 % of nearby-lightning-triggered upward flashes are initiated from downward flashes which occur before the initiation of the upward leader.

It is important to note that the remaining 29 upward flashes are not necessarily self-initiated. Of the 29 upward flashes, some might have been triggered by IC lightning. Additionally, the SALDN might not have detected some of the triggering events outside of the field of view and the triggering events might have been on the outside of the coordinates to which the SALDN was filtered by. Therefore, this data is only to show an estimate of the number of CG nearby-lightning-triggered upward flashes in this dataset.

As discussed in chapter 2 section 2.3, the detection of a CG triggering event in an upward flash is not strictly a detection of an upward flash. Therefore, in this research, a detected CG triggering event was classified as a downward flash.

6.4.2 Detected M-components and ICC pulses

In the *time-correlated dataset* it was observed that the SALDN stroke data detected M-components and ICC pulses. M-components and ICC pulses are not considered strokes since they are transient effects which occur during the CC or ICC phase.

The total number of M-components (for downward and upward flashes) and ICC pulses the SALDN detected is 15 and 57 respectively as seen in table 5.1. The total number of M-components (for downward and upwards flashes) and ICC pulses in the high-speed camera data is 111 and 387 respectively. Therefore 13.5 % of M-components and 14.7 % of ICC pulses are classified as strokes. These values are very similar which is expect since M-components are similar to ICC pulses as discussed by Flache et al. (2008) [28].

The numbers have been summarised in table 6.4 below. The total number of M-components and ICC pulses that were filmed by the high-speed camera is 498. The total number of M-components and ICC pulses that were detected by the SALDN is 72. The SALDN classified 14.5 % of M-components and ICC pulses as strokes.

Table 6.4: The amount of ICC pulses and M-components captured with the high-speed camera and detected by the SALDN

Lightning events	**High-speed camera**	**SALDN**
M-components	111	15
ICC pulses	387	57
Total	498	72

6.4.3 SALDN dual stroke entry

As seen in table 3.4, chapter 3, the SALDN provides the time, location and current along with other information about a stroke. Throughout this research dual stroke entries in the CG stroke SALDN data were observed. The dual stroke entries were two strokes detected at the same millisecond, with a similar geographical location and similar peak current values. The dual stroke entries are shown in table 6.5 below. Entry 5 is a SRS in an upward flash. The remaining entries were strokes in a downward flash. Of the 10 entries, 6 were of negative polarity and 4 were of positive polarity. These dual strokes entries did not present any difference with regards to the high-speed camera footage of other strokes which were analysed. If a dual stroke entry occurred in the data, the stroke with the highest peak current was chosen.

Table 6.5: Dual stroke entries from the SALDN

Dual stroke entry	**Polarity**	**Time**	**Latitude**	**Longitude**	**Peak current (kA)**
1	Positive	18:46:27.321	-26.2313	28.0727	50
		18:46:27.321	-26.2297	28.0729	52
2	Negative	20:05:13.575	-26.2073	28.0800	-16
		20:05:13.575	-26.2073	28.0800	-16
3	Negative	20:24:47.100	-26.2520	28.2096	-13
		20:24:47.100	-26.2520	28.2096	-13
4	Negative	20:28:35.709	-26.2349	28.1947	-16
		20:28:35.709	-26.2339	28.1945	-17
5	Negative	15:46:51.678	-26.1863	28.0491	-27
		15:46:51.678	-26.1867	28.0494	-24
6	Positive	18:44:39.426	-26.1554	27.9289	28
		18:44:39.426	-26.1535	27.9291	27
7	Negative	14:45:50.361	-26.2016	28.0368	-36
		14:45:50.361	-26.2026	28.0352	-34
8	Negative	14:51:13.770	-26.2025	28.0312	-12
		14:51:13.770	-26.2047	28.0288	-14
9	Positive	18:52:19.801	-26.1488	28.1130	37
		18:52:19.801	-26.1586	28.1124	40
10	Positive	18:32:48.994	-26.2680	28.1506	38
		18:32:48.994	-26.2664	28.1507	34

6.5 Summary

The flash detection efficiency of downward flashes can be compared to upward flashes with subsequent return strokes. This indicates the importance of subsequent return strokes for the detection of a flash. The stroke detection efficiency of a subsequent return stroke, whether from a downward flash or upward flash, is very similar. The stroke detection efficiency and reported peak current generally decrease from the 1^{st} return stroke to the 9th subsequent return stroke of a flash. The flash and stroke detection of the SALDN proved to be comparable to the studies presented in chapter 2. A comparison of the locations of known attachment and flash cluster method indicated that either method could be used to determine the location accuracy of a lightning location system. However, the flash cluster method is regarded as the upper bound of the location accuracy.

There were several upward flashes which were initiated by a cloud-to-ground triggering event. However, the amount of self-initiated upward flashes is unknown. SALDN cloud-to-ground stroke data detected some M-components and initial continuing current pulses. M-components and initial continuing current pulses are not regarded as strokes. The SALDN had some dual stroke entries within the data, meaning that two strokes were detected at the same time, geographical location and similar peak currents when in fact there was one stroke seen on the high-speed camera.

The following chapter concludes the dissertation.

CHAPTER 7

Conclusion

Lightning location systems provide information about lightning events in many countries. This information is used in a number of applications. However, the application is only as accurate as the lightning location systems data. For this reason many studies evaluate the performance of a lightning location system. This gives an indication of how accurate the applications are and how the lightning location system can be improved in the future. The South African Lightning Detection Network has not had a performance evaluation where the flash detection efficiency, stroke detection efficiency and location accuracy are determined with the use of high-speed cameras. A methodology is presented that discusses how lightning location system data and ground truth data can be time-correlated and from this, how the detection efficiency and location accuracy of a lightning location system can be determined. This methodology was used to evaluate the performance of the South African Lighting Detection Network. Results show that the South African Lightning Detection Network has a flash detection efficiency of 84.9 %, stroke detection of 68.5 % and has a median location accuracy of 59.2 m. The location accuracy was found using ground truth lightning events which occurred on structures with known locations. Additionally, the location accuracy was found using locations errors within a flash cluster which produced a median location accuracy of 124.4 m, however this is regarded as the upper bound of the location accuracy of the South African Lightning Detection Network. Interesting cases regarding upward triggering events, detected M-components and initial continuing current pulses and dual South African Lightning Detection Network stroke entries were discussed.

References

[1] H. G. P. Hunt, K. J. Nixon, and I. R. Jandrell, "Establishing a methodology to investigate ldn median error ellipses used as corroborating evidence for a lightning event at a specific geographic location," *Electric Power Systems Research, Volume 113*, 2014.

[2] A. Nag, M. J. Murphy, W. Schulz, and K. L. Cummins, "Lightning locating systems: Insights on characteristics and validation techniques," *Earth and Space Science*, vol. 2, no. 4, pp. 65–93, 2015.

[3] Y. Zhang, W. Lu, Y. Zhang, D. Zheng, L. Chen, S. Chen, and X. Yan, "Evaluation for the performance of the guangdong-hongkong-macau lightning location system," *23rd international Lightning Detection Conference*, March 2014.

[4] D. R. Poelman, L. Delobbe, M. Crabbé, and C. Bouquegneau, "Lightning activity in belgium during 2001-2011," in *2012 International Conference on Lightning Protection (ICLP)*, 2012.

[5] T. Gill, "Initial steps in the development of a comprehensive lightning climatology of south africa," *University of the Witwatersrand*, 2008.

[6] V. A. Rakov and M. A. Uman, "Lightning physics and effects." Press syndicate of the University of Cambridge, 2007.

[7] V. Cooray, "The lightning flash." The Institution of Engineering and Technology, London, United Kingdom, 2014.

[8] J. Hanke, "Calibration of the recording of far fields radiated by lightning strikes to the gaisberg tower," *Diploma thesis- Vienna University of Technology*, September 2014.

[9] G. Diendorfer, M. Mair, and W. Schulz, "Detailed brightness versus lightning current amplitude correlation of flashes to the gaisberg tower," January 2002.

[10] L. Z. S. Campos, M. M. F. Saba, O. Pinto, and M. G. Ballarotti, "Waveshapes of continuing currents and properties of m-components in natural positive cloud-to-ground lightning," *Atmospheric Research*, vol. 91, no. 2, pp. 416 – 424, 2009.

[11] H. Zhou, G. Diendorfer, R. Thottappillil, H. Pichler, and M. Mair, "Measured current and close electric field changes associated with the initiation of upward lightning from a tall tower," *Journal of Geophysical Research: Atmospheres*, vol. 117, no. D8, 2012.

[12] C. Schumann, H. G. P. Hunt, M. M. F. Saba, M. A. S. Ferro, T. A. Warner, J. Souza, R. Albrecht, J. Tilles, T. J. Lang, and R. Thomas, "Analysis of the charge distribution and leaders inside the cloud for upward flash initiation," in *25th International Lightning Detection Conference and 7th International Lightning Meteorology Conference*, March 2018.

[13] M. M. F. Saba, C. Schumann, T. A. Warner, M. A. S. Ferro, A. R. Paiva, J. Helsdon, and R. E. Orville, "Upward lightning flashes characteristics from high-speed videos," *Journal of Geophysical Research: Atmospheres*, vol. 121, no. 14, pp. 8493–8505, 2016.

[14] W. Schulz, "Performance evaluation of lightning location systems," *Dissertation- Universitat Wien Fakultat fur Elektrotechnik*, 1997.

[15] V. Cooray, "An introduction to lightning." Springer Netherlands, 2015.

[16] H. G. P. Hunt, K. J. Nixon, and I. R. Jandrell., "Comparison between south african lightning detection network interpretation of single- channel and branched upward lightning flashes to a tall structure," *2013 International Symposium on Lightning Protection (XII SIPDA), Belo Horizonte, Brazil, October*, 2013.

[17] H. G. P. Hunt, Y. C. Liu, and K. J. Nixon, "Evaluation of the south african lightning detection network using photographed tall tower lightning events from 2009 - 2013," *International Conference on Lightning Protection (ICLP)*, 2014.

[18] K. L. Cummins and M. J. Murphy, "An overview of lightning locating systems: History, techniques, and data uses, with an in-depth look at the u.s. nldn," *IEEE Transactions on Electromagnetic Compatibility, vol. 51, no. 3*, 2009.

[19] W. Schulz, G. Diendorfer, S. Pedeboy, and D. R. Poelman, "The european lightning location system euclid – part 1: Performance analysis and validation paper," *Natural Hazards and Earth System Sciences*, 2016.

[20] M. G. Ballarotti, M. M. F. Saba, and O. Pinto, "A new performance evaluation of the brazilian lightning location system (rindat) based on high-speed camera observations of natural negative ground flashes," 2006.

[21] S. Mallick, V. A. Rakov, T. Ngin, W. R. Gamerota, J. T. Pilkey, J. D. Hill, M. A. Uman, D. M. Jordan, J. A. Cramer, and A. Nag, "An update on the performance characteristics of the nldn," *23rd international Lightning Detection Conference*, March 2014.

[22] M. Gijben, "The lightning climatology of south africa," *S Afr J Sci. 2012;108(3/4), Art. 740, 10 pages*, 2012.

[23] C. A. Stall, K. L. Cummins, E. P. Krider, and J. A. Cramer, "Detecting multiple ground contacts in cloud-to-ground lightning flashes," *Journal of Atmospheric and Oceanic Technology*, vol. 26, no. 11, pp. 2392–2402, 2009.

[24] S. Pedeboy, "Identification of the multiple ground contacts flashes with lightning location systems," in *22nd International Lightning Detection Conference and 4th International Lightning Meteorology Conference*, 2012.

[25] W. Schulz, S. Pedeboy, and M. M. F. Saba, "Lls detection efficiency of ground strike points," in *2014 International Conference on Lightning Protection (ICLP)*, 2014.

[26] S. Pedeboy and W. Schulz, "Validation of a ground strike point identification algorithm based on ground truth data," in *23rd International Lightning Detection Conference and 5th International Lightning Meteorology Conference*, 2014.

[27] W. Schulz, C. Vergeiner, H. Pichler, G. Diendorfer, and K. L. Cummins, "Location accuracy evaluation of the austrian lightning location system aldis," in *22nd International Lightning Detection Conference (ILDC)*, 2012.

[28] D. Flache, V. A. Rakov, F. Heidler, W. Zischank, and R. Thottappillil, "Initial-stage pulses in upward lightning: Leader/return stroke versus m-component mode of charge transfer to ground," *Geophysical Research Letters*, vol. 35, no. 13, 2008.

Appendix A

Investigating the performance of the SALDN

A.1 Preamble

This appendix contains a paper titled: **Performance evaluation of the SALDN using high-speed camera footage of ground truth lightning events over Johannesburg, South Africa** this paper was presented and accepted to be published at the *34th International Conference on Lightning Protection (ICLP)* in September 2018, which took place in Rzeszow, Poland.

A.2 Paper description

This papers purpose was to present the preliminary results of this research with a smaller dataset of ground truth lightning events. Therefore, this paper evaluates the performance of the SALDN with regards to the DE and LA and discusses interesting cases in the research. A methodology is included to explain step by step the process taken to get the results.

34th International Conference on Lightning Protection
02-07 September 2018
Rzeszow, Poland

Performance evaluation of the SALDN using high-speed camera footage of ground truth lightning events over Johannesburg, South Africa

H.G. Fensham, C. Schumann, H.G.P. Hunt, J.D. Tasman, K.J. Nixon
School of Electrical & Information Engineering
University of the Witwatersrand
Johannesburg, South Africa
hgfensham@gmail.com

T.A. Warner
ZT Research
Rapid City-SD-USA
Tom.Warner@ztresearch.com

M. Gijben
South Africa Weather Service
Pretoria, South Africa
Morne.Gijben@weathersa.co.za

***Abstract*— The performance of the South African Lightning Detection Network (SALDN) with regards to detection efficiency and location accuracy is presented in this paper. The performance is evaluated over a region in South Africa by using high-speed camera footage of ground truth lightning events, time-correlated with data from the SALDN. The data set contains 128 flashes which were recorded with high-speed cameras. The flash detection efficiency of the network is 88.3 % and the stroke detection efficiency is 72.1 %. The location accuracy has a median location error of 67.7 m based on 71 events which attached to the Hillbrow and Sentech Towers.**

Keywords- Detection efficiency, Location accuracy, SALDN

I. INTRODUCTION

Lightning Detection Networks (LDNs) consist of sensors which measure magnetic and/or electric fields propagated from lightning events. These lightning events are time-correlated and in certain instances, given a geographical location [1]. However, there are errors in these measurements, whether the LDN detected a lightning event and if the location given for a lightning event is correct. The performance of LDNs can be evaluated by determining the detection efficiency (DE) and the location accuracy (LA) of the system.

Around the world many LDNs have been evaluated with regards to their DE and LA. These include: the Guangdong-Hongkong-Macau Lightning Location System (GHMLLS), U.S. National Lightning Detection Network (NLDN), the European Lightning Location System (EUCLID) and the Austrian Lightning Detection and Information System (ALDIS) [2-5]. There are different ways to collect ground truth lightning event data to evaluate an LDN, to list a few: rocket triggered lightning events, high-speed camera footage and E-field measurements and natural lightning events on tall towers [4].

This paper aims to determine the DE, with regards to flash and stroke detection, and LA of the South African Lightning Detection Network (SALDN) over Johannesburg, South Africa, using high-speed camera footage of ground truth lightning events.

II. SALDN

The SALDN was established in 2005, consisting of 19 sensors throughout the country. Since 2009 there have been 2 upgrades to the system. In the early part of 2010 the systems number of sensors increased to 22 and in 2011 sensors were relocated and a further 2 sensors were added. As of 2014, the SALDN contains 24 Vaisala LS7000 sensors positioned throughout South Africa as seen in Fig. 1 [6]. The SALDN has a self-evaluated performance of 90 % for flash DE and a median location error of 0.5 km for LA [7].

The flash DE and LA of the SALDN was determined previously in 2014. This was done by using low speed cameras which meant the stroke DE could not be determined. Additionally, the camera was only recording lightning events which took place on the Sentech Tower. Therefore, the flash DE was calculated for one specific location, nonetheless it was found to be 76 %. The LA of the system was found to have a median location error of 290 m since the lightning events had a known geographical location from the tower [6].

The data provided by the SALDN was cloud-to-ground stroke data for the whole of South Africa which needed to be time-correlated with the high-speed camera footage.

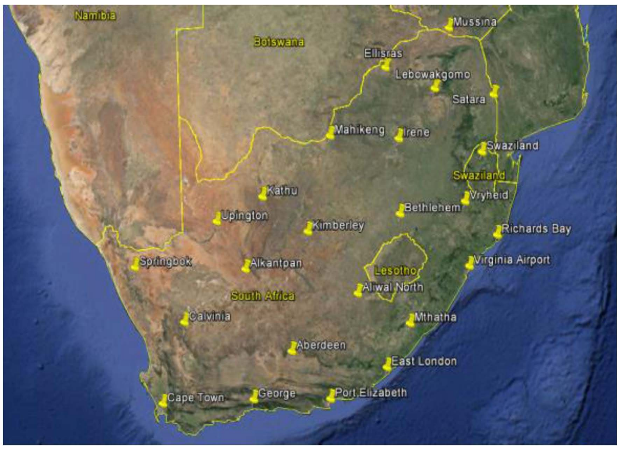

Fig. 1. Location of the 24 Vaisala sensors in South Africa as of 2014 [6].

978-1-5386-6635-7/18/$31.00 ©2018 IEEE

III. High-Speed Camera Footage

The high-speed cameras used were the Phantom v310 and the Phantom v7.1. The camera footage was collected between the 5th of February 2017 and the 6th of February 2018. Table I, gives a summary of the data collected by the cameras, this data set was used in finding the DE and LA of the SALDN.

This data was found by positioning the cameras where the blue pin is situated (26.16283°S, 27.95986°E) in Fig. 2. From this location the cameras looked over Johannesburg, South Africa. The field of view which is illustrated by the black lines, encloses the Hillbrow (26.18696°S, 28.04948°E) and Sentech (26.1925°S, 28.00666°E) Towers illustrated by the black pins. The red pins illustrate the region that was focused on for the SALDN data. The respective decimal coordinates are given with each red pin.

TABLE I. High-speed Camera Data

Lightning events	High-speed camera events
Thunderstorms	22
Flashes	128
Downward flashes	101
Strokes	431
M-components	82
Upward flashes	27
Upward leaders	34
ICC pulses	246
Subsequent return strokes	30
M-components	8

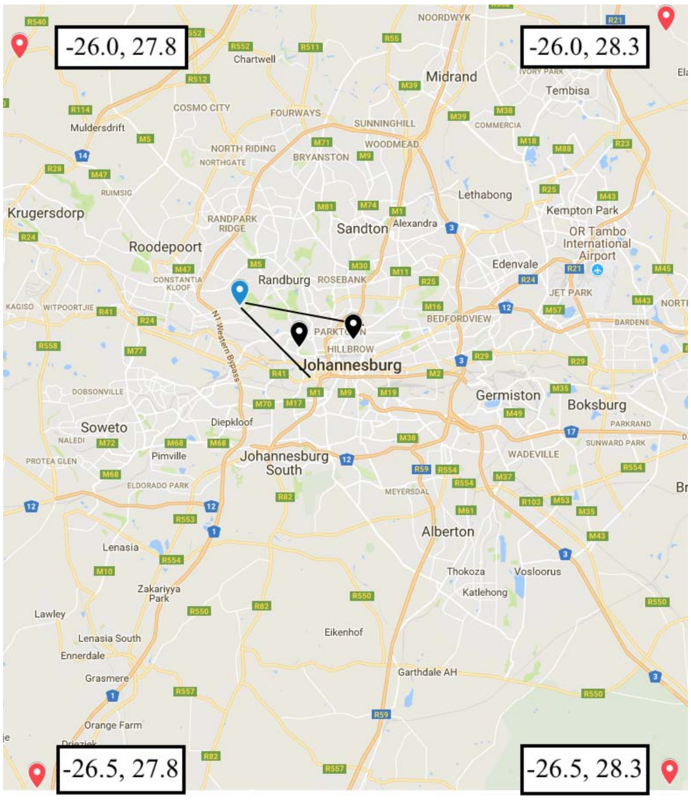

Fig. 2. Map of region which SALDN data is filtered by, camera location and Hillbrow and Sentech Tower

IV. Methodology

In order to evaluate the performance of the SALDN, the two data sets needed to be time-correlated. From this time-correlation the DE and LA methodology can be applied.

A. *Time-correlation between SALDN data and high-speed camera footage*

- Filter the cloud-to-ground SALDN stroke data to only contain strokes between the red pins illustrated in Fig. 2 in order to find the localized SALDN data.
- Time-correlate the lightning events seen in the high-speed camera data with the localized SALDN data.
- Determine if the SALDN detected the events.

B. *Detection Efficiency*

The DE of the SALDN is comprised of the flash DE and the stroke DE.

1) *Flash Detection Efficiency*

- Find the number of flashes captured with the high-speed cameras.
- Determine if the SALDN stroke data detected any strokes (return strokes and subsequent return strokes), upward leaders, M-components or ICC pulses in the time-correlated data.
- If the SALDN detected any one of the above-mentioned lightning events, then a flash has been detected by the SALDN.
- Calculate the percentage of flashes detected by the SALDN compared to the total number of high-speed camera flashes.

2) *Stroke Detection Efficiency*

- Find the number of strokes for downward and upward flashes captured with the high speed cameras.
- Calculate the number of strokes that were detected by the SALDN, in the time-correlated data.
- Calculate the percentage of SALDN strokes that were detected compared to the number of strokes in the high-speed camera footage.

C. *Location accuracy*

- Create a subset of the data from the high-speed camera footage with the lightning events that occurred on the Hillbrow and Sentech Tower.
- Calculate the distance between the coordinates of the towers and the coordinates given by the SALDN data for the events which were detected on these towers.

- Determine the number of samples, maximum, minimum, median, standard deviation, mode and arithmetic mean of the distances calculated.

V. RESULTS

The following section will provide the results obtained from applying the methodology in section IV as well as interesting cases which were found throughout the evaluation of the performance of the SALDN.

A. Time-correlation Results

Table II is the summarized results of the time-correlation between the high-speed camera footage and the SALDN data.

TABLE II. TIME-CORRELATED DATA OF THE HIGH-SPEED CAMERA DATA AND THE SALDN DATA

Lightning events	High-speed camera events	SALDN events
Flashes	128	113
Downward flashes	101	95
Strokes	431	311
M-components	82	9
Upward flashes	27	18
Upward leaders	34	0
ICC pulses	246	45
Subsequent return strokes	35	25
M-components	8	2

B. Detection Efficiency

The DE has been defined for both flash and stroke levels. Naturally, a network will have a greater chance of detecting a flash compared to a stroke. This is because a single detected stroke, within a flash, will constitute a flash [8].

1) Flash Detection Efficiency

The SALDN was found to have detected 113 flashes as seen in table II. This was found by using section IV. With the camera footage recording 128 flashes, this meant the SALDN has a flash DE of 88.3 % as seen in table III.

TABLE III. FLASH DETECTION EFFICIENCY

Number of flashes recorded by high-speed camera	128
Number of flashes detected by SALDN	113
Flash Detection Efficiency	**88.3 %**

This compared with the self-evaluation value DE of 90 %, shows that the system is performing close to its expectation. Additionally, the flash DE for downward flashes is 94 %. This is greater than the flash DE for upward flashes which is 66.7 %.

2) Stroke Detection Efficiency

The high-speed camera data had a total of 466 strokes for downward and upward flashes. Of this, the SALDN detected a total of 336, equating to a stroke DE of 72.1 %. This can be seen in table IV.

TABLE IV. STROKE DETECTION EFFICIECNY

Number of strokes recorded by high-speed camera	466
Number of strokes detected by SALDN	336
Stroke Detection Efficiency	**72.1 %**

It must be noted that in upward lightning, the upward leader is generally not detected and sometimes the superimposed ICC pulses can be classified as intra-cloud (IC) discharges [9, 10]. Unfortunately, the IC SALDN data was not obtainable for this dataset.

C. Location Accuracy

The high-speed camera footage is crucial for determining the LA of the SALDN. The high-speed cameras allow the lightning events on the Hillbrow and Sentech Tower to be viewed, meaning the true location of the event is known. As described above in section IV, the coordinates for the events which made attachment with the two towers in the video footage and were detected by the SALDN were used to form a subset of the data set. The coordinates given by the SALDN could then be compared to the true coordinates of the Hillbrow and Sentech Tower. From this the distance between the towers and the SALDN detection coordinates could be calculated.

The amount of events which occurred on both of the towers totals to 71. The SALDN has a LA with a median location error of 68.5 m. This value is well within the self-performance evaluation for the LA which has a 0.5 km median location error. The results of this data for both towers together and each tower separately can be seen in table V. The following two subsections will discuss the LA on each tower.

1) Sentech Tower

Of the 71 events which took place on the towers, 36 of them took place on the Sentech Tower. However, one of the events which took place on the tower was an outlier. This event was calculated to be 1.7 km away from the tower. In Fig. 3 a) one can see this outlier and in Fig. 3 b) this outlier has been excluded to get a better view of the SALDN locations detected around the Sentech Tower. Table V shows the results of the LA on the Sentech Tower, having a median location error of 80.5 m.

2) Hillbrow Tower

Of the 71 events, 35 occurred on the Hillbrow Tower. Two of these events were found to be outliers as the one event had a distance of 11.65 km and the other event having a distance of 3.85 km from the tower. This can be seen in Fig. 3 c). In Fig. 3 d) the two events were excluded to give a closer view on the distribution around the Hillbrow Tower.

Table V gives the results of the LA on the Hillbrow Tower with all the events taken into account. It shows that the median location error is 60.1 m.

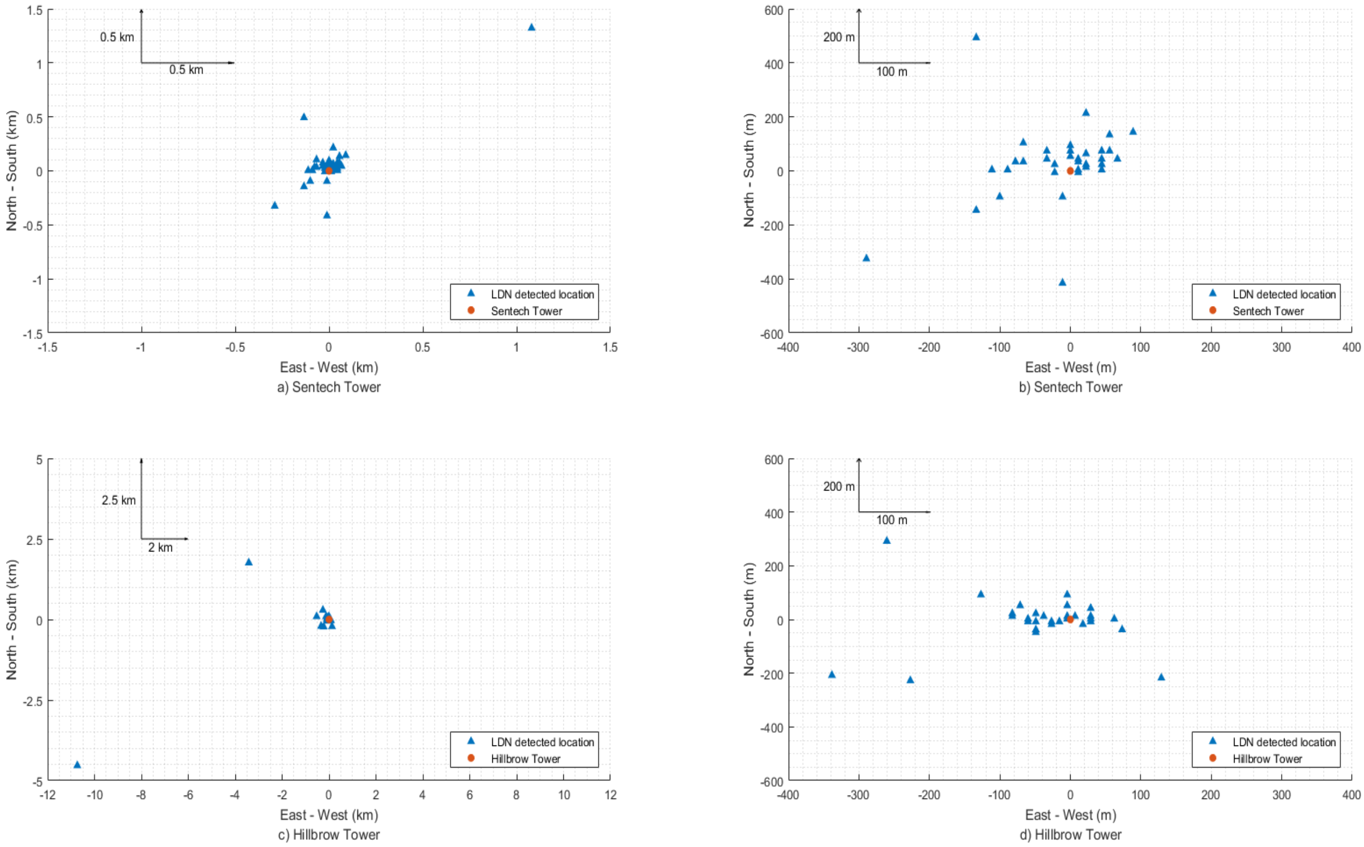

Fig. 3. Detected locations of the SALDN data which has been time-correlated with the high-speed video footage for the Sentech and Hillbrow Towers

TABLE V. LOCATION ACCURACY OF TOWER EVENTS

Tower	N	Max	Min	Median	σ	Mode	Mean
Both Towers	71	11650.7 m	4.9 m	68.5 m	1501.0 m	4.9 m	363.0 m
Sentech Tower	36	1707.1 m	11.8 m	80.5 m	285.5 m	53.9 m	156.4 m
Hillbrow Tower	35	11650.7 m	4.9 m	60.1 m	2009.5 m	4.9 m	536.5 m

D. *Interesting Cases*

In the process of evaluating the performance of the SALDN, it was seen that there were upward triggering events, M-components and ICC pulses which were detected as strokes by the SALDN and the odd case where two strokes would be detected at the same time and geographical location by the SALDN.

1) *Upward triggering event*

Of the 18 detected upward flashes in the high-speed camera footage, approximately 8 upward flashes had a positive lightning stroke before the upward flash was initiated and then seen on camera. These positive lightning strokes were detected by the SALDN with positive current and would initiate an upward leader within 100 ms.

2) *Detected M-components and ICC pulses*

In the comparison between the high-speed camera footage and the SALDN data, it was noticed that strokes were detected by the SALDN which were actually M-components or ICC pulses as observed in the high-speed camera footage.

From table II, the number of M-components and ICC pulses detected by the SALDN equate to 56. The total number of ICC pulses and M-components in the high-speed camera data equates to 336. This means that 16.6 % of M-components and ICC pulses were classified as a stroke by the SALDN. It must be noted that of this percentage, ICC pulses are responsible for 13.4 %.

3) *SALDN dual stroke entry*

During the time-correlation between the high-speed camera data and the SALDN data, it was noticed that a small amount of strokes in the SALDN data were detected twice. Meaning the SALDN data detected two strokes at the same time, down to the millisecond, with a similar geographical location. These strokes were all downward negatives within a downward or upward flash. The strokes were also given current estimates which were similar if not the exact same.

In the high-speed video footage these dual entry strokes did not have any substantial differences to other strokes which were analyzed. These entries can be seen in table VI.

TABLE VI. DUAL STROKE ENTRIES BY SALDN

Dual stroke entry	Time	Latitude	Longitude	Current (kA)
1	20:05:13.575 20:05:13.575	-26.2071 -26.2073	28.0791 28.0800	-16 -16
2	20:28:35.709 20:28:35.709	-26.2339 -26.2349	28.1945 28.1947	-17 -16
3	15:46:51.678 15:46:51.678	-26.1863 -26.1867	28.0491 28.0494	-27 -24

VI. CONCLUSION

The South African Lightning Detection Network is still a relatively new LDN which has a self-evaluated performance of 90 % for flash detection efficiency and a location accuracy with a median location error of 0.5 km. Using high-speed camera footage over Johannesburg, South Africa, time-correlated with cloud-to-ground SALDN stroke data, the flash detection efficiency and stroke detection efficiency was calculated to be 88.3 % and 72.1 % respectively. Additionally, the SALDN was found to have a flash detection efficiency of 94 % for downward flashes and a flash detection efficiency of 66.7 % for upward flashes. The location accuracy had an overall median location error of 68.5 m with 71 events in total making attachment on the Sentech and Hillbrow Tower. The Sentech Tower had a location accuracy with a median location error of 80.5 m and the Hillbrow Tower had a location accuracy with a median location error of 60.1 m.

ACKNOWLEGDMENTS

The authors would like to thank the South African Weather Service (SAWS) for their support and for providing the SALDN data used in this paper. They would also like to thank Eskom for the support of the Lightning/EMCResearch Group through the TESP programme. Thanks are extended to the Department of Trade and Industry (DTI) for THRIP funding as well as to the National Research Foundation (NRF) for direct funding of the Research Group.

REFERENCES

[1] H. G. P. Hunt, K. J. Nixon and I. R. Jandrell, “Establishing a methodology to investigate LDN median error ellipses used as corroborating evidence for a lightning event at a specific geographic location,” Electric Power Systems Research, vol. 113, 2014.

[2] Y. Zhang, W. Lu, Y. Zhang, D. Zheng, L. Chen, S. Chen, and X. Yan, “Evaluation for the performance of the Guangdong-Hongkong-Macau Lightning Location System,” 23rd International Lightning Detection Conference, March 2014.

[3] S. Mallick, V. A. Rakov, T. Ngin, W. R. Gamerota, J. T. Pilkey, J. D. Hill, M. A. Uman, D. M. Jordan, J. A. Cramer and A. Nag, “An update on the performance characteristics of the NLDN,” 23rd International Lightning Detection Conference, March 2014.

[4] W. Schulz, G. Diendorfer, S. Pedeboy, and D. R. Poelman, “The European Lightning Location System EUCLID – Part 1: Performance analysis and validation,” Natural Hazards and Earth System Sciences, March 2016.

[5] C. Vergeiner, W. Schulz and S. Pack, “On the performance of the Austrian Lightning Detection and Information System (ALDIS),” Institute of High Voltage Engineering and System Management, Graz University of Technology, Graz, Austria, November 2013.

[6] H. G. P. Hunt, Y. C. Liu, and K. J. Nixon, “Evaluation of the South African Lightning Detection Network using photographed tall tower lightning events from 2009 – 2013,” 2014 International Conference on Lightning Protection (ICLP), 2014.

[7] M. Gijben, “The lightning climatology of South Africa,” South African Journal of Science, vol. 108, 2012.

[8] H. G. P. Hunt, K. J. Nixon and I. R. Jandrell, “Comparison between South African Lightning Detection Network interpretation of single-channel and branched upward lightning flashes to a tall structure,” 2013 International Symposium on Lightning Protection (XII SIPDA), Belo Horizonte, Brazil, October 2013.

[9] T. A. Warner, K. L. Cummins and R. E. Orville, “Upward lightning observations from towers in Rapid City, South Dakota and comparison with National Lightning Detection Network data, 2004-2010,” Journal of Geophysical Research, 2012.

[10] G. Diendorfer, H. Pichler and W. Schulz, “LLS detection of upward initiated lightning flashes,” 2015 Asia-Pacific International Conference on Lightning (APL), Nagoya, Japan, 2015.

Appendix B

Summary of high-speed video analysis over Johannesburg, South Africa

B.1 Preamble

This appendix contains a paper titled: **High-speed video analysis of lightning flashes over Johannesburg, South Africa** this paper was showcased with a poster at the 26th *Southern African Universities Power Engineering Conference (SAUPEC)* in January 2018, which took place at the university of the Witwatersrand, South Africa.

B.2 Paper description

This paper gives an overview of the lightning events seen on high-speed cameras over Johannesburg, South Africa. The equipment that was used was discussed in detail and a methodology was presented before the data analysis. 100 flashes were analysed and the following data analysis was done: Multiplicity, number of strike points, inter-stroke interval, continuing current duration and stroke duration.

HIGH-SPEED VIDEO ANALYSIS OF LIGHTNING FLASHES OVER JOHANNESBURG, SOUTH AFRICA

J. Tasman*, **H. Fensham***, **C. Schumann***, **H. G.P. Hunt***, **K.J.Nixon***, **T.A.Warner** †

* *School of Electrical & Information Engineering, University of the Witwatersrand, Private Bag 3, 2050, Johannesburg, South Africa.*

† *ZT Research, Rapid City-SD-USA.*

Abstract: A discussion based on data attained from analysing high-speed footage of lightning flashes in Johannesburg, South Africa, is presented. A total of 100 lightning flashes, comprising of 346 visible strokes and 57 M-components, were analysed. The high-speed cameras used to attain the data were the Phantom v310, Phantom v7.1 and the MIRO4. From the data attained, a multiplicity of 3.6 strokes-per-flash was calculated and the arithmetic mean of 62.3 *ms* and 29.8 *ms* was calculated for the interstroke intervals and the stroke durations, respectively. Long continuous current (> 40 *ms*) was seen the most in negative upward flashes, with it being present in 47.5% of all its strokes.

Key words: Continuing current, flash, high-speed camera, lightning characteristics, M-component, stroke

1. INTRODUCTION

Fundamentally, lightning flashes can be categorised into three types; cloud-to-ground (CG), ground-to-cloud (GC) and intra/inter-cloud (IC) [1]. These labels classify the lightning's direction of propagation from its start to termination point. The research and data collected was focused on CG and GC flashes only. Each flash is made up of a certain number of strokes. Once initial attachment has been made, a return stroke will deliver current through the channel. This will cause the channel to emit a large amount of luminosity. The first return stroke will have the greatest current magnitude and luminosity and when completed, will leave behind a channel of ionised air. IC discharges will re-establish the electric field (E-field) and the channel provides an easy path for subsequent return strokes to travel through. If the channel has not disappeared completely and the E-field has not been re-established before the occurrence of another current impulse, an M-component, as opposed to a return stroke, has occurred [2].

Due to the microphysics and other conditions inside the cloud such as: wind, dust particles, temperature among others; the particles separate themselves in positive or negative, creating large charge centers.

Both CG and GC flashes can be classified as either positive or negative. Due to the microphysics involved, as well as many other physical conditions such as temperature and wind, particles within the cloud separate themselves into positive and negative - this creates large charge centers. These most commonly separate with the positive charge centers at the top of the cloud and the negative at the bottom. The strong E-fields within the clouds are the cause of IC flashes. The difference in potential between the cloud and the ground also causes an E-field to develop. In the negative CG case (nCG), this enhanced E-field causes a downward propagation of negative charge (a stepped leader) from a charge center in the cloud toward the ground. This causes a further enhancement of the field and can result in this stepped leader attaching to a point on the ground [2]. From consulting similar discussion papers and studies, it can be concluded that nGC is the most common type of lightning throughout the regions of São Paulo in Brazil, New Mexico and Arizona in the United States and the eastern Mediterranean [3–6].

Depending on the charge magnitude and density in the cloud and on the ground, it is possible for a stepped leader to originate from the ground and propagate towards the cloud. Due to how charge is most commonly separated in the cloud, the ground is generally dense with positive charge. If this charge causes a sufficient enhancement of the E-field, positive streamers can develop and begin propagating upwards. Once these streamers have attached to either a charge center in the cloud or to downward propagating negative stepped leaders, return strokes consisting of negative current impulses will be initiated - this is negative GC (nGC) [2, 7].

Depending on the type of thunderstorm or the stage of the thunderstorm, the positive charge centers can be situated at the bottom of the cloud with the negative charges at the top. This would cause the ground underneath the cloud to be dense with negative charge. Once again, if the enhancement of the E-field is strong enough, this can cause a downward propagating positive CG flash (pCG). Alternatively, upward propagating negative streamers can occur. If these find a point of termination in the cloud, return strokes consisting of positive current impulses would be initiated - this is positive GC (pGC) [2, 8].

The human eye is not able to detect, in real time, individual strokes within a flash. Therefore, in order to analyse and capture flash data, specialised high-speed cameras were used. These were set up in different locations and primarily focused on flashes occurring in the Johannesburg central business district (CBD). The high frame rate and resolution capabilities of the cameras allowed the behaviour of each individual stroke within a flash to be independently analysed and recorded.

Many studies have been performed that discuss the behaviour of lightning flashes in different geographical locations, such as São Paulo, New Mexico, Arizona and the eastern Mediterranean. The Johannesburg CBD has not yet been focused on in this line of research and the data attained and presented in this report aims to contribute to furthering the communal understanding of lightning processes.

2. EQUIPMENT

In order to attain footage that would enable the characterisation of lightning flashes, three high-speed cameras were used. These were the Phantom v310, Phantom v7.1 and the MIRO4. For the v310 and v7.1, the Phantom Camera Control Software version 2.8 was used to run the cameras and analyse the footage [9].

The v310 recorded at 15000 fps and had an exposure time of 58 μs. The Phantom v7.1 recorded at 5000 fps and had an exposure time of 990 μs. The different frame rates of the cameras and their subsequent exposure times and resolution allowed for each flash to be analysed separately - this optimised the accuracy of the characterisation process.

The Phantom v310 has internal memory of 32 GB which is split into 2 individual memory partitions (2 of 16 GB each). A 512 GB CINEMAG external hard drive is attached to the camera, which allows it to save all 16 GB in about 2-3 seconds. Since it has two memory banks, this means another flashed can be saved in those 2-3 seconds. After completion of the thunderstorm, this footage could then be transferred onto a computer from the CINEMAG and analysed using the above mentioned software.

Initially, the v7.1 had a 16 GB internal memory capacity that was split into 10 individual memory partitions of 1.6 GB each. After filming, each partition was saved. The current settings include the memory being split into two 8 GB partitions that are set to save automatically to the computer after each trigger.

The physical setup of the camera allowed for them to be orientated at any angle or position. This allowed for different, more specific areas to be focused on.

3. METHODOLOGY

Between the dates February to December 2017, the high speed cameras (Phantom v310 and Phantom v7.1) were positioned 6 km away from the CBD to capture CG and GC lightning in the Johannesburg CBD (Braamfontein CBD), centered at $26°11'28''S$ $28°02'16''E$. Within the area, is the Hillbrow tower at a height of 270 m with coordinates $26°18'70''S$ $28°04'95''E$ and the Brixton tower at a height of 232 m and with coordinates $26°19'25''S$ $28°00'67''E$ [10].

Before a storm, the cameras were switched on and setup to ensure that the correct amount of light was able to pass through the cameras.

Personal were required to sit and watch the lightning storm and press the trigger once a lightning flash was completed. The trigger was a single trigger system, which triggered the Phantom v310 and the Phantom v7.1 with a single press of the button. Each camera was running off a laptop of its own, with the above mentioned program, and had pre-trigger time of 1.6 s and post-trigger time of 0.2 s.

Videos were analysed and summarised and the results will be present in the Section 4 on data analysis. Using the two different cameras for the same lightning flash allowed a more precise visual analysis as each camera has benefits with regards to their fps and exposure time. Figure 1, below, shows an example of the high-speed camera's videos captured over Johannesburg. The figure contains two nGC flashes from both the Hillbrow tower (pictured left) and the Brixton tower (pictured right). A nCG flash is also present and can be identified as the channel to the right of the Brixton tower (making attachment with the ground).

Figure 1: Frame taken from high-speed camera footage

4. DATA ANALYSIS

One hundred lightning flashes were analysed and characterised in a database. As mentioned in the introduction, IC was not a focus for this research. The database has 100 flashes that were recorded during 14 days with thunderstorms. Of these, 81 were downward flashes and 19 were upward flashes. It was observed that there were 346 strokes and 57 M-components in these flashes. Strokes that made attachment out of the camera's field of view were classified as 'non-visible' and not included. Accompanying the figures in this section are quantities N, AM and GM. These refer to the number of samples, the arithmetic mean and the geometric mean, respectively. Table 1 presents the summary of the collected data.

Of the 100 classified flashes, 79 were nCG, 2 were pCG, 17

Table 1: Summarised results of collected lightning flash data

Classification	Quantity
Thunderstorms	14
Flashes	100
Visible strokes	346
M-component	57

were nGC and 2 were pGC. Table 2 provides a percentage summary on the polarity of the lightning flashes relative to all of the collected lightning flash data.

Table 2: Summarised results of the polarity of the collected lightning flash data

Type	Polarity	Percentage
CG	Negative	79%
	Positive	2%
GC	Negative	17%
	Positive	2%

4.1 Multiplicity

The multiplicity is defined as the number of strokes in a flash. This is generally represented as a strokes-per-flash average taken from the full data set [2]. From Table 2, it is noted that nGC flashes occurred considerably more often than other types.

An M-component is defined as a return stroke with the occurrence of subsequent strokes before the ionised channel disappears [2]. The luminosity of the channel increases as discharge occurs. If the channel has not disappeared and there is an increase in luminosity after the original attachment and the return stroke, then the time stamps need to be analysed to determine if it is due to residual charge from the return stroke of if it is an M-component. If a luminosity variation occurs within the μs range after the return stroke's variation, then it is classified as residual charge and caution was taken as to not confuse the two and incorrectly classify the flash. The way in which the flashes were analysed excluded M-components in the sense that they did not contribute to the strokes per flash statistic.

Figure 2 is a bar graph plotting the number of strokes per flash against the number of flashes. This graph is representative of the entire data set. It was seen that 21% of all recorded flashes had two strokes and along with the outlying flash that had 27 strokes, a multiplicity of 3.6 was calculated for the entirety of the flash data.

4.2 Number of strike points

In order to say that a lightning flash has multiple strike points, return strokes need to have multiple points of attachment. This means that different strokes in the same flash should terminate at different or alternating points [2]. From the 100 recorded flashes, nine were found to have multiple strike points, however, none more than two. All of these were from nCG flashes.

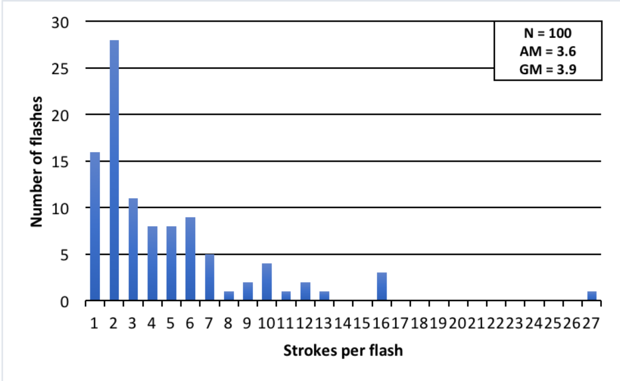

Figure 2: Bar graph showing the number of strokes per flash

4.3 Interstroke interval

According to the way in which the data was recorded, the interstroke interval can be defined as the time between the attachment of subsequent return strokes within the same flash. As previously discussed, an M-component is different to a single stroke and therefore, an interstroke interval was not computed if a return stroke was followed by an M-component. It is difficult to accurately determine, from visual analysis, the exact point at which the stroke's continuing current has concluded and the channel disappears. The interstroke interval was therefore taken between times of attachment as this can be determined with significantly less of an error. The accuracy of this method would come down to the frame rate of the camera - the higher the frame rate, the more precise one can be when determining the time of attachment.

Table 3: Overall interstroke interval results

Interval information	time (ms)
Arithmetic mean	62.3
Minimum	6
Maximum	546

Table 3 presents the minimum, maximum and arithmetic mean of all recorded interstroke intervals. Table 4 presents the number of interstroke intervals that fall within specific time ranges. It is seen that 57.8% of recorded interstroke intervals lasted less than 50 *ms*.

4.4 Continuing current

Continuing current (CC) is the continuous flow of charge through the ionised channel after initial attachment of the stroke [2]. There are three different ways to characterise CC. A "long" CC is a CC with a duration greater than 40 *ms* whereas a "short" CC has a duration between 10 *ms* and

Table 4: Summarised results of the number of interstroke intervals that fell within different time ranges

Intervals (*ms*)	**Number**
0<x⩽50	134
50<x⩽100	64
100<x⩽150	17
150<x⩽200	10
200<x⩽250	2
250<x⩽300	1
300<x⩽350	1
350<x⩽400	1
400<x⩽450	1
450<x⩽500	0
500<x⩽550	1
Total	232

40 *ms*. Additionally, a ”questionable” CC has a duration between 1 and 10 *ms* [11].

The results were based off the data were the initial attachment of the strike was noted and then when the channel was seen to disappear. Using the software for the cameras, the brightness of the video was changed to ensure that the channel had disappeared meaning that the CC had stopped. The flashes were recorded by two different cameras to ensure that the channel had legitimately ceased.

It was found that 40 strokes had long CC with 31 occurring from nCG flashes, 8 from nGC and 1 from pGC. Table 5 below shows the results of how many strokes had long CC in each data set. The table shows that nCG has the greatest amount of long CC, this however could be skewed due to the amount of nCG which has been captured in the results in comparison to the other types of lightning. Relative to the specific type of lightning, 39.3% percent of nCG has long CC as opposed to 47.5% percent of nGC. This shows that nGC might be more prone the having long CC.

Table 5: Summarised results of continuing current

Data set	**Long CC**
nCG	31
pCG	0
nGC	8
pGC	1
All	40

4.5 Stroke Duration

The stroke duration in the context of this investigation, was defined as the amount of time taken from attachment until the ionised channel of the stroke on the high-speed footage had completely disappeared. The arithmetically calculated mean stroke duration of all recorded strokes was calculated to be 29.8 *ms*. The maximum stroke duration was found to be 619 *ms*. Figure 3 below shows the number of strokes in a flash that are between 1 and 40 *ms*. It can be seen that the majority of strokes have a duration between 1 and 15 *ms*. This accounts for 265 of the 346 strokes, that is 76.6% of all recorded strokes lay in this time duration region.

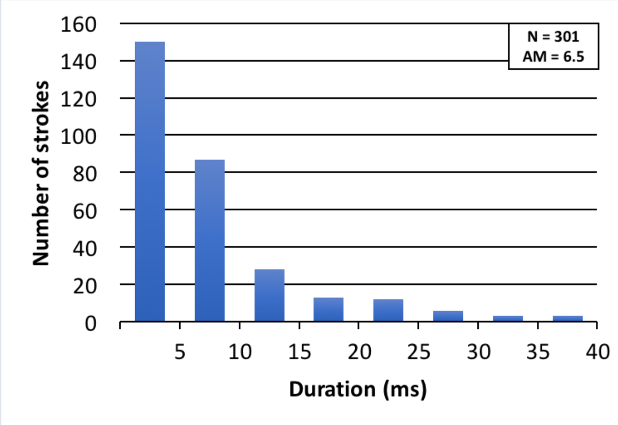

Figure 3: Bar graph showing the duration of strokes between 1 and 40 *ms*

The number of strokes with larger durations steadily decrease as seen in Figure 4 below which accounts for strokes that have a duration of greater than 40 *ms*.

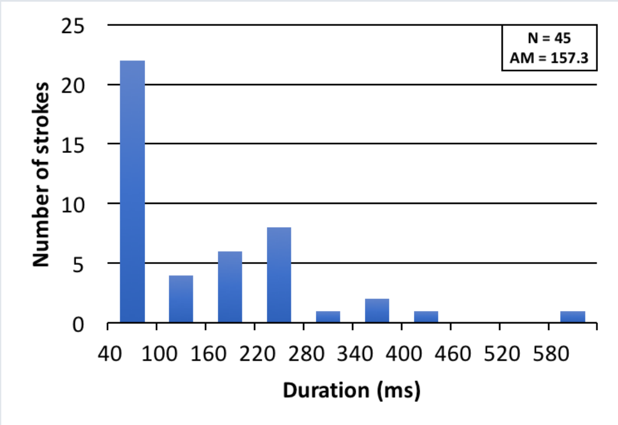

Figure 4: Bar graph showing the duration of strokes greater than 40 *ms* (Long CC)

Table 6 below shows the mean stroke duration for the different types of lightning that has been characterised in the dataset.

Table 6: Summarised results of mean stroke duration

Data set	**Mean duration** (*ms*)
nCG	23.1
pCG	97.5
nGC	437.7
pGC	256.0
All	29.8

5. SUMMARY

Of the 100 flashes which were analysed, each flash had arithmetic mean of 3.6 strokes. Strokes within a flash ranged from 1 to 27. Within the data it was seen that 9 of the 100 flashes had two strike points, there were no cases were a flash had more than 2 strike points. The interstroke intervals in the data had an arithmetic mean of 62.3 *ms* with a range of 6 to 546 *ms*. 134 out of 232 interstroke intervals were found to have a duration of 0-50 *ms*. With regards to long CC, it was seen nGC has 47.5% long CC which is the highest in this dataset in comparison to the other lightning types. The stroke duration in the entire dataset had an arithmetic mean 29.8 *ms*. It was seen that nGC had the longest mean stroke duration with 437.7 *ms*.

REFERENCES

[1] V. A. Rakov. "Fundamentals of Lightning." *International Symposium on Lightning Protection*, October 2011.

[2] V. A. Rakov. "The Physics of Lightning." *Surveys in Geophysics - Springer*, pp. 701–729, April 2013.

[3] M. M. F. Saba, M. G. Ballarotti, and O. Pinto Jr. "Negative cloud-to-ground lightning properties from high-speed video observations." *Journal of Geophysical Research*, vol. 111, no. D3, February 2006.

[4] A. C. V. Saraiva, M. M. F. Saba, O. Pinto Jr., K. L. Cummins, E. P. Krider, and L. Z. S. Campos. "A comparative study of negative cloud?to?ground lightning characteristics in So Paulo (Brazil) and Arizona (United States) based on high?speed video observations." *Journal of Geophysical Research*, vol. 115, no. D11, June 2010.

[5] Y. Yair, S. Shalev, Z. Erlich, A. Agrachov, E. Katz, H. Saaroni, C. Price, and B. Ziv. "Lightning flash multiplicity in eastern Mediterranean thunderstorms." *Natural Hazards and Earth System Sciences*, vol. 14, no. 165, February 2014.

[6] M. M. F. Saba, T. A. Warner, and C. Schumann. "Features of lightning flashes obtained from high-speed video recordings." *The Lightning Flash*, pp. 231–266, February 2014.

[7] M. M. F. Saba, C. Schumann, T. A. Warner, M. A. S. Ferro, A. R. de Paiva, J. Helsdon Jr., and R. E. Orville. "Upward lightning flashes characteristics from high-speed videos." *Journal of Geophysical Research: Atmospheres*, vol. 121, no. 14, pp. 8493–8505, July 2016.

[8] M. M. F. Saba, W. Schulz, T. A. Warner, L. Z. S. Campos, C. Schumann, E. P. Krider, K. L. Cummins, and R. E. Orville. "Negative cloud-to-ground lightning properties from high-speed video observations." *Journal of Geophysical Research*, vol. 115, no. D24, December 2010.

[9] "PCC Software version 2.8.", October 2016. URL `http://www.phantomhighspeed.com/`. Last accessed: 11 December 2017.

[10] "GOOGLE Maps.", December 2017. URL `https://www.google.co.za/maps/place/Johannesburg/`. Last accessed: 13 December 2017.

[11] M. M. F. Saba, W. Schulz, T. A. Warner, L. Z. S. Campos, C. Schumann, E. P. Krider, K. L. Cummins, and R. E. Orville. "High?speed video observations of positive lightning flashes to ground." *Journal of Geophysical Research:*, vol. 115, no. D24, December 2010.

Appendix C

Further summary of high-speed video analysis over Johannesburg, South Africa

C.1 Preamble

This appendix contains a paper titled: **High-speed video observation of lightning flashes over Johannesburg, South Africa 2017 - 2018** this paper was presented and accepted to be published at the *34th International Conference on Lightning Protection (ICLP)* in September 2018, which took place in Rzeszow, Poland.

C.2 Paper description

This paper gives a further overview of the lightning events seen on high-speed cameras over Johannesburg, South Africa. There are 168 flashes which were categorised into positive and negative, upward and downward flashes and then the following attributes are assessed: strike points, inter-stroke interval and CC duration. Additionally, one building in particular is studied and presents itself as a location for future current measurements.

34th International Conference on Lightning Protection
02-07 September 2018
Rzeszow, Poland

High-speed video observation of lightning flashes over Johannesburg, South Africa 2017 - 2018

Carina Schumann
School of Electrical and Information Engineering
University of the Witwatersrand
Johannesburg, South Africa
Email: carina.schumann@wits.ac.za

Hugh.G.P. Hunt
School of Electrical and Information Engineering
University of the Witwatersrand
Johannesburg, South Africa
Email: hugh.hunt@wits.ac.za

Jesse Tasman
School of Electrical and Information Engineering
University of the Witwatersrand
Johannesburg, South Africa

Haydn Fensham
School of Electrical and Information Engineering
University of the Witwatersrand
Johannesburg, South Africa

Ken J. Nixon
School of Electrical and Information Engineering
University of the Witwatersrand
Johannesburg, South Africa
Email: ken.nixon@wits.ac.za

Tom A. Warner
ZT Research,
Rapid City, USA
Email: tom.warner@ztresearch.com

Marcelo M.F. Saba
Atmospheric Electricity Group
Brazilian National Institute for Space Research
São José dos Campos, Brazil
Email: marcelo.saba@inpe.br

Abstract— **South Africa has a long history of lightning research. Tall towers provide a useful tool for investigating lightning as they generally have a high repeatability of events. The Johannesburg region in the Gauteng province has two tall towers, the Brixton tower and the Hillbrow tower, with a high frequency of lightning events. This paper presents a project beginning in January 2017 and aims to study the physics of lightning through high-speed video observation and fast electric field measurements. Thunderstorms over Johannesburg have a high cloud base which allows for visible channels from the tall towers. More than 200 videos of downward and upward flashes were observed since the project started. Also, 6 flashes to a 53 m tall building were observed. The project also aims to raise awareness around lightning dangers in Africa.**

Keywords- South African lightning; high-speed camera; upward lightning; downward lightning

I. Introduction

South Africa has a long history of research into lightning to tall structures [1,2]. The purpose of this paper is to present a project that is to be undertaken in 2017-2018. This is a scientific project that aims to investigate the physics of lightning by high-speed video observation along with electric field measurements and potential current measurements as well in Johannesburg, South Africa. It is part of an international collaboration between Brazil, USA, Austria and Sweden. Historically, these are all locations where tall tower investigations of lightning have been performed (using high-speed camera observations, electric field measurements, current measurements or a combination of these). Tall towers provide a useful tool for investigating lightning as they generally have a high repeatability of events. The Johannesburg region has two tall towers, the Brixton tower and the Hillbrow tower, with a high frequency of lightning events. However, these events are usually upward in nature, and an investigation of the density of lightning over Johannesburg to determine other, less tall locations is considered.

II. Johannesburg, South Africa

Johannesburg is the main economic city in South Africa and can be found in the north-east of the country. It is the location of much of the industry in South Africa. It is also notable for its altitude – approximately 1600 m above sea level. Figure 1 shows the skyline of Johannesburg.

Claude Leon Post-doctoral fellowship, Eskom TESP Programme

978-1-5386-6635-7/18/$31.00 ©2018 IEEE

Figure 1. The skyline of Johannesburg city, view from the north looking south through the city.

This photograph is taken from the north facing south through the city. Two tall towers on either ends of the skyline can be seen. These are the Brixton (right) and Hillbrow (left) tower. The Brixton tower is west of the city and Hillbrow tower is east. Figure 2 is a sketch of the height, and distance between the towers.

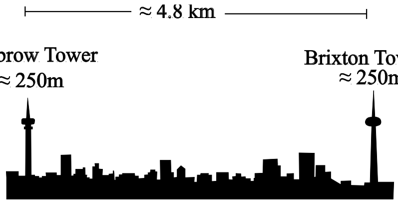

Figure 2. The two tall towers in Johannesburg city, Brixton (right) and Hillbrow (left) tower.

While these are the two tallest buildings, a number of other locations and buildings of interest fall within the city. The University of the Witwatersrand is located approximately halfway between the Brixton and Hillbrow tower.

Figure 3 shows the lightning flash density map of South Africa as of 2014. This map was created by the South African Weather Service (SAWS) utilizing data from the South African Lightning Detection Network (SALDN) – the lightning location system in operation in South Africa.

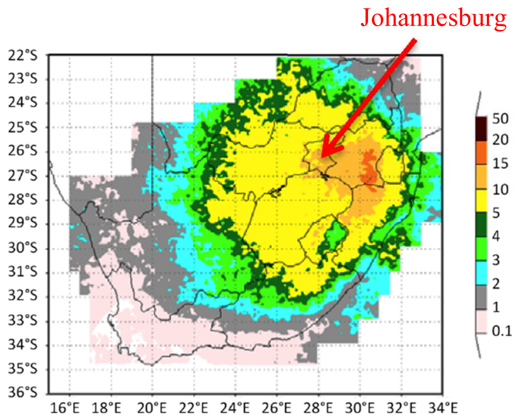

Figure 3. Lightning flash density over South Africa. Image used with permission, courtesy Morné Gijben [3]. The location of Johannesburg is indicated.

The SALDN consists of 25 Vaisala LS7000 sensors located across the country (with one sensor located in Swaziland) and has been operational since 2006. SAWS has collected more than 10 years worth of lightning data over the whole country. The network has an estimated average detection efficiency of 90% and approximately 500 m median location accuracy.

As can be seen in figure 3, the areas of highest lightning flash density are to the north-east of the country, in region known as the Mpumalanga province. Johannesburg is located close to this region (indicated in the figure), not quite in the highest flash density region but still high with approximately 10-15 *flashes/km²/year*. The combination of the tall towers, altitude, cloud base and high flash density make Johannesburg a unique and relevant choice for lightning studies.

A. Lightning Occurrence over Johannesburg

Utilizing Gaussian smoothing techniques, lightning location system data can be further interrogated for more detail. Gaussian smoothing techniques utilize the confidence ellipses of stroke reports to represent a stroke as a distribution rather than a single point. In this way, it is possible to create flash density maps that are independent of resolution - ideal for looking at areas smaller than 10×10 km. Given that each attachment point has been “spread out” and is rather represented as a fraction over the grid, no actual values can be attributed to the values but visual density trends are clearly displayed.

Figure 4 shows a Gaussian smoothed map over Johannesburg city. The map utilizes data from the SALDN from 2007 – 2015. The locations of the Brixton tower and the Hillbrow tower are shown. As is clear in the figure, there is a high density around the location of the two towers indicating that they are regularly struck – and much more than other locations within the city.

Figure 4. Gaussian smoothed lightning density map based on SALDN data from 2007 - 2015. The Brixton and Hillbrow towers are indicated in the image and can be distinguished by the “hotspots”.

Gaussian smoothed maps can be used to investigate even further – figure 5 shows a similar image but only over the University of the Witwatersrand campus, located roughly in the city center about half-way between the Brixton and the Hillbrow tower.

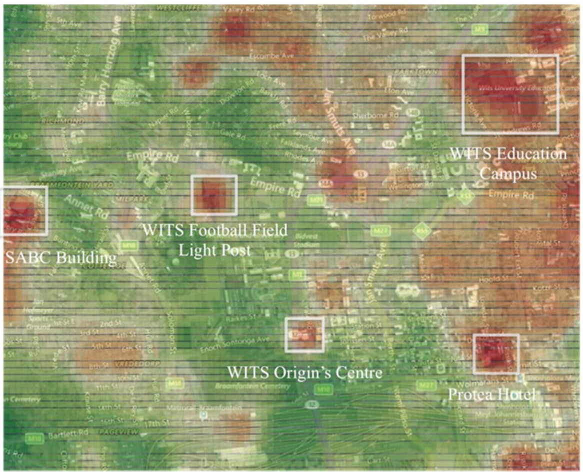

Figure 5. Gaussian smoothed lightning density map over Johannesburg, WITS University campus.

By examining the smaller area and excluding the Brixton and Hillbrow tower, more detail can be gained on specific locations around the city center and campus. It can be seen in the Figure 5 that there are a number of locations that seem to have been struck multiple times in the last 10 years. Five locations are identified on the map:

- The SABC broadcasting buildings
- A light post on a WITS football field
- The Origins Centre building on WITS campus
- The Protea Hotel in Braamfontein, Johannesburg
- The WITS Education Campus

None of these locations are significantly tall towers and it is very likely that the events they have endured are downward lightning events. The SABC broadcasting buildings, while close to the Brixton tower is sufficiently far away (1 km) so as not to be protected by the Brixton tower. Also of interest, is the Protea hotel in the Braamfontein area, a dense city area and yet, the Protea hotel clearly is struck fairly regularly, likely due to its height.

B. *Previous Photographic Studies*

Since 2009, a simple surveillance system to photograph lightning attachments to the Brixton tower was in operation. The system was initially installed to capture lightning images for 3-dimensional modeling of the lightning channel but was later used as a ground-truth location for comparison with the SALDN. The system consisted of a simple motion-triggered camera located at the University of the Witwatersrand and looking east towards the Brixton tower with an approximate field of view of 55° [4]

The system initially operated from 2009-2013 but was shutdown in 2014. It was reinitiated in 2015 with a second camera added looking at the tower from a different perspective. Figure 6(a) and (b) shows an example of the type of images captured by the system – a lightning flash attaching to the Brixton tower on Friday, 20 November 2015 at 22:24:48 SAST.

(a) (b)

Figure 6. A lightning strike to the Brixton tower on the 20 November 2015 at 22:24:48 SAST. Two cameras observe the Brixton tower – (a) one situated at WITS university and facing east, (b) the other situated 1 km north of the tower and facing south.

Table 1 shows the number of flashes to the Brixton tower photographed by the camera for each season since 2009. The cases are separated between upward flashes and downward flashes and, as expected, the majority of flashes to the tower are upward. However, some downward events do also attach to the tower.

TABLE I. PHOTOGRAPHED FLASHES TO BRIXTON TOWER

Season	***Number Upward Flashes***	***Number Downward Flashes***	***Total Number Flashes***
2009-2010	12	0	12
2010-2011	24	2	26
2011-2012	6	1	7
2012-2013	17	4	21
2015-2016	46	9	55
Total	105	16	121

Also notable in the photographs is the clarity of the channel – the cloud base is far above the top of the tower allowing for a complete view of the channel, unlike many other tall towers in the world, which find themselves reaching into the clouds and therefore obscuring the visibility of any lightning events that may attach to them.

III. HIGH-SPEED VIDEO STUDY

Before Abbreviations and Acronyms

A. *Collaborators*

The project has a number of collaborators who assist both with equipment and experience: ZT Research in South Dakota, USA and INPE in São Paulo, Brazil have performed similar studies in their respective countries and SAWS and EarthNetworks operate lightning location systems. This section details the nature of the projects performed by these collaborators and highlights how their knowledge and results feed into the South African project.

1) *ZT Research*

Tom Warner, of ZT Research, has worked with high-speed cameras since 2010 in Rapid City, USA. The city has 10 towers that produce upward lightning [5]. Figure 7 shows a frame from a high-speed video, which captured upward lightning events from towers in Rapid City. The researchers spent four summers recording flashes in Rapid City along with electric field measurements provided the Brazilian National Institute for Space Research (INPE). Tom Warner lent two high-speed cameras (10,000 and 1,000 frames per second) to the project in South Africa and is involved in all research analysis.

Figure 7. Upward lightning from towers in Rapid City, South Dakota.

2) Brazilian National Institute of Space Research (INPE)

The INPE team has experience with high-speed cameras and flat plate electric field measurements since 2003, and are pioneers on the characterization of the different polarities of flashes by images [6-7]. The team are have lent a flat plate electric field sensor, able to record data continuously at 5 MSamples/s to the South African project. Collaboration and comparison with ongoing research in São Paulo, Brazil (upward lightning to Jaraguá peak and downward lightning to normal apartment buildings) allows for comparison between data sets.

3) SAWS

SAWS has a long-standing agreement with the research group regarding the use of the SALDN data. The data provides insight into the filmed high-speed cases and simultaneously the video observation provide and ideal ground-truth data set for comparison with SALDN stroke detections and reports.

4) EarthNetworks□

EarthNetworks□ have recently begun implementing a lightning location system in South Africa and similarly, there is value in comparing high-speed video observations with reports from such a network.

B. *Equipment and Experimental Setup*

The two high-speed cameras provided by ZT Research and being used for the study are the Phantom v310, Phantom v7.1. In general, the v310 records at approximately 15000 fps with an exposure time of 58µs and the v7.1 at 5000 fps with an exposure time of 990µs. The different frame rates of the cameras and their subsequent exposure times and resolution allow for each recorded flash to be separately analysed. analysed separately - optimising the accuracy of the characterization process.

Figure 8 shows where the two high-speed cameras are located – an area north-west of the Johannesburg city center on a ridge known as Northcliff hill – along with the locations of the Brixton and the Hillbrow tower, and the city center between them. The camera view over the city is therefore the same as shown in figure 1, the skyline of Johannesburg.

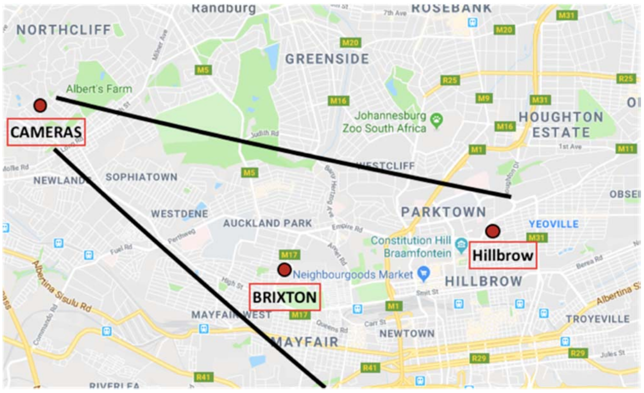

Figure 8. Location of high-speed cameras and the Brixton and Hillbrow towers, indicating Johannesburg city.

Also shown in figure 8 the locations of a number of simple surveillance camera setups similar to those used in the previous photographic study. However, here cameras located at the University of the Witwatersrand look not only to the Brixton tower but also at the Hillbrow tower and the city centre. Another on of these camera setups is located on the 52nd floor of a building known as Ponte, a tall apartment building in the city not far from the Hillbrow tower. Figure 9 shows a photograph of a lightning event to the Hillbrow tower taken by the South African photographer Jonathan Wood.

Figure 9. Photograph lightning event to Hillbrow tower taken from the Ponte building. Courtesy Jonathan Wood.

These simple surveillance camera setups provide additional information to the high-speed video observations, giving a different perspective on the channel and allowing for identification of strike-points that may not have been visible from the high-speed footage.

C. *Methodology*

For the end of the season (January – May 2017) and the following season (October 2017 – May 2018), the high-speed camera setup and surveillance camera setup were activated and capturing video footage of lightning during thunderstorm over South Africa.

For each filmed lightning flash, the following categorizations were performed based on the video:

- Downward flashes
  - Continuing current duration
  - Polarity
  - Multiplicity
  - Multiple strike points
  - Total flash duration
- Upward flashes
  - Triggering events
  - Duration and continuing current
  - Polarity
  - Subsequent return strokes
  - ICC pulses
  - Tall towers involved

Also discussed in the analysis are a number of bipolar events observed by the camera. Upward and downward events are categorized based on the direction of propagation of the leader. Polarity is determined based on the presence of branching and recoil leaders.

IV. FIRST RESULTS: 2017 - 2018

During this first year of high-speed video recording in Johannesburg, 168 downward flashes were recorded. Upward flashes also were observed from Johannesburg towers and tall buildings. A total of 45 upward flashes were registered. Table 2 shows a summary of the lightning events captured by high-speed video over Johannesburg from February 2017 to February 2018.

TABLE II. NUMBER OF FLASHES RECORDED FEB 2017-2018

Type		***Quantity***
Downward	Negative	155
	Positive	6
Upward	Negative	43
	Positive	2
Triggering events		6
Bi-polar		1
Total		262

A. Downward flashes

A total of 155 negative downward flashes, 6 positive downward flashes and 1 bipolar downward flash were recorded. A bipolar flashes was considered only when a channel was used to transfer different polarities of charge. In addition to this amount, 6 downward flashes were classified as triggering flashes due to the occurrence at the same time and framed in the same camera view of upward flashes. These triggering flashes were observed to be 5 positive downward flashes and 1 bipolar flash.

The number of strokes and statistics for the duration of each flash consider all registered downward strokes, including triggering events. A total of 605 negative strokes and 13 positive strokes were recorded. Figure 10 shows a frame taken for a high-speed video of a downward flash over Johannesburg. Table III summarizes the characteristics of the downward flashes recorded over Johannesburg.

Figure 10. Frame taken from high-speed video of downward lightning over Johannesburg, South Africa.

The two bipolar flashes began with a single positive stroke followed by 2 and 3 negative strokes respectively. The strokes followed the same channel and attached to the same strike point. The bipolar flash that had 4 strokes, triggered an upward leader from the Brixton tower 2 kilometers from the downward strike point. The upward leader started after the positive stroke and the following 3 negative strokes happened during the continuous current of the upward leader. Both bipolar flashes follow the same structure as that seen by Saba et al. [8].

Figure 11. Downward bipolar flash struck the building and triggered an upward leader from a 250 meter-tower 2 kilometer away.

TABLE III. DOWNWARD FLASH STROKES

	N	AM	Min	Max
NEGATIVE FLASHES	155			
Max Number of Strike Points	3			
Multiplicity - Average of Strokes per flash		3,1	1	26

Max Duration Negative strokes	605	28,7	1	929
Time between Strokes (ms)	460	66,5	6	546
Time with no current (ms)	425	43,3	2	360
Total duration (ms)	206	320,4	2	1162

POSITIVE FLASHES	**N**	**AM**	**Min**	**Max**
Positive strokes	6			
Max Duration Positive strokes* (*Including bipolar and triggering events)	13	230	2	567

As presented by Kitagawa et al. [9], Brook et al. [10] Shindo and Uman [11], Ballarotti et al. [12] the continuous current can be defined by the duration and the terms are "*very short*" for durations from 3 ms up to 10 ms, "*short*" for durations between 10ms up and 40 ms and "*long*" for cases where the duration is more than 40 ms. The continuous current duration for negative and positive strokes is presented in Table IV.

TABLE IV. CONTINUOUS CURRENT DURATION

	Negative Strokes	Positive Strokes
	605	13
Number of strokes without CC	108	1
CC Very short 3>CC>10	264	1
CC Short 10>CC>40ms	160	0
CC Long more than 40ms	73	11

B. Upward Flashes

From a total of 43 upward flashes that were recorded, 41 were negative upward flashes and 2 were positive upward flashes. Negative upward flashes are the flashes that transfer negative charge to the ground, i.e. the upward positive leader propagates toward to the cloud. The image obtained from the high-speed camera shows a leader with no branches. On the other hand, positive upward flashes have branched negative upward leaders propagating towards the cloud. Figure 12 shows the two types of upward leader: a) positive and no-branched upward leader and b) negative and branched upward leader.

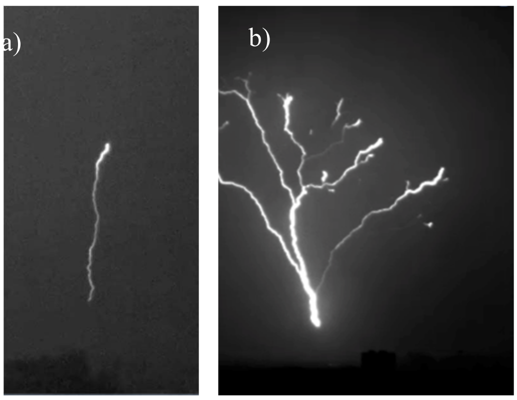

Figure 12. Frames taken from high-speed video of (a) positive upward leader (negative upward flash) and (b) negative upward leader (Positive upward flash)

Upward flashes were recorded mainly from the Brixton and Hillbrow tower. For the multiple tower-involved cases, 10 out of 11 had both towers producing upward leaders (4.8 km from each other), one case had three upward leaders from both towers and also the SABC building (115-meter building). One other case involved a 90 m tall tower 2.5 km from the Hillbrow tower and the Hillbrow tower.

Upward flashes start with an upward leader propagation that is known in the literature as a Initial Continuous Current (ICC), any fluctuation of luminosity in this stage are designated as ICC pulses. After this stage the upward flash can end or, after some tens of milliseconds, a downward leader can use the ionized channel to transfer charge to the ground (Return Stroke). These return strokes can then be followed by continuous current. The luminosity of upward flashes can be summarized as in the figure 13.

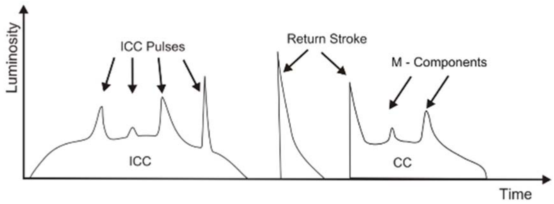

Figure 13. Upward flash luminosity profile (Saba et al. 2016)

The average and maximum duration of upward initial continuous current stages were 405ms and 990ms respectively. 398 pulses were registered in the 41 negative upward flashes. Table V shows some of the characteristics of the upward flashes filmed over Johannesburg.

TABLE V. NEGATIVE UPWARD FLASH

Negative upward flashes	41
Negative Leaders	53
w/ multiple tower involved	11
Max duration ICC	990 ms (AM=405ms)
ICC Pulses (N)	398
RS in negative upward flash (N)	38
Max Duration RS	269 (AM=28ms)
Triggering event:	
w/ triggering event visible:	6
Positive Flashes	5
Bipolar flashes (+CG > UP > -CG)	1

C. Potential current measurement:

A number of lightning events were observed attaching to a 53 m tall apartment building (Figure 14). From the SALDN and videos, this building was struck by positive, negative and bipolar downward flashes.

V. SUMMARY

The Johannesburg scientific project aims to investigate the physics of lightning by high-speed video observation along with electric field measurements. All equipment and collaborations available were presented. Previous studies about the location were also provided.

A total of 168 downward flashes and 43 upward flashes were characterized. Characteristics of 13 positive and 605 negative strokes and 41 negative upward flashes were presented. Flashes with almost 1 second connected to ground: negative downward flash (929ms) and upward flash (990ms).

One building in particular presented an ideal location to install a current system for natural downward flash measurement. Towers approximately 250 meters-tall and 4.8 km from each also are potential locations for the installation of a current measurement system due to number of upward flashes. The current system combined with high-speed video and the high cloud base in Johannesburg would provide more information about the initiation of flashes.

ACKNOWLEDGMENT

The author Carina Schumann would like to thank the Claude Leon Foundation for the Post-doctoral fellowship. The authors also like to thank South African Weather Service (SAWS) for their support and for providing the SALDN data used in this paper. They would also like to thank Eskom for the support of the Lightning/EMC Research Group through the TESP programme. Thanks are extended to the Department of Trade and Industry (DTI) for THRIP funding as well as to the National Research Foundation (NRF) for direct funding of the Research Group.

REFERENCES

[1] Eriksson, A.J. (1978), Lightning and tall structures, Transactions: The SA Institute of Electrical Engineering, pp. 238-252.

[2] Anderson, R.B. and A. J. Eriksson (1980), Lightning parameters for engineering application.Electra Vol.69, 65–102, 1980.

[3] Gijben M. The lightning climatology of South Africa. S Afr J Sci. 2012;108(3/4), Art. #740, 10 pages.

[4] H.G.P Hunt, K.J. Nixon and I.R. Jandrell: "Establishing a methodology to investigate LDN median error ellipses used as corroborating evidence for a lightning event at a specific geographic locations." *Electric Power Systems Research Journal*, 2014.

[5] T.A. Warner, K.L. Cummins and R.E. Orville: "Upward lightning observations from towers in Rapid City, South Dakota and comparison with National Lightning Detection Network data, 2004–2010", Journal of Geophysical Research, Res. 117, D19109, doi:10.1029/2012JD018346

[6] M.M.F. Saba, M.G. Ballarotti, O. Pinto, Jr: "Negative cloud-to-ground lightning properties from high-speed video observations." Journal of Geophysical Research, vol. 111, p. D03101, 2006.

[7] M.M.F. Saba, W. Schulz, T.A. Warner, L.Z.S. Campos, K.L. Cummins, R.E. Orville: "High-speed video observations of positive lightning flashes to ground." Journal of Geophysical Research: Atmospheres, vol. 115, p. D24201, 2010.

[8] M.M.F. Saba, C. Schumann, T.A Warner, J.H. Helsdon, W. Schulz, R.E Orville: "Bipolar cloud-to-ground lightning flash oberservations." Journal of Geophysical Research: Atmospheres, vol. 118, p. 1-9, 2013.

[9] N. Kitagawa, M. Brook, E.J. Workman, ―Continuing currents in cloud-to-ground lightning discharges, J. Geophys. Res. 67, pp. 637–647, 1962.

[10] M. Brook, N. Kitagawa, E.J. Workman, ―Quantitative study of strokes and continuing currents in lightning discharges to ground, J. Geophys. Res. 67, pp. 649‑659, 1962.

[11] T. Shindo, M.A. Uman, ―Continuing current in negative cloud- to-ground lightning, J. Geophys. Res. 94, pp. 5189‑5198, 1989.

[12] M.G. Ballarotti, M.M.F. Saba, O. Pinto Jr., ―High-speed camera observations of negative ground flashes on a millisecond-scale. Geophys. Res. Lett. 32, L23802.doi:10.1029/2005GL023889, 2005.

Appendix D

Summary of electric field measurements of lightning flashes over Johannesburg, South Africa

D.1 Preamble

This appendix contains a paper titled: **Characterisation of lightning flashes from changing electric field measurements in Johannesburg, South Africa** this paper was presented and accepted to be published at the *34th International Conference on Lightning Protection (ICLP)* in September 2018, which took place in Rzeszow, Poland.

D.2 Paper description

This paper gives an overview of lightning events which were captured using changing electric field measurements. The equipment that was used is discussed and the methodology to finding the results is presented. There is a comparison of the results in this paper and other studies with regards to the electric field intensity and the 0-100% and 10-90% rise times.

34th International Conference on Lightning Protection
02-07 September 2018
Rzeszow, Poland

Characterisation of lightning flashes from changing electric field measurements in Johannesburg, South Africa

J. D. Tasman, C. Schumann,
H. G. P. Hunt , H. G. Fensham,
K. J. Nixon
School of Electrical and Information Engineering
University of the Witwatersrand
Johannesburg, South Africa
jesstasman@gmail.com

M. M. F. Saba
Atmospheric Electricity Group
Brazilian National Institute for Space Research
São José dos Campos, Brazil
marcelo.saba@inpe.br

T. A. Warner
ZT Research
Rapid City, South Dakota, USA
tom.warner@ztresearch.com

***Abstract*—Presented are results obtained from changing electric field measurements and high-speed video analysis on lightning flashes over Johannesburg, South Africa. A flat-plate antenna and integrator were used to record changing electric fields and the high-speed footage was recorded using Phantom v310 and v7.1 (15,000 fps and 5,000 fps respectively) cameras. A total of 34 negative strokes and 3 positive strokes were analysed. The recorded negative strokes presented an average peak intensity of 8.0 V/m, 0 - 100 % rise time of 3.3 µs, 10 - 90 % rise time of 1.8 µs and pulse duration of 6.4 µs. The positive strokes presented an average peak intensity of 36.7 V/m, 0 - 100 % rise time of 22.9 µs, 10 - 90 % rise time of 7.4 µs and pulse duration of 33.4 µs. The average continuing current durations, determined using high-speed videos, was 6.3 ms for the negative strokes and 81.5 ms for the positive strokes.**

Keywords—changing E-field; flat-plate antenna; high-speed video; rise time

I. Introduction

Previous studies have been performed using changing electric field (E-field) measurements to characterise and record data from cloud-to-ground (CG) lightning flashes. These include studies performed in Brazil, Austria, Malaysia and Florida (USA), among others [1-4]. The common parameters recorded from the changing electric field profiles measured in these studies include rise times, intensities and durations. These parameters correspond to the attachment of a leader and the magnitude and duration of the current impulse. If the strike-point is too close to the measurement device, the electronics could be driven into saturation and an accurate profile may not be obtainable. The ideal setup would have sensors installed at a range of distances. The presence of a near and far E-field measurement sensor ensures that all recorded strokes can be analysed.

High-speed videos and changing electric field measurements are two accurate ways in which lightning flashes can be characterised and analysed. From 10 February 2017 to 6 February 2018, both methods were applied in assessing lightning flashes that occurred in Johannesburg, South Africa. For the changing electric field data to be viewed, the E-field files were analysed using the Dataviewer 1.4 software.

A flat-plate antenna is set up to perform changing electric field measurements and is detailed in Section II. The high-speed video and changing E-field measurement studies are presented in Section III and IV. These sections include a detailed methodology on the extraction of the aforementioned parameters from the recorded measurements. Comparisons between previous studies and the results from this study are presented in Section V.

II. Changing Electric Field Measurements

Measuring a change in the electric field between a thundercloud and the ground is a highly effective way of characterising lightning flashes. In this study, a flat-plate antenna was used to perform these changing electric field measurements. Using the assumption of an infinite ground plane, justified by Cooray [5], the flat-plate antenna measures a change in the vertical electric field by using a capacitive antenna. The output signal from the antenna is then integrated and amplified, which allows for a waveform to be resolved that is proportional to the time derivative of the measured electric field.

A flat-plate antenna and integrator system was installed at coordinates 26.19134° S, 28.02712° E, on the roof of a four-story building in Johannesburg, South Africa. The integrator has a decay time-constant of 0.47 s and operates at a bandwidth between 300 Hz and 1.5 MHz. The measurement system comprises of a 12-bit, 5 MS/s PCI N-6110 National Instruments digitiser, which allows for continuous recording. An external antenna and a Meinberg PCI-170GPS board is integrated into the system to ensure accurate time stamping of recordings. This allows for time correlation with other measurement equipment, such as high-speed cameras. The process that the changing E-field measurement equipment follows is presented in Fig. 1.

The flat-plate antenna set-up is shown in Fig. 2. A PV panel is utilised to ensure the battery used to power the integrator is always sufficiently charged.

978-1-5386-6635-7/18/$31.00

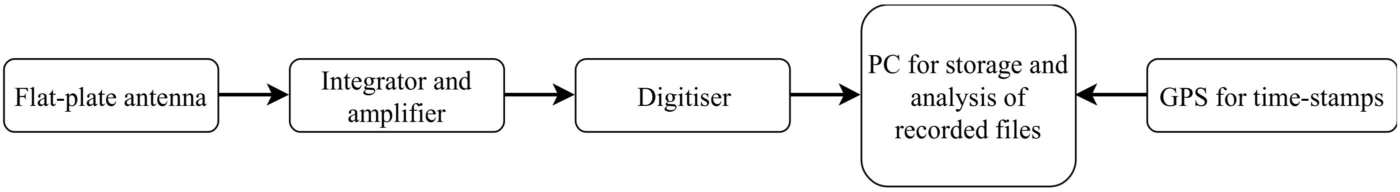

Fig. 1. High-level flow diagram of changing electric field measurement process

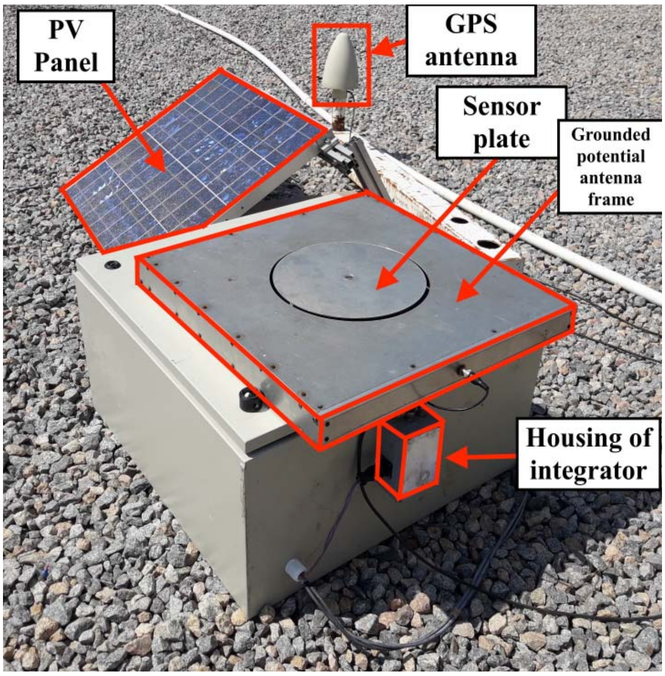

Fig. 2. Flat-plate antenna set-up

III. HIGH-SPEED VIDEO CAMERAS

The high-speed cameras used in this study are the Phantom v310 (15,000 fps, exposure time 58 µs) and the Phantom v7.1 (5,000 fps, exposure time 990 µs). The difference in frame rate and exposure time of each camera allows for the footage to be compared and ultimately, more accurate characterisation of lightning flashes.

The cameras are installed at coordinates 26.1614° S, 27.957° E. This is approximately 8 km Northwest of central Johannesburg. The field of view of the cameras relative to the Brixton and Hillbrow towers and the changing E-field measurement set-up is shown in Fig. 3.

IV. ANALYSIS

The following section presents an analysis of the changing electric field data. This includes a detailed methodology on the characterisation process of the recorded changing E-field data and the overall results. Previous studies were consulted to ensure the analysis procedure produced comparable results [6 – 8].

A. Data

The changing electric field data consists of lightning flashes occurring between 10 February 2017 and 6 February 2018. A sample waveform of a negative flash registered by the flat-plate antenna system is presented in Fig. 4. Peak intensity magnitudes, rise times (0 - 100 % and

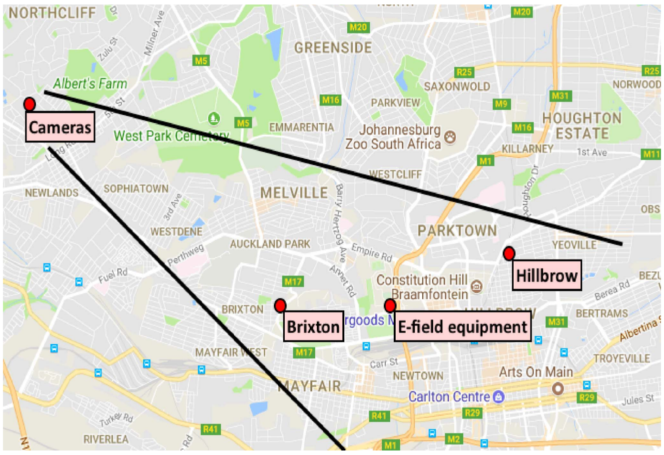

Fig. 3. Map illustrating field of view of high-speed cameras (developed using Google Maps software)

10 – 90 %) and pulse durations were obtained from the waveforms.

In this study, the distance from the sensor to the strike-point of the flashes ranged from 5.7 km to 28.2 km. In this distance range, the radiation field component of the propagated electromagnetic field is prominent. Distances were claculated using the strike-point coordinates obtained from the South African Lightning Detection Network (SALDN). The recorded intensity of the change in the electric field is dependent on the distance the strike-point was relative to the flat-plate antenna. To allow for this parameter to be compared objectively with other studies, the recorded peak intensities were normalised to 100 km.

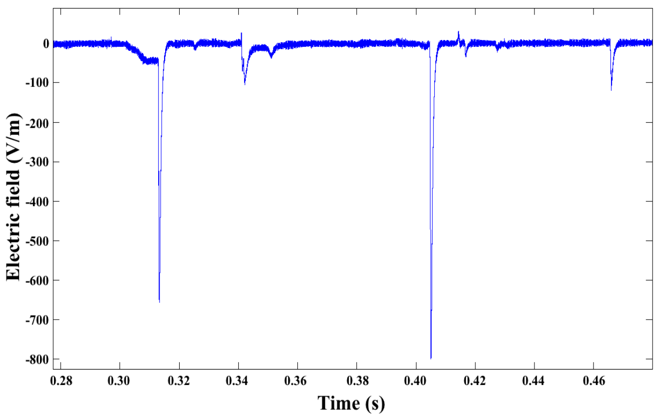

Fig. 4. Sample of a negative flash waveform

B. Methodology

The waveform of a negative stroke is shown in Fig. 5. The slow front (SF) and fast transition (FT) phases associated with this stroke is discussed by Tran and Rakov [9] and illustrated on Fig. 5. With reference to the time (T) and intensity (i) parameters used in this section, the points indicated in Fig. 5 are defined by the following parameters:

- A: (T_0, i_0)
- B: (T_{100}, i_{100})
- C: (T_{end}, i_{50})

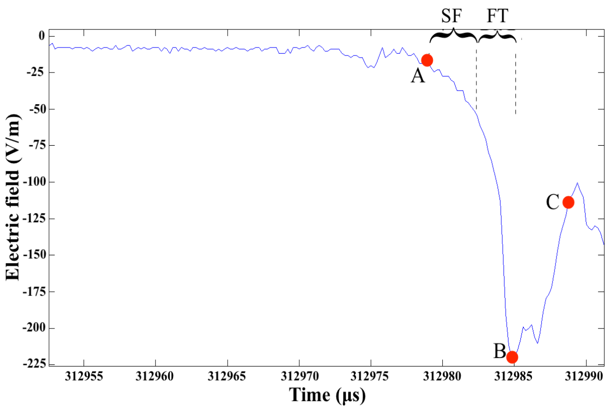

Fig. 5. Slow front (SF) and fast transition (FT) of a changing electric field waveform of a negative return stroke

Determination of changing E-field parameters:

1) *Changing E-field intensity*

- Take point A as the intensity where the waveform gradient begins its decay to infinity.
- Take point B as the intensity at the peak of the stroke.
- $i_{max} = i_{100} - i_0$

2) *Normalised peak intensity*

- Determine distance between strike-point and changing E-field measurement device using SALDN coordinates of strike-point.
- Normalise peak intensity to 100 km.

3) *0 % - 100 % rise time ($T_{0\text{-}100}$)*

- T_0 is the time at i_0
- T_{100} is the time at i_{100}
- $T_{0\text{-}100} = T_{100} - T_0$

4) *10 % - 90 % rise time ($T_{10\text{-}90}$)*

- T_{10} is the time corresponding to i_{10}
  - $i_{10} = i_0 + 0.1(i_{100} - i_0)$
- T_{90} is the time corresponding to i_{90}
  - $i_{90} = i_0 + 0.9(i_{100} - i_0)$
- $T_{10\text{-}90} = T_{90} - T_{10}$

5) *Pulse duration ($T_{duration}$)*

- T_{end} at point C on Fig. 5 is the time taken for the intensity to return to 50 % of i_{100} from point A (T_0).
- $T_{duration} = T_{end} - T_0$

6) *Polarity*

- Classified as positive if $i_{100} > i_0$
- Classified as negative if $i_{100} < i_0$

C. *Results*

From a total of 18 recorded flashes, 15 were classified as negative CG and 3 as positive CG. From the 15 negative flashes, a total of 34 strokes were observed and only two consisted of more than 3 strokes (6 strokes and 9 strokes). All three positive flashes consisted of only one stroke. The arithmetic means (AM) and geometric means (GM) of the data obtained from the positive strokes and negative strokes are presented in Table I and Table II, respectively.

TABLE I. POSITIVE STROKES (3 SAMPLES)

Parameter	AM	GM	Unit
Normalised peak intensity	40.5	36.7	V/m
$T_{0\text{-}100}$	23.7	22.9	µs
$T_{10\text{-}90}$	7.8	7.4	µs
$T_{duration}$	34.5	33.4	µs

TABLE II. NEGATIVE STROKES

Samples		Parameter	AM	GM	Unit
1st RS	12	Normalised peak intensity	9.4	8.6	V/m
		$T_{0\text{-}100}$	4.6	4.5	µs
		$T_{10\text{-}90}$	2.8	2.5	µs
		$T_{duration}$	9.3	8.5	µs
2nd RS	9	Normalised peak intensity	7.5	6.3	V/m
		$T_{0\text{-}100}$	4.0	3.5	µs
		$T_{10\text{-}90}$	2.6	2.3	µs
		$T_{duration}$	5.8	5.3	µs
3rd RS	5	Normalised peak intensity	8.1	7.7	V/m
		$T_{0\text{-}100}$	2.4	2.3	µs
		$T_{10\text{-}90}$	1.0	0.9	µs
		$T_{duration}$	7.0	6.4	µs
All	34	Normalised peak intensity	9.5	8.0	V/m
		$T_{0\text{-}100}$	3.9	3.3	µs
		$T_{10\text{-}90}$	2.2	1.8	µs
		$T_{duration}$	7.4	6.4	µs

V. DISCUSSION

The results of the changing E-field measurements are discussed below and are compared with other studies. The durations measured from the changing electric field waveforms correspond to the pulse duration of the impulse phase of the lightning flash. The duration parameter attained from the high-speed videos represents the duration of the continuing current phase of the lightning flash.

A. Changing electric field

The Geometric mean (GM) of changing E-field peak intensities, normalised to 100 km, for South Africa and Austria are provided in Table III. The Austrian data set used is made up of 31 return strokes. The integrator used for the flat-plate antenna in the Austrian study has a decay time-constant of 0.5 s resulting in a similar bandwidth to the equipment used in this study, hence, ensuring comparable peak intensities.

TABLE III. GEOMETRIC MEAN OF NORMALISED CHANGING ELECTRIC FIELD INTENSITIES

RS	SA	Austria [1]	Units
All	9.5*	8.6	V/m

* TAKEN FROM NEGATIVE STROKE DATA ONLY

The Austrian data used in Table III lists a 0-100 % rise time of 7.4 μs (GM) for all return strokes. For comparison, the GM for the same parameter from the data obtained in this study is 3.3 μs. A comparison of 0 – 100 % and 10 – 90 % rise times with studies conducted in Malaysia and Florida is presented in Table IV. A possible reason for the discrepancies in these rise-times could be due to the measurement equipment operating in different bandwidths.

TABLE IV. GEOMETRIC MEANS OF RISE TIMES FOR NEGATIVE FIRST RETURN STROKES

RS	%	SA	Malaysia [3]	Florida [2]
1st	0 - 100	4.5 μs	9.1 μs	6.5 μs
	10 - 90	2.5 μs	5.0 μs	3.6 μs

The data obtained from the positive flashes is compared with other studies and presented in Table V. The data collected in this study along with the study performed by Schumann, et al. [4] are tabulated in bold text as the antenna and integrator used were the same. This means the frequency content in both measurements are similar and, therefore, allow for accurate rise time comparisons. With the flat-plate antenna being placed on the roof of a building, a significant local, vertical electric field enhancement occurs. This effect will be accounted for by determining a scalar factor that will normalise the results.

B. High-speed video correlation

A set of data was compiled from high-speed video footage of all flashes corresponding to those recorded by the changing electric field measurement system. From these recordings, the luminosity persistence in the lightning channel after attachment had been made was used as an indicator for continuing current duration. A statistical summary of the continuing current durations for both negative and positive flashes is presented in Table VI. From the videos, the end of the continuing current was determined by when the channel disappeared. Visibility of the channel can vary based on the lighting environment and the computer monitor that was used for analysis and, therefore, could account for possible inaccuracies in recorded duration times.

TABLE V. COMPARISON OF CHANGING ELECTRIC FIELD PARAMETERS FOR POSITIVE STROKES

Parameter	Studies	Samples	AM
Peak instensities (V/m)	**This study**	**3**	**40.5**
	Schumann, et al. [4]	**66**	**17.0**
	Cooray, et al. [10]	46	11.5
Rise time (0 – 100 %, μs)	**This study**	**3**	**23.7**
	Schumann, et al. [4]	**72**	**9.5**
	Hojo, et al. [11]	32	22.3
	Cooray [12]	20	8.9
	Ushio, et al. [13]	19	18.0
Rise time (10 – 90 %, μs)	**This work**	**3**	**7.8**
	Schumann, et al. [4]	**72**	**5.7**
	Hojo, et al. [11]	32	6.7
	Cooray [12]	15	6.2

TABLE VI. RECORDED CONTINUING CURRENT DURATIONS FROM LUMINOSITY PERSISTENCE IN HIGH-SPEED VIDEO FOOTAGE

Polarity	Samples	Duration AM	Duration GM	Max	Min	Units
Negative	34	21.4	6.3	271	1	ms
Positive	3	348.7	81.5	567	2	ms

C. Notable points

Throughout this study, certain constraints existed due to the equipment used and the data acquisition methodology. These, along with other noteworthy observations, are presented below:

- The peak changing E-field intensities could only be normalised if there was corresponding SALDN coordinate data on the strike-point locations of the recorded flashes.
- The changing E-field stroke data that could be correlated to the videos was limited to flashes with strike-points in the field of view of the cameras (illustrated in Fig. 3).
- The beginning stages of the electric field collapse are observable before T_0. This information, if studied further, could have significant practical applications,

such as improving the response time of certain lightning protection systems.

- An advantage of using both changing E-field measurements in collaboration with high-speed videos is that if unfamiliar anomalies occur in the electric field, the videos can be used to provide clarity. The converse also applies.
- A disadvantage of using both analysis techniques is that the field of view of the cameras is the limiting factor in the number of strokes that can be correlated to the changing E-field data. The antenna sensors register more flashes than the high-speed cameras can capture.
- The localised enhancement of the vertical electric field on the building that the antenna was placed has been noted. An enhancement factor is yet to be developed and as such, the presented electric field peaks are assumed to be marginally higher than the true values.

VI. CONCLUSION

Presented in this paper are the results obtained from analysing the data obtained from 18 separate lightning flashes over Johannesburg, South Africa. A flat-plate antenna with an integrator was used to record the peak intensity, rise times and pulse duration parameters of the propagated vertical electric field from lightning flashes. The normalised peak intensities for the 34 recorded negative strokes and 3 positive strokes were 8.0 V/m and 36.7 V/m, respectively. The pulse durations for the negative and positive stroke samples were 6.4 µs and 33.4 µs, respectively. From high-speed video recordings of the corresponding flashes, the negative and positive strokes presented an average continuing current duration of 6.3 ms and 81.5 ms, respectively.

ACKNOWLEDGEMENTS

The authors would like to thank the South African Weather Service (SAWS) for their support and for providing the SALDN data used in this paper. They would also like to thank Eskom for the support of the Lightning/EMC Research Group through the TESP programme. Thanks are extended to the Department of Trade and Industry (DTI) for THRIP funding as well as to the National Research Fund (NRF) for direct funding of the Research Group.

REFERENCES

[1] H. Pichler, G. Diendorfer and M. Mair. “Some Parameters of Correlated and Radiated Field Pulses from Lightning to the Gaisberg Tower” IEEJ Transactions on Electrical and Electronic Engineering, 2010.

[2] A. Nag, V. A. Rakow, D. Tsalikis, J. S. Howard, C. J. Biagi, J. D. Hill, M. A. Uman and D. M. Jordan. “Characteristics of the initial rising portion of near and far lightning return stroke electric field waveforms” ICLP, 2010.

[3] M. N. Hamzah, M. Z. A. Ab Kadir, C. Gomes and S. N. M. Arshad. “Unusually Long Duration Lightning Electric Field Return Strokes in Malaysia” ICLP, 2014.

[4] C. Schumann, M. M. F. Saba, R. B. G. Da Silva and W. Schulz. “Electric fields changes produced by positive cloud-to-ground lightning flashes” Journal of Atmospheric and Solar-Terrestrial Physics, Volume 92, 2012.

[5] V. Cooray. An Introduction to Lightning. Springer Netherlands, 1st ed., 2015. □

[6] S. N. M. Arshad, M. Z. A. Ab Kadir, M. Izadi, M. N. Hamzah, C. Gomes and J. Jasni. “Characterization of Measured Lightning Electric Fields Observed in Malaysia” ICLP, 2014.

[7] M. A. Haddad, V. A. Rakov, S. A. Cummer. “New measurements of lightning electric fields in Florida: Waveform characteristics, interaction with the ionosphere, and peak current estimates” Journal of Geophysical Research, Volume 117, 2012.

[8] A. D. Watt. “ELF Electric Fields From Thunderstorms” Journal of Research of the National Bureau of Standards, Volume 64D, 1960.

[9] M. D. Tran and V. A. Rakov. “A study of the ground-attachment process in natural lightning with emphasis on its breakthrough phase” Scientific Reports, 2017.

[10] V. Cooray, M. Fernando, C. Gomes, and T. Sorenssen. “The fine structure of positive lightning return-stroke radiation fields” IEEE Transactions on Electromagnetic Compatibility, Volume 46 (1), pp. 87–95, 2004.

[11] J. Hojo, M. Ishii, T. Kawamura, F. Suzuki and R. Funayama. “The fine structure in the field change produced by positve ground strokes” Journal of Geophysical Research, Volume 90, pp. 6139–6143, 1985.

[12] V. Cooray. “A novel method to identify the radiation fields produced by positive return strokes and their submicrosecond structure” Journal of Geophysical Research 91 (D7), pp. 7907–7911, 1986.

[13] T. Ushio, Z. Kawasaki, K. Matsu-ura and D. Wang. “Electric fields of initial breakdown in positive ground flash” American Geophysical Union. Paper no. 97d01975–0148-0227/97/97JD-01975, 1998.